PHYSIOLOGICAL AND PHARMACOLOGICAL PROPERTIES OF THE ATP-SENSITIVE POTASSIUM CHANNEL FROM THE INNER MITOCHONDRIAL MEMBRANE

Vladimir Yarov-Yarovoy
M.S., Moscow State University, Russia, 1993

A dissertation submitted to the faculty of the
Oregon Graduate Institute of Science and Technology
in partial fulfillment of the
requirements for the degree
Doctor of Philosophy
in
Biochemistry and Molecular Biology

October 1998

The dissertation "Physiological and Pharmacological Properties of the ATP-Sensitive Potassium Channel from the Inner Mitochondrial Membrane" by Vladimir Yarov-Yarovoy has been examined and approved by the following Examination Committee:

Keith D. Garlid
Professor, Thesis Advisor

James M. Cregg
Professor

Gebre Woldegiorgis
Associate Professor

Kent L. Thornburg
Professor
Oregon Health Sciences University

DEDICATION

This work is dedicated to my wife Yuliya.

ACKNOWLEDGMENTS

I would like to thank my advisor, Dr. Keith D. Garlid, for his support, thoughtful advice, encouragement, and patience throughout my tenure as a graduate student.

I am also grateful to the other members of my dissertation committee, Drs. James Cregg, Gebre Woldegiorgis, and Kent Thornburg, for their careful evaluation of my work and their helpful comments. In particular, I would like to thank Dr. Woldegiorgis for many valuable discussions concerning all aspects of my study and for his constant encouragement of my work.

I am grateful to Dr. Petr Paucek for guiding me through this project and for his experimental expertise.

I am indebted to my M.S. thesis advisor, Dr. Galina Mironova, for introducing me to the mitochondrial research field and for her high aspirations for my work.

I greatly appreciate the technical advice, editing expertise, and patient cooperation of Craig Semrad. Many thanks to Martin Jabůrek, Martin Modriansky, Peter Schindler, Hongfa Zhu, Jianying Shi, Oleg Stasyk, Pierre Moënne-Loccoz, and Monique Johnson for their friendship, support, and interest in my work.

I would like to thank Nancy Christie and Terrie Hadfield for their great assistance in editing and correcting my work, all the smiles, and the beautiful cake at my graduation party.

I am grateful to Carol Resco, Julianne Williams, Kristine Roley, Nancy Henderson, Mary Hultine, and Kathleen Stewart for their assistance in the library and their friendliness.

Finally, I am thankful to my wife, Yuliya Yarova-Yarovaya, for her love, support and constant encouragement which made this all worthwhile.

TABLE OF CONTENTS

LIST OF FIGURES

ABBREVIATIONS

8-azido-[α-^{32}P]ATP	8-azido-[α-^{32}P] adenosine 5′-triphosphate
4-Br-A23187	4-bromo-A23187
ADP	adenosine 5′-diphosphate
APD	action potential duration
ATP	adenosine 5′-triphosphate
ATP_i	intracellular ATP
BLM	bilayer lipid membrane
BSA	bovine serum albumin
$CellK_{ATP}$	plasma membrane K_{ATP} channel
CoA	coenzyme A
CPT-1	carnitine palmitoyltransferase I
CDP	cytidine 5′-diphosphate
DEAE-cellulose	diethylaminoethyl-cellulose
DTT	dithiothreitol
EDTA	ethylene diaminetetraacetic acid
EGTA	ethylene glycol-bis(β-aminoethyl ether)-N,N,N′,N′-tetraacetic acid
$\Delta\Psi$	electrical membrane potential
FA	fatty acid
FAD	flavin adenine dinucleotide
FCCP	carbonyl cyanide *p*-(trifluoromethoxy)phenylhydrazone
FL-glyburide	BODIPY® FL glibenclamide
GDP	guanosine 5′-diphosphate
3xGMs	guanidine-treated inner mitochondrial membranes
GTP	guanosine 5′-triphosphate

5-HD	5-hydroxydecanoate
HEPES	N-[2-hydroxyethyl]piperazine-N′-[2-ethanesulfonic acid]
IDP	inosine 5′-diphosphate
KCO	potassium channel opener
KIR	inward rectifying K^+ channel
MitoK_{ATP}	mitochondrial K_{ATP} channel
NADH	α-nicotinamide-adenine dinucleotide
NDP	nucleotide diphosphates
NBF	nucleotide-binding fold
Octyl-POE	n-octylpentaoxyethylene ether
PAGE	polyacrylamide-gel electrophoresis
PBFI	potassium-binding benzofuran isophthalate
PKC	protein kinase C
POPE	1-palmitoyl-2-oleyl-*sn*-glycero-3-phosphoethanolamine
POPS	1-palmitoyl-2-oleoyl-*sn*-glycero-3-[phospho-L-serine]
RPM	revolutions per minute
SDS	sodium dodecyl sulfate
SMPs	submitochondrial particles
SUR	sulfonylurea receptor
TEA	tetraethylammonium cation
TES	*N*-tris(hydroxymethyl)methylaminoethenesulfonic acid
TMPD	N,N,N′,N′-tetramethyl-*p*-phenylenediamine
TRIS	tris(hydroxymethyl) aminomethane
UDP	uridine 5′-diphosphate
W_A	Walker A motif
W_B	Walker B motif

ABSTRACT

Physiological and Pharmacological Properties of the ATP-Sensitive Potassium Channel from the Inner Mitochondrial Membrane

Vladimir Yarov-Yarovoy

Supervising Professor: Keith D. Garlid, M.D., dr. techn.

The ATP-sensitive potassium channel from the inner mitochondrial membrane (mitoK_{ATP}) is highly selective for conducting K^+ ions and is inhibited with high affinity by ATP. The primary function of this channel is regulation of mitochondrial matrix volume. Any net K^+ flux across the inner mitochondrial membrane is accompanied by electroneutral flux of anions and osmotically obligated water. Electrophoretic K^+ uptake into the matrix is conducted through mitoK_{ATP} and K^+ leak, while K^+ efflux is mediated by the electroneutral K^+/H^+ antiporter. Net K^+ flux has little effect on matrix K^+ concentration, which is about 180 mM, but does have a significant effect on matrix volume.

The objective of this project was the investigation of the physiological and pharmacological properties of mitoK_{ATP}. Measurements of K^+ flux enabled characterization of the biochemical properties of mitoK_{ATP} through either purified mitoK_{ATP} reconstituted into liposomes or bilayer lipid membranes or mitoK_{ATP} in intact mitochondria using light scattering. Using these models, it was possible to demonstrate that mitoK_{ATP} is activated by guanine nucleotides and K_{ATP} channel openers, such as diazoxide and cromakalim; it is inhibited by long-chain acyl-CoA esters and K_{ATP} channel inhibitors, such as glyburide and 5-hydroxydecanoate. We also demonstrated that the nucleotide regulatory sites on mitoK_{ATP} face the cytosol.

Regulation of mitoK_{ATP} by long-chain acyl-CoA esters, together with matrix volume-dependent regulation of oxidative phosphorylation, β-oxidation of fatty acids, and the fact that mitoK_{ATP} regulates the matrix volume, suggests that mitoK_{ATP} has a role in regulation of oxidative phosphorylation and β-oxidation of fatty acids. Activation of cardiac mitoK_{ATP} by diazoxide and inhibition of this activation by 5-hydroxydecanoate, in addition to the cardioprotective effect of diazoxide, abolishing of this effect by 5-hydroxydecanoate, and the fact that both of these drugs are specific for regulation of mitoK_{ATP} but not the plasma membrane K_{ATP} channel, implies that mitoK_{ATP} has a role in cardioprotection against myocardial ischemia. The studies presented in this work suggest that mitoK_{ATP} is an important regulator of cellular bioenergetics. The opening of mitoK_{ATP} may be required to support cellular demands for increased work in heart, glucogenesis in liver, and thermogenesis in brown adipose tissue.

Chapter 1
INTRODUCTION

1.1 Plasma Membrane K_{ATP} Channels (CellK_{ATP})

Potassium channels in the plasma membrane of many kinds of cells set the resting membrane potential and thereby regulate electrical activity and ion transport of those cells. One class of K^+ channels, ATP-sensitive K^+ channels, is inhibited by micromolar concentrations of cytosolic ATP, thus coupling the metabolic state of the cell to electrical activity in the plasma membrane. K_{ATP} channels were first discovered by Noma (1) in 1983 in the plasma membrane of cardiac muscle, using patch clamp techniques. Later, K_{ATP} channels were found in a variety of tissues, including pancreatic β-cells (2, 3), skeletal muscle (4), smooth muscle (5), and brain (6). The role of these K_{ATP} channels has been associated with diverse cellular functions, such as the shortening of action potential duration and cellular loss of K^+ ions during metabolic inhibition in heart (7, 8), insulin secretion from pancreatic β-cells (7), smooth muscle relaxation (9), regulation of skeletal muscle excitability (7), and neurotransmitter release (7).

1.1.1 Physiological roles of cellK_{ATP}

Opening of cellK_{ATP} hyperpolarizes the plasma membrane of the cell. In pancreatic β-cells, opening of the K_{ATP} channel prevents elevation of the intracellular $[Ca^{2+}]$ through voltage-gated Ca^{2+} channels and therefore inhibits glucose-stimulated insulin secretion (10). Closing of cellK_{ATP} in pancreatic β-cells leads to plasma membrane depolarization and opening of the voltage-gated Ca^{2+} channels. The increased Ca^{2+} influx into the cell and consequent rise in intracellular $[Ca^{2+}]$ triggers exocytosis of insulin granules (11). In heart, elevated K^+ efflux shortens the action

potential duration and decreases influx of Ca^{2+}, leading to reduced contraction, which can cause arrhythmias during ischemia (12, 13). In arterioles, opening of cellK_{ATP} relaxes smooth muscle and lowers blood pressure (14).

1.1.2 Regulation of cellK_{ATP} by intracellular nucleotides

Intracellular ATP (ATP_i) is believed to be the main regulator of cellK_{ATP}. It has two functions: to close the channel and to maintain channel activity in the presence of Mg^{2+} (15–18). The first function of ATP_i is assumed to require the binding of ATP_i to cellK_{ATP} and persists as long as ATP_i is bound to the channel. Under physiological concentrations of ATP_i, there is a very low probability that cellK_{ATP} will be open. Half-maximal inhibition of most types of cellK_{ATP} by ATP_i is achieved in the low micromolar range (7). The second action of ATP_i restores the opening of cellK_{ATP} following a decline in channel activity, an effect referred to as channel "run-down." This action requires the hydrolysis of ATP in the presence of Mg^{2+} and therefore suggests an essential role of protein phosphorylation for maintenance of the channel activity. There is also new evidence that MgATP is able to stimulate K_{ATP} channel activity, but this effect normally is masked by the potent inhibitory effect of the nucleotide (19).

Nucleotide diphosphates (NDP) and GTP also regulate cellK_{ATP} activity. The presence of ADP_i at low micromolar concentrations reduces the inhibitory action of ATP_i on cellK_{ATP} (20–25) and suggests that the ATP/ADP ratio could be important in regulating channel activity in intact cells. The effect of ADP can be mimicked by GTP, GDP and the non-hydrolyzable analogues ADPβS, GDPβS and GTPγS (26). UDP, IDP and CDP have been shown to induce opening of cellK_{ATP} after "run down" (27).

Thus, cellK_{ATP} has distinct sites for ATP, NDP, and phosphorylation. The transduction of information from these sites to the gaiting mechanism is important for channel regulation.

1.1.3 Pharmacological regulation of cellK_{ATP}

A class of drugs called K^+ channel openers (KCOs) reverses the ATP inhibition of K_{ATP} channels. KCOs include diverse chemical compounds, such as levocromakalim, diazoxide, minoxidil, nicorandil, and pinacidil. CellK_{ATP} is considered to mediate the hypotensive and diabetogenic effects of diazoxide (14) and the cardioprotective effects of pinacidil (28), cromakalim and its derivatives (29–32). In different tissues, K_{ATP} channels exhibit considerable variations in response to KCOs (7–9, 33, 34). For example, cardiac cellK_{ATP} is activated by pinacidil but not by diazoxide. Pancreatic β-cell cellK_{ATP} is activated by diazoxide in the 100-μM range and only weakly by pinacidil. Smooth muscle cellK_{ATP} is activated effectively by both of these drugs. Thus, the properties of K_{ATP} channels vary among tissues, leading to the premise that there are receptor subtypes among cellK_{ATP}.

Sulfonylureas, such as glyburide and tolbutamide, are a class of hypoglycemic drugs that have been used for many years in the treatment of non-insulin-dependent diabetes mellitus and also have been found to block K_{ATP} channel activity. Glyburide is the most potent specific K_{ATP} channel blocker in pancreatic β-cells where half-maximal inhibition of the channel is reached in the low nanomolar range (35, 36). Inhibition of the channel by glyburide triggers a cascade of events leading to insulin release (37, 38). Glyburide and tolbutamide can also block K_{ATP} channels in cardiac and smooth muscle cells, but they require higher concentrations than in β-cells (5, 39–45). Glyburide has been found to reverse the cardioprotective effects of KCOs in experimental ischemia and thus is contraindicated in patients susceptible to cardiac ischemia (14, 30, 46). Glyburide also prevents the arrhythmias frequently seen in ischemic hearts (47).

1.1.4 Structure of cellK_{ATP}

CellK_{ATP} is formed by interaction of at least two distinct protein subunits: an inward-rectifying potassium channel (Kir6.1 or Kir6.2) (19, 48), a member of the inward-rectifying K^+ channel family (49), and the sulfonylurea receptor (SUR1 or SUR2A, or SUR2B) (50–52), a member of the ATP-binding cassette transporter

family (53, 54). The Kir6.x subunit serves as a K^+-conducting pore, and SURx is the regulator of cellK_{ATP} activity (50, 51, 55–57).

cDNA encoding Kir6.1 was first isolated from a rat pancreatic islet cDNA library (48). Rat Kir6.1 is a 424-amino acid residue protein (M_r = 47,960) having two transmembrane regions. Subsequently Kir6.2 was isolated by screening a human genomic library with Kir6.1 as a probe, and its mouse homolog was also isolated from an insulin-secreting cell line cDNA library (55). The predicted amino acid sequences showed that Kir6.1 has roughly 70% identity with Kir6.2 and 40–50% identity with other cloned Kir channels (55, 56). The highly conserved motif in the pore region (GYG) found in all other cloned Kir channels with two transmembrane regions was transmuted to GFG in both Kir6.1 and Kir6.2. These findings suggested that Kir6.1 and Kir6.2 belong to the same subfamily of inward-rectifying potassium channels. The truncated isoform of Kir6.2, in which either the last 26 or 36 amino acids had been deleted, when expressed in the absence of SUR, produced a K^+ channel blocked with low affinity by ATP but insensitive to sulfonylureas, diazoxide, and the potentiatory action of MgADP (19, 57).

SUR1 was identified and isolated in pancreatic β-cells as a 140-kD protein (on SDS-PAGE) by photoaffinity labeling using radiolabeled analogs of glyburide (39, 58). A value of 500 fmol of high affinity receptor per mg of membrane protein was estimated (39). Molecular cloning of SUR1 has revealed that the open reading frames of hamster and rat SUR1 cDNAs encode proteins of 1582 amino acids (M_r = 177,000) with 13 transmembrane domains and two nucleotide-binding folds (NBF) (52). Co-expression of SUR1 and Kir6.2 exhibits the characteristic properties of cellK_{ATP} from the pancreatic β-cell (55). Mutations in NBF1 and NBF2 are associated with familial persistent hyperinsulinemic hypoglycemia of infancy (59, 60). Disruption of the Walker A (W_A) or B (W_B) consensus motifs of NBF1 in SUR1 dramatically decreased channel activity and glibenclamide binding to SUR1, suggesting that NBF1 may confer some of the sulfonylurea sensitivity of cellK_{ATP} (50). W_A motifs of NBF1 and NBF2 have been shown to be the sites of Mg-ADP activation of cellK_{ATP} (61). The W_A motif of NBF1 (but not NBF2) was shown to be essential for activation of K_{ATP} channels by diazoxide (61). Recently, isoforms of

SUR1 have been identified that confer different sensitivities to KCOs when coexpressed with Kir6.2. Thus, the SUR2A/Kir6.2 complex is sensitive to pinacidil, but not to diazoxide, and is thought to regulate cellK_{ATP} in cardiac and skeletal muscle (50), whereas the SUR2B/Kir6.2 complex is sensitive to both pinacidil and diazoxide, and is thought to regulate cellK_{ATP} of smooth muscle (51). Thus, SUR is required for the sensitivity of cellK_{ATP} to sulfonylureas and diazoxide, as well as for activation by Mg-ADP (57).

Because SUR1 contains two NBF whereas Kir6.2 has none, it is assumed that inhibition of the channel by ATP requires binding of ATP to SUR (50, 52). Indeed, SUR1 was shown to enhance sensitivity of truncated Kir6.2 to ATP, shifting K_i from $\sim 100\ \mu M$ to $\sim 10\ \mu M$ (57).

Recent studies from several groups have demonstrated that to form an active β-cell K_{ATP} channel, the Kir6.2 and SUR1 subunits must associate with 1:1 stoichiometry (62–64). The data indicate that the K_{ATP} channel pore is lined by four Kir6.2 subunits, each requiring one SUR1 subunit to generate a functional channel in an octameric structure.

1.2 Mitochondrial K_{ATP} Channels (MitoK_{ATP})

ATP-sensitive K^+ channels in the mitochondrial inner membrane were first reported by Inoue et al. in 1991 (65), with electrophysiological evidence from patch clamp studies of fused giant mitoplasts prepared from rat liver mitochondria. At the same time, Garlid's group reported reconstitution of partially purified mitoK_{ATP} from rat liver and beef heart mitochondria (66–68). The basic properties of mitoK_{ATP} include selectivity of K^+ over Na^+ and TEA^+ (68); inhibition with high affinity by ATP (68) or long-chain acyl-CoA esters (69), which both require the presence of divalent cations; activation of the ATP-inhibited channel by GTP, GDP, or KCOs (69, 70, 71); and inhibition by glyburide or 5-hydroxydecanoate (65, 68, 71, 72). Thus, mitoK_{ATP} exhibits physiological and pharmacological properties that are remarkably similar to those of cellK_{ATP}.

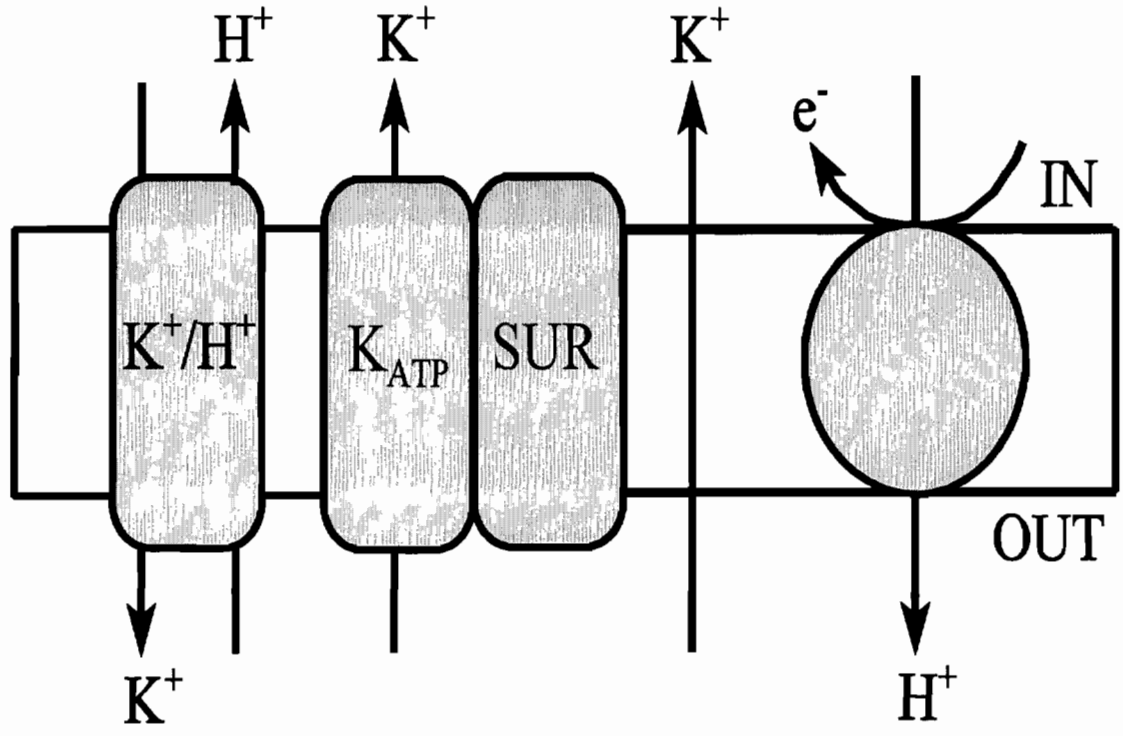

Figure 1.1 The mitochondrial K^+ cycle. Electrogenic H^+ ejection by the respiratory chain drives electrophoretic K^+ uptake into the matrix by parallel K_{ATP} channel and K^+ leak pathways. Matrix K^+ is then released into the intermembrane space in exchange for H^+ via the electroneutral K^+/H^+ antiporter, which is regulated by matrix $[Mg^{2+}]$ and $[H^+]$ and is exquisitely sensitive to changes in the matrix volume.

As the high-energy electrons from the hydrogens on NADH and $FADH_2$ are transported through the respiratory chain in the inner mitochondrial membrane, the energy released as they pass from one carrier molecule to the next is used to pump H^+ ions across the inner mitochondrial membrane from the matrix to the intermembrane space. The electrochemical gradient thus generated drives the synthesis of ATP by ATP synthase, which catalyzes the conversion of ADP and P_i to ATP, thus completing the oxidative phosphorylation process.

Oxidative metabolism in mitochondria is also fueled by fatty acids. β-oxidation of fatty acids begins with the complex enzymatic activation of fatty acids in the cytosol and their transport across the mitochondrial membranes into the mitochondrial matrix. There the fatty acyl group is transferred to intramitochondrial coenzyme A (CoA), to form a fatty acyl-CoA thioester. The fatty acyl-CoA undergoes dehydrogenation and hydrogenation steps, followed by enzymatic cleavage by reaction with a second molecule of CoA to produce acetyl-CoA and a long-chain saturated fatty acyl-CoA with two fewer carbon atoms than the original fatty acid. The latter now becomes the substrate for another round of the above described reactions. The hydrogen atoms from the dehydrogenation of the fatty acid enter the respiratory chain, while acetyl-CoA, the product of the fatty acid oxidation, enters the tricarboxylic acid cycle.

1.2.3 MitoK$_{ATP}$ is an intracellular signaling device involved in the regulation of electron transport and fatty acid oxidation

Substrate oxidation is mediated by changes in mitochondrial matrix volume independently of the means used to change the volume (77, 78). Changes in the matrix volume over the physiological range (1.0–1.5 μl/mg protein) have been shown to stimulate electron transport and β-oxidation of fatty acids in heart, liver, and brown adipose tissue mitochondria (78–81). β-Oxidation of fatty acids is greatly stimulated by an increase in electron transfer between flavoprotein and ubiquinone (79). Changes in the matrix volume secondary to the hormonal regulation of brown adipose tissue (82) and liver (80) have also been observed in the intact cell.

The role of mitoK$_{ATP}$ in cellular bioenergetics has been suggested by a number of authors (75, 83, 84). The fact that both electron transport and fatty acid oxidation are controlled by the matrix volume suggests that mitoK$_{ATP}$ is an important element in their regulation. Thus, opening of mitoK$_{ATP}$ may be necessary to support increased cellular demands for work in heart, gluconeogenesis in liver, and thermogenesis in brown adipose tissue.

1.2.4 Regulation of mitoK$_{ATP}$ by nucleotides and long-chain acyl-CoA esters

K^+ flux through mitoK$_{ATP}$ is inhibited by ATP and ADP with high affinity in both reconstituted and intact mitochondrial systems (68, 69, 85). MitoK$_{ATP}$ is also inhibited by oleoyl-CoA and palmitoyl-CoA in the nanomolar range in both proteoliposomes (68) and intact mitochondria (85). Compared to its effects on other transporters, palmitoyl-CoA is a very potent inhibitor of mitoK$_{ATP}$. For example, its half-maximal value for inhibition of the mitochondrial uncoupling protein is higher by an order of magnitude (86). Inhibition of mitoK$_{ATP}$ by both adenine nucleotides and long-chain acyl-CoA esters exhibits an absolute requirement for divalent cations (68, 69) and is reversed by the addition of a chelator to the assay medium (85). Mg^{2+} alone has no effect on mitoK$_{ATP}$ activity.

The inhibition of mitoK$_{ATP}$ with high affinity by adenine nucleotides or long-chain acyl-CoA esters raises the question of how this channel can be open under physiological conditions. By measuring K^+ flux in liposomes reconstituted with purified mitoK$_{ATP}$, Paucek et al. (69) found that guanine nucleotides are potent activators of this channel. ATP- or ADP-inhibited K^+ flux was completely restored by GTP in the low micromolar range, which is roughly two orders of magnitude less than normal cytosolic [GTP] (69). In the absence of adenine nucleotides, GTP had no effect on mitoK$_{ATP}$ activity. Inhibition of K^+ flux through reconstituted mitoK$_{ATP}$ by palmitoyl-CoA was reversed by GTP in its physiological range (69). The fact that both long-chain acyl-CoA esters and GTP regulate activity of mitoK$_{ATP}$ within their physiological range suggests that the open/closed state of mitoK$_{ATP}$ is principally determined by the cytosolic concentrations of GTP and long-chain acyl-CoA esters.

1.2.5 Cardioprotection against myocardial ischemia

Myocardial ischemia is an imbalance between the myocardial demand for, and the vascular supply of, coronary arterial blood. This creates a deficit of oxygen, substrates, and energy in the tissue, as well as an insufficient capacity for the removal of potentially toxic metabolites such as protons, carbon dioxide, and lactate. Myocardial tissue is normally aerobic and its metabolism is closely dependent on oxygen availability. The contractile process, or more precisely, myosin ATPase activity, represents the major part of myocardial energy requirements and is almost exclusively met by mitochondrial oxidative phosphorylation. Thus, myocardial cells have high sensitivity to oxygen deficiency, and mitochondrial function is likely to play a key role in the molecular events that lead to myocardial ischemia.

Ischemic preconditioning is a series of repetitive brief ischemic episodes, each of which causes cumulative ATP depletion, separated by intermittent reperfusion which washes out ischemic catabolites (87). Following the initial ischemic period, ATP levels are not depleted further by subsequent ischemic challenges. KCOs protect ischemic myocardial tissue and thus mimic ischemic preconditioning (31, 88). These protective effects of KCOs are abolished by K_{ATP} channel blockers such as glyburide and 5-hydroxydecanoate (30, 31, 89). Several studies suggested that opening of cardiac cellK_{ATP} by KCOs protected the ischemic myocardium by shortening the action potential duration (APD) (90). However, more recent studies contradict this hypothesis by demonstrating a lack of correlation between monophasic APD and cardioprotection by KCOs (91, 92). These data suggest the possibility of a site of action of KCOs in cardiac myocytes that is distinct from cellK_{ATP}.

1.2.6 MitoK_{ATP} is a receptor for potassium channel openers and inhibitors

MitoK_{ATP} is an important intracellular pharmacological receptor (70–72, 93, 94). KCOs are very potent activators of ATP-inhibited mitoK_{ATP}. Cromakalim and diazoxide activate mitoK_{ATP} in the low micromolar range (70), while two cromakalim analogues (EMD60480 and EMD57970) activate mitoK_{ATP} in the low nanomolar range (70). Diazoxide is about 2000 times more potent in activation of cardiac mitoK_{ATP}

than in activation of cardiac cellK_{ATP} (70), making it a potentially useful drug for distinguishing between the activities of these two K_{ATP} channels.

K^+ flux through reconstituted mitoK_{ATP} is inhibited by the specific cellK_{ATP} blocker, glyburide, in the nanomolar range (68, 71). However, when studied in intact mitochondria, the presence of ATP, Mg^{2+}, and a pharmacological opener, such as diazoxide or cromakalim or a physiological opener such as GTP, are required to observe inhibition of mitoK_{ATP} by glyburide or 5-hydroxydecanoate (72).

Diazoxide has been shown to protect ischemic/reperfused rat hearts in the low micromolar range, and 5-hydroxydecanoate completely abolished this effect (71). Cardiac mitoK_{ATP}, but not cardiac cellK_{ATP}, is sensitive to both of these drugs (71). Based on these observations, Garlid et al. (71) hypothesized that cardioprotection by KCOs in cardiac myocytes is mediated via mitoK_{ATP}. Measuring the channel activity in intact ventricular myocytes, Liu et al. (93) also demonstrated that diazoxide targets the mitochondrial, but not sarcolemmal, K_{ATP} channel. Recently, Sato et al. (94) provided evidence for modulation of mitoK_{ATP} activity by protein kinase C (PKC) in intact ventricular myocytes. PKC activation has been shown to be a key element in ischemic preconditioning (95–98). Stimulation of mitoK_{ATP} opening by PKC thus provides a specific link between the signal transduction of ischemic preconditioning and the cardioprotective effects of KCOs targeted at mitoK_{ATP}.

1.2.7 Orientation of mitoK_{ATP} in the inner membrane

In order to understand the signaling role of mitoK_{ATP} in cell bioenergetics, it is important to know whether its regulatory sites face the matrix or the cytosol or both. Inoue et al. (65) and Halestrap (83) have suggested that nucleotide regulatory sites of mitoK_{ATP} face the matrix. Studies by Garlid's group (85) of mitoK_{ATP} reconstituted into proteoliposomes and bilayer lipid membranes (BLM) demonstrated that mitoK_{ATP} is unidirectional with respect to nucleotide access. Studies of ATP-dependent K^+ flux in intact mitochondria demonstrated inhibition by external ATP or palmitoyl-CoA and activation of the inhibited flux by external GTP (85). Since there are no transport pathways for GTP or palmitoyl CoA (in the absence of carnitine) in the inner mitochondrial membrane, it was concluded that the nucleotide binding sites of

mitoK_{ATP} face the cytosol (85). Thus, mitoK_{ATP} and cellK_{ATP} appear to be accessible to the same pool of cytosolic regulatory metabolites.

1.2.8 Sulfonylurea receptor of mitoK_{ATP}

Garlid et al. (75, 99) suggested that mitoK_{ATP}, like cellK_{ATP}, consists of an inward-rectifying K^+ channel (mitoKIR) and a regulatory sulfonylurea receptor (mitoSUR). Using BODIPY-FL glyburide to photolabel inner mitochondrial membrane vesicles, Paucek et al. (100, 101) found that only one protein was labeled with high affinity and specificity (labeling was displaced by 1 μM unlabeled glyburide), and that this protein migrated at 63 kD on SDS-PAGE. A value of 90 fmol of 63-kD protein per mg of total mitochondrial protein was estimated based on purification yield (101). Partially purified on DEAE-cellulose column, a fraction containing the 63-kD protein showed properties of mitoK_{ATP} when reconstituted in lipid vesicles (101). Thus, the 63-kD protein was hypothesized to be a regulatory sulfonylurea receptor of mitoK_{ATP} (101).

Recently, by photoaffinity labeling of submitochondrial particles with [^{125}I]-glibenclamide, Szewczyk et al. (102) identified a 28-kD inner mitochondrial membrane protein as a low affinity sulfonylurea receptor (labeling of this protein was displaced by 30 μM unlabeled glyburide); they demonstrated the presence of a single class of low-affinity binding sites for glibenclamide in the inner mitochondrial membrane with an apparent K_D of 360 nM and B_{MAX} of 48 pmol per mg of inner membrane protein. Future studies should clarify the nature and physiological role of this low-affinity sulfonylurea-binding protein.

1.2.9 K^+ channel pore subunit of mitoK_{ATP}

Several laboratories have attempted to identify a specific K^+ conducting pore subunit of mitoK_{ATP}. Paucek et al. (68) demonstrated mitoK_{ATP} activity in liposomes reconstituted with a partially purified fraction from rat liver and beef heart mitochondria containing a major protein band at 54 kD. Mironova et al. (103) partially purified and reconstituted an ATP-dependent K^+ channel in the bilayer lipid membrane from rat liver mitochondria and identified its activity with a 55-kD protein.

Suzuki et al. (104) detected a single band at 51 kD when an antibody to a C-terminal epitope of Kir6.1 was used to label the inner membrane of mitochondria from rat skeletal muscle and liver by immunogold chemistry. Further studies should be conducted to identify, sequence, and express the putative K^+ conducting pore subunit of mitoK_{ATP}.

Chapter 2

INHIBITION OF THE MITOCHONDRIAL K_{ATP} CHANNEL BY LONG-CHAIN ACYL-CoA ESTERS AND ACTIVATION BY GUANINE NUCLEOTIDES*

The mitochondrial K_{ATP} channel (mitoK_{ATP}) is inhibited with high affinity by ATP and ADP, and this inhibition exhibits an absolute requirement for divalent cations (68). We have shown that ATP inhibition of K^+ flux through mitoK_{ATP} is reversed by submicromolar levels of K^+ channel openers (70). These studies left us with a conundrum: given the high affinity for ATP, how can mitoK_{ATP} ever be opened under normal physiological conditions? We hypothesized (68) that endogenous activators of mitoK_{ATP} must exist to overcome the high affinity for ATP, and this study presents support for this hypothesis. K^+ flux through the MgATP-inhibited channel is restored to full activity by GTP and GDP, neither of which has any effect in the absence of MgATP. GTP and GDP are competitive with ATP, and their reversal of ATP inhibition exhibits hyperlinear kinetics consistent with two guanine nucleotide binding sites. We also report that palmitoyl-CoA and oleoyl-CoA inhibit mitoK_{ATP} with high potency, and this inhibition is also reversed by GTP and by the potassium channel openers, cromakalim and diazoxide. Inhibition by long-chain acyl-CoA esters, like inhibition by ATP, exhibits an absolute requirement for Mg^{2+} ions and is immediately reversed upon chelation of Mg^{2+}. From these findings, we infer that GTP and long-chain acyl-CoA esters may be the physiological regulators of mitoK_{ATP} and that this channel may play a role *in vivo* in regulating fatty acid oxidation.

---

* This material has been published in this or similar form in *The Journal of Biological Chemistry* and is used here with permission of the American Society for Biochemistry and Molecular Biology.

Paucek, P., Yarov-Yarovoy, V., Xun, S., and Garlid, K. D. (1996) Inhibition of the mitochondrial K_{ATP} channel by long chain acyl-CoA esters and activation by guanine nucleotides. *J. Biol. Chem.* **271**, 32084–32088.

2.1 Materials and Methods

2.1.1 Isolation of rat liver mitochondria

Mitochondria were isolated using a modification of protocol described by Beavis et al. (105). Male Sprague-Dawley rats were starved overnight and killed by decapitation. The livers were immediately excised, placed in ice cold isolation medium containing 220 mM D-mannitol, 70 mM sucrose, 5 mM K-EGTA, 5 mM K-TES 6.8 and 0.5 mg BSA/ml, and cut in small pieces by sharp scissors. The following steps were carried at 0–4°C. The liver pieces were rinsed three times in the isolation medium, homogenized with 4 strokes of a motorized glass-Teflon homogenizer at 600 RPM. The homogenate was centrifuged at 1,900 RPM (520 × *g*) in the SA-600 rotor of a Sorvall RC2B centrifuge for 10 min. The resulting supernatant was passed through cheese-cloth and saved, and the pellet was resuspended in the isolation medium by glass tube filled with ice and centrifuged at 1,900 RPM (520 × *g*) for 10 min. The resulting supernatant was combined with saved supernatant after the first spin and they were centrifuged at 7,500 RPM (8,130 × *g*) for 10 min. For subsequent steps the isolation medium contained 0.5 mM K-EGTA. The resulting pellet was resuspended in the isolation medium and centrifuged at 6,200 RPM (5,560 × *g*) for 10 min. The resulting pellet was resuspended and centrifuged at 2,700 RPM (1,050 × *g*) for 3 min to remove contaminating red cells and nuclei and then centrifuged at 6,200 RPM (5,560 × *g*) for 10 min to collect the mitochondria. After final wash and centrifugation at 10,600 RPM (16,250 × *g*) for 15 min, the mitochondria were resuspended to 100 mg protein/ml in 220 mM D-mannitol, 70 mM sucrose and 5 mM K-TES, pH 6.8 and stored at -70°C for subsequent preparation of submitochondrial particles.

2.1.2 Preparation of submitochondrial particles

Submitochondrial particles (SMPs) were prepared using a modification of protocol described by Brierly et al. (106). The frozen mitochondria were thawed and diluted to final concentration of 10 mg protein/ml with SMP preparation medium containing 220 mM D-mannitol, 70 mM sucrose, 0.5 mg/ml BSA, and 20 mM K-

HEPES, pH 7.4. The mitochondrial suspension was sonicated in 30 ml Corex tubes (10 ml of suspension per tube) for 20 s at 25 W at 0–4°C using a Branson 250 sonifier and then cooled on ice. After eight sonication-cooling cycles, the suspension was centrifuged at 10,800 RPM (16,870 × *g*) in the SA-600 rotor of a Sorvall RC2B centrifuge for 15 min at 4°C, and the resulting supernatant was centrifuged at 35,000 RPM (86,980 × *g*) in the Type 60 Ti rotor of a Beckman L8-80M ultracentrifuge for 35 min at 4°C. The resulting pellet was resuspended in SMP preparation medium at a protein concentration of 50 mg/ml and stored at -70°C until ready to use.

2.1.3 Preparation of guanidine-treated inner mitochondrial membrane vesicles

Preparation of guanidine-treated inner mitochondrial membrane vesicles (3xGMs) generally followed the procedure described by McEnery et al. (107). The frozen SMPs were thawed and diluted to a protein concentration of 2 mg/ml in *PA buffer* containing 150 mM potassium phosphate, 1 mM ATP, 25 mM EDTA, 0.5 mM dithiothreitol, 5% ethylene glycol, pH 7.9, and centrifuged at 50,000 RPM (177,520 × *g*) in the Type 60 Ti rotor of a Beckman L8-80M ultracentrifuge for 45 min at 4°C. The resulting pellet was resuspended in *PA buffer* and centrifuged as described before, and this washing step was repeated one more time. The final membrane pellet was suspended to 15 mg/ml in *PA buffer* and stored at -70° C until needed. Prior to use, the vesicles were incubated in *PA buffer* containing 3 M guanidine-HCl to remove F_1-ATPase and bound chaperonins. Guanidine-treated vesicles were then washed three times in *PA buffer* by centrifugation at 50,000 RPM (177,520 × *g*) for 30 min at 4°C and final pellet was resuspended in 250 mM sucrose, 50 mM Tris-HCl, pH 7.2, and 1 mM TEA-EDTA and stored at -70°C until ready to use.

2.1.4 Estimation of protein concentration

Protein concentrations in mitochondria, SMPs, or 3xGMs were estimated using a modification of the Biuret method described by Layne (108). To 80 μl of a protein sample containing 20–100 mg of protein/ml was added 20 μl of 10% Triton X-100

and the suspension was vortexed. Then 1.6 ml of 150 mM TEA-acetate, pH 7.0, was added to the protein–detergent mixture and the suspension was vortexed again. Five dilutions of a protein standard (BSA) containing from 1 to 5 mg/ml protein were prepared in the same buffer as the sample for protein measurement. Blank standard was also prepared and did not contain protein. 500-μl aliquots of standards and the protein sample were pipetted into clean, dry test tubes. 2 ml of Total Protein Reagent (Sigma Diagnostics) were added into each tube, and each tube was vortexed. After boiling at 100°C for 1 min, samples were cooled to room temperature and absorbance of each sample was measured at 543 nm. The protein sample concentration was obtained by reference to a calibration curve established with protein standards.

Protein concentrations in purified fractions were measured by the Amido Black method (109).

2.1.5 Extraction and purification of mitoK$_{ATP}$

3xGMs were solubilized at 2 mg of protein/ml in 3% Triton X-100, 20% glycerol, 0.1% β-mercaptoethanol, 0.2 mM EGTA, 1 mM $MgCl_2$, and 50 mM Tris-HCl, pH 7.2. After incubation on ice for 20 min, the mixture was centrifuged at 44,000 RPM (124,240 $\times$ *g*) in the Type 65 rotor of a Beckman L8-80M ultracentrifuge for 35 min at 4°C. Supernatant (10 ml), typically containing 50–80 mg of extracted proteins, was loaded onto a DEAE-cellulose column (10-ml bed volume) that had been equilibrated with a column buffer containing 1% Triton X-100, 0.1% β-mercaptoethanol, 1 mM EDTA, and 50 mM Tris-HCl, pH 7.2. The column was washed sequentially with 2 bed volumes each of the column buffer containing 50, 100, 150, 200, 250, and 300 mM KCl. The fraction eluted at 250 mM KCl was desalted and concentrated by filtration and contained mitoK$_{ATP}$ activity (68).

2.1.6 Reconstitution of mitoK$_{ATP}$ into liposomes

The purified mitoK$_{ATP}$ fraction was added to a 10:1 mixture of L-α-lecithin (Avanti) and cardiolipin in 10% octylpentaoxyethylene. The buffer composition at this stage defines the *internal medium*, which contained 300 μM PBFI, 100 mM TEA-SO_4, 0.14 mM KCl, 1 mM TEA-EDTA, and 25 mM TEA-HEPES, pH 6.8. This

mixture was loaded onto a 2-ml Bio-Beads SM-2 column (Bio-Rad) to remove detergent and form proteoliposomes. After incubation for 90 min at 0–4°C, the column was centrifuged at 2,000 RPM (810 × *g*) for 2 min in a Sorvall GLC-2B centrifuge to collect the proteoliposomes. To remove extravesicular PBFI, 200-μl aliquots of the proteoliposome suspension were passed twice through 4-ml Sephadex G-25-300 columns by centrifugation at 2,000 RPM (810 × *g*) for 2 min. The final stock vesicle suspension (nominally 50 mg lipid/ml) was stored on ice during the experiment. Protein content, measured by the Amido Black method (109), was normally 10 ng of protein per mg of lipid. Intraliposomal volume of each preparation was estimated from the volume of distribution of PBFI and was normally found to be 1 μl per mg of starting lipid.

2.1.7 Assay of K^+ flux through reconstituted mitoK_{ATP}

Stock vesicles (15 μl) were added to 1.985 ml of *external medium* containing 150 mM KCl, 1 mM TEA-EDTA, and 25 mM TEA-HEPES, pH 7.4. Electrophoretic K^+ flux was initiated by 1 μM FCCP to provide charge compensation via H^+ flux. K^+ flux was quantitated from the fluorescence of intraliposomal PBFI, which increases with increasing $[K^+]_{in}$. Fluorescence was followed with an SLM/Aminco 8000C spectrofluorometer (SLM, Urbana, IL) with excitation set at 344 nm (bandpass 8 nm) and emission set at 485 nm (bandpass 8 nm). The K^+ response of intravesicular PBFI was calibrated by stepwise additions of KCl to proteoliposomes in internal medium in the presence of 0.5 μM nigericin and 5 μM tributyltin chloride (110).

2.1.8 Materials

Tris salts of adenine and guanine nucleotides were titrated to pH 7.2 with Tris base. PBFI was from Molecular Probes Inc. (Eugene, OR). All other chemicals were obtained from Sigma Chemical (St. Louis, MO) unless otherwise indicated.

2.2 Results

2.2.1 Activation of the ATP-inhibited K_{ATP} channel by GTP and GDP

The results in Fig. 2.1 demonstrate activation of ATP- and ADP-sensitive K^+ flux by GTP and GDP. The following observations can be made from these data:

(i) K^+ flux was completely restored by both GTP and GDP.

(ii) GTP was 20–30 times more potent than GDP, irrespective of whether ATP or ADP was used to inhibit K^+ flux.

In 0.5 mM ATP, the $K_{1/2}$ values for GTP and GDP activation were 6.9 μM and 143 μM, respectively. In 0.5 mM ADP, the $K_{1/2}$ values for GTP and GDP activation were 0.12 μM and 3.4 μM, respectively.

Additional experiments (not shown) further characterize guanine nucleotide reversal of ATP inhibition of K^+ flux through mitoK_{ATP}:

(i) Guanine nucleotides had no effect on K^+ flux through the open channel, measured in the absence of MgATP.

(ii) Activation required that guanine nucleotides be added to the same side as MgATP. Thus, external GTP had no effect on K^+ flux when it was inhibited by internal MgATP.

(iii) GTP or GDP activated K^+ flux when added 30 s after inhibition by MgATP had already been established.

2.2.2 Kinetics of guanine nucleotide activation of the K_{ATP} channel

To examine the kinetics of activation, we measured ATP inhibition of K^+ flux in the presence of 3 mM Mg^{2+} and different concentrations of GTP or GDP. Fig. 2.2 contains representative dose–response curves.

In the *absence* of GTP, ATP inhibited K^+ flux through reconstituted mitoK_{ATP} with a $K_{1/2}$ of 21 μM in this experiment (•, Fig. 2.2). We observed $K_{1/2}$ values for ATP ranging between 20 and 30 μM in four independent experiments, and the Hill coefficient was always 1.0 $\pm$ 0.1. These $K_{1/2}$ values are lower than our previously reported value of 39 μM (68) because they are calculated from ATP-sensitive, rather than total, K^+ flux. We have recently established that 10–15% of channels are

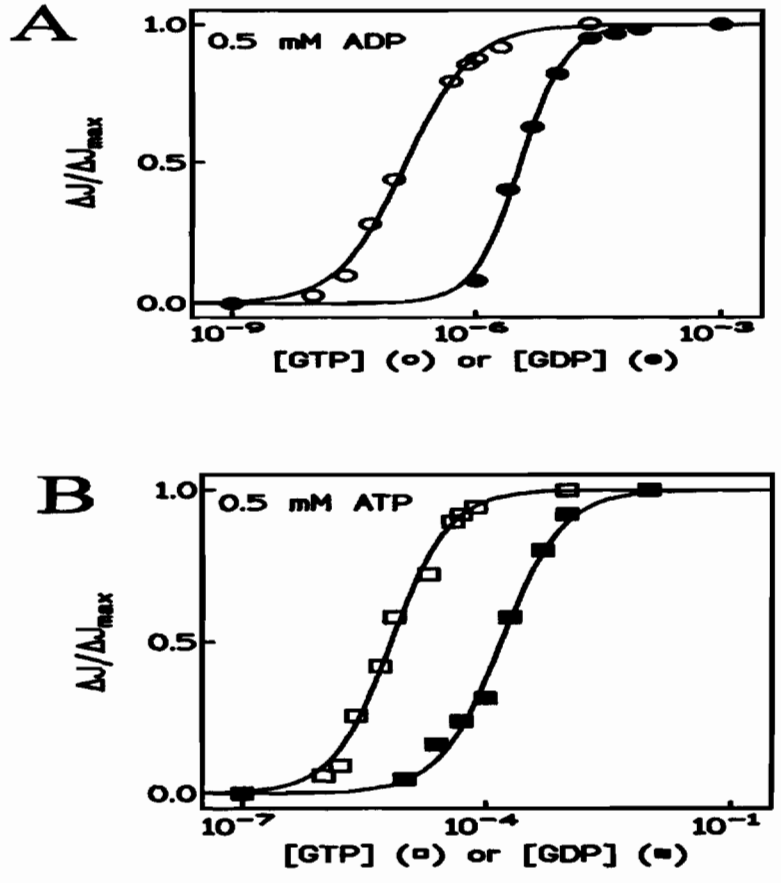

Figure 2.1 Activation of ATP- and ADP-inhibited mitoK$_{ATP}$ by GTP and GDP. The relative ATP-sensitive K^+ uptake into liposomes reconstituted with mitoK$_{ATP}$, $\Delta J/\Delta J_{max}$, is plotted versus concentration of GTP or GDP. All assay media contained 3 mM Mg^{2+}, and K^+ influx was initiated by adding 1 μM FCCP to assay medium at 10 s. Nucleotides were added to assay medium.

Panel A: Activation of ADP-inhibited K^+ flux. GTP or GDP was added to assay medium containing 0.5 mM ADP. ΔJ_{max} is the difference between control fluxes in the absence or presence of 0.5 mM ADP, which inhibited *total* K^+ flux by 65% (68). ΔJ is the difference between fluxes in the presence or absence of guanine nucleotide measured in the presence of 0.5 mM ADP. The $K_{1/2}$ values and Hill slopes (in parentheses) for activation were 0.12 μM (1.0) for GTP and 1.55 μM (1.6) for GDP.

Panel B: Activation of ATP-inhibited K^+ flux. GTP or GDP was added to assay medium containing 0.5 mM ATP. ΔJ_{max} is the difference between control fluxes in the absence or presence of 0.5 mM ATP, which inhibited *total* K^+ flux by 85–90% (4). ΔJ is the difference between fluxes in the presence or absence of guanine nucleotide with both fluxes measured in the presence of 0.5 mM ATP. The $K_{1/2}$ values and Hill slopes (in parentheses) for activation were 6.9 μM (1.2) for GTP and 140 μM (1.2) for GDP.

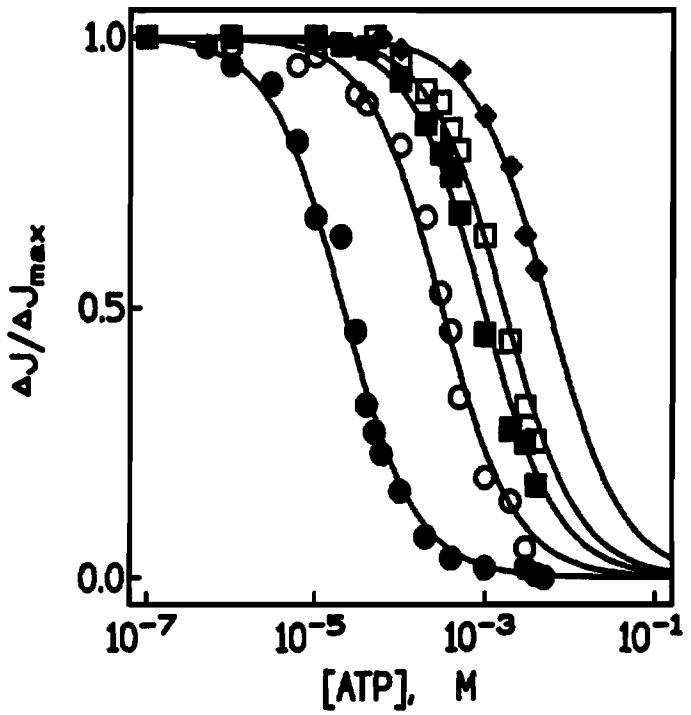

Figure 2.2 Effect of GTP on the kinetics of ATP inhibition of mitoK$_{ATP}$. Figure contains dose–response curves for ATP inhibition of K^+ flux through reconstituted mitoK$_{ATP}$. ATP titrations were done in the presence of GTP added to assay medium in concentrations of 0 μM (●), 2 μM (○), 4 μM (■), 8 μM (□), and 20 μM (◆). ΔJ_{max} is the difference between control fluxes in the absence or presence of 0.5 mM ATP measured in the absence of GTP. ΔJ is the difference between fluxes in the presence or absence of GTP measured in the presence of 0.5 mM ATP (90% inhibition of *total* K^+ flux). In four separate experiments carried out in the *absence* of GTP, $K_{1/2}$ values for ATP inhibition ranged between 20 and 30 μM, and the Hill slope was 1.0 $\pm$ 0.1.

reconstituted with their regulatory sites facing inward and are, therefore, inaccessible to external ATP (99, 111).

In the *presence* of increasing doses of GTP, the $K_{1/2}$ value for ATP inhibition was shifted sharply higher (see Fig. 2.2). It is striking that 20 μM GTP increased the $K_{1/2}$ for ATP inhibition from 21 μM to 6 mM. ATP was ineffective in the presence of 3 mM GTP (not shown).

Fig. 2.3 contains a summary of the results of five experiments in which the $K_{1/2}$ for ATP inhibition of mitoK$_{ATP}$ was measured at various concentrations of GTP (•) or GDP (○). These data show that the apparent affinity of mitoK$_{ATP}$ for ATP decreases ($K_{1/2}$ increases) in a quadratic manner with guanine nucleotides. In order to extract parameters from the data in Fig. 2.3, we constructed a simple model for nucleotide interaction with the mitoK$_{ATP}$ receptor, R:

$$\mathrm{ATP \cdot R} \overset{K_i}{\rightleftharpoons} \mathrm{R} \overset{k_1}{\rightleftharpoons} \mathrm{GTP \cdot R} \overset{k_2}{\rightleftharpoons} \mathrm{GTP_2 \cdot R}$$

This model is consistent with available data. For example, if ATP binds to a second binding site, its affinity is too low to be detected. Solving the kinetic equations for $K_{1/2}$(ATP),

$$K_{1/2}/K_i = 1 + [G]/k_1 + [G]^2/k_1k_2$$

where [G] refers to GTP or GDP concentrations. The data were fit to this equation (solid lines in Fig. 2.3), using K_i(ATP) $\approx$ 21 μM. The derived dissociation constants for GTP were $k_1 \approx 0.18$ μM and $k_2 \approx 14$ μM. For GDP, the values were $k_1 \approx$ 21 μM and $k_2 \approx 25$ μM. A simple qualitative interpretation of these results is that GTP reacts at a high-affinity and a low-affinity site, whereas GDP reacts with two low-affinity sites. The low-affinity sites appear to have similar affinities for ATP, GTP, and GDP.

2.2.3 Inhibition of the K_{ATP} channel by long-chain acyl-CoA esters

Fig. 2.4 contains the results of experiments on the effects of oleoyl-CoA and palmitoyl-CoA on K^+ flux through reconstituted mitoK$_{ATP}$. Long-chain acyl-CoA esters are known to inhibit other ATP-binding transport proteins in mitochondria (112), and they are potent inhibitors of K^+ flux through mitoK$_{ATP}$. Oleoyl-CoA

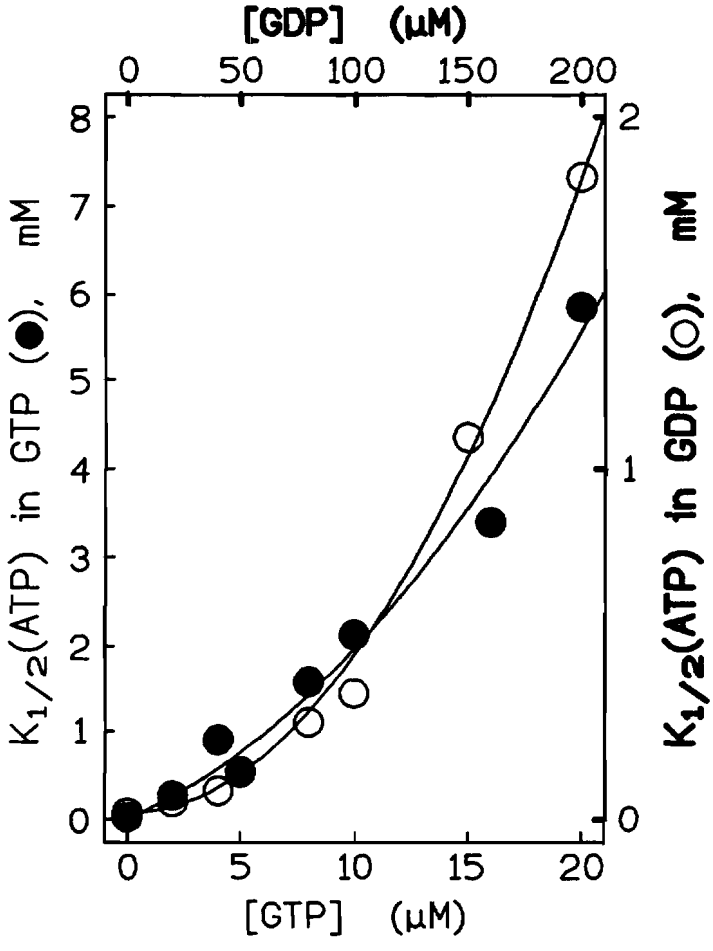

Figure 2.3 Quadratic competitive opening of the ATP-inhibited mitoK_{ATP} by GTP and GDP. Observed $K_{1/2}$ values for ATP inhibition of K^+ flux through the reconstituted mitoK_{ATP} channel are plotted versus [GTP] (●) and [GDP] (○). The $K_{1/2}$ values were obtained from nonlinear regression of dose–response curves ($\Delta J/\Delta J_{max}$ versus log[ATP]) for ATP inhibition in the presence of indicated concentrations of GTP or GDP. The data plotted were from three separate experiments, each with GTP and GDP. The solid lines were fitted to the second-order polynomial, $K_{1/2}/K_I = 1 + [G]/k_1 + [G]/k_1k_2$, as described in Section 2.2.

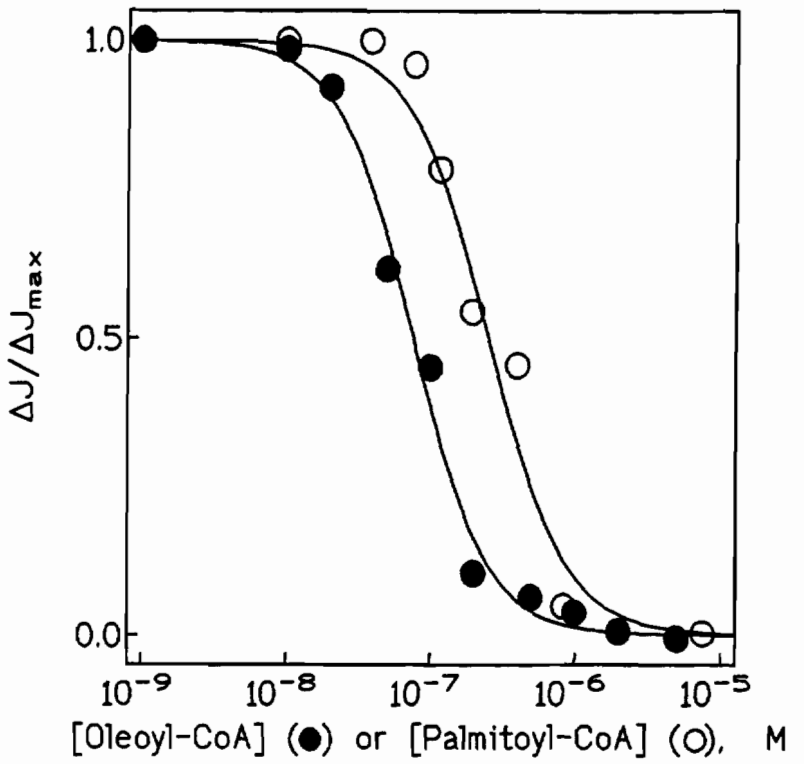

Figure 2.4 Oleoyl-CoA and palmitoyl-CoA inhibit K^+ flux through mitoK_{ATP}. The relative ATP-sensitive K^+ uptake, $\Delta J/\Delta J_{max}$, into liposomes reconstituted with mitoK_{ATP} is plotted versus concentrations of oleoyl-CoA and palmitoyl-CoA. ΔJ_{max} is the difference between control fluxes in the absence or presence of 0.5 mM ATP, which inhibited *total* K^+ flux by 90%. ΔJ is the difference between fluxes in the presence or absence of acyl-CoA ester measured in the absence of ATP. $K_{1/2}$ values for oleoyl-CoA and palmitoyl-CoA inhibition were 260 and 80 nM, respectively (averages of three independent experiments). Assay medium contained 3 mM Mg^{2+}. Oleoyl-CoA and palmitoyl-CoA had no effect on K^+ flux in the absence of Mg^{2+}.

inhibited with $K_{1/2} \approx 80$ nM and Hill coefficient of 1.7. Palmitoyl-CoA inhibited with $K_{1/2} \approx 260$ nM and Hill coefficient of 2. These experiments were carried out in the presence of 3 mM Mg^{2+}. Strikingly, acyl-CoA esters had no effect on K^+ flux in the absence of Mg^{2+} (0.5 mM EDTA) (not shown).

2.2.4 Activation of the palmitoyl-CoA-inhibited K_{ATP} channel by GTP and K^+ channel openers

Fig. 2.5A contains fluorescence traces from experiments designed to determine whether palmitoyl-CoA inhibition of K^+ flux is reversed by K^+ channel openers. Control flux (*trace a*) was inhibited by 1 μM palmitoyl-CoA (*trace b*), and this inhibition was prevented in the presence of 10 μM diazoxide (*trace c*) or 20 μM cromakalim (*trace d*). Fig. 2.5B contains fluorescence traces from experiments designed to determine whether palmitoyl CoA inhibition of K^+ flux is reversed by GTP. Control flux (*trace a*) was inhibited by 1 μM palmitoyl-CoA (*trace b*), and this inhibition was prevented by the inclusion of 1 mM GTP in the assay medium (trace c). GTP and K^+ channel openers also activated K^+ flux when added after flux was inhibited by palmitoyl-CoA (not shown).

The dose–response curves in Fig. 2.6 demonstrate GTP for activation of K^+ flux inhibited by ATP (•), palmitoyl CoA (○), or a combination of ATP and palmitoyl CoA (▲). In these experiments, the $K_{1/2}$ values were 4 μM (in 0.5 mM ATP), 232 μM (in 1 μM palmitoyl-CoA), and 283 μM (ATP plus palmitoyl-CoA). The two important features of these results are that palmitoyl-CoA moved the $K_{1/2}$ for GTP activation toward the physiological range of GTP concentration and that ATP had no effect on the $K_{1/2}$ for GTP in the presence of palmitoyl-CoA.

2.3 Discussion

2.3.1 Regulation of the mitochondrial K_{ATP} channel

The purpose of these experiments was to explore regulation of mitoK_{ATP} by physiological ligands. MitoK_{ATP} is inhibited by ATP, ADP (68), and long-chain acyl-

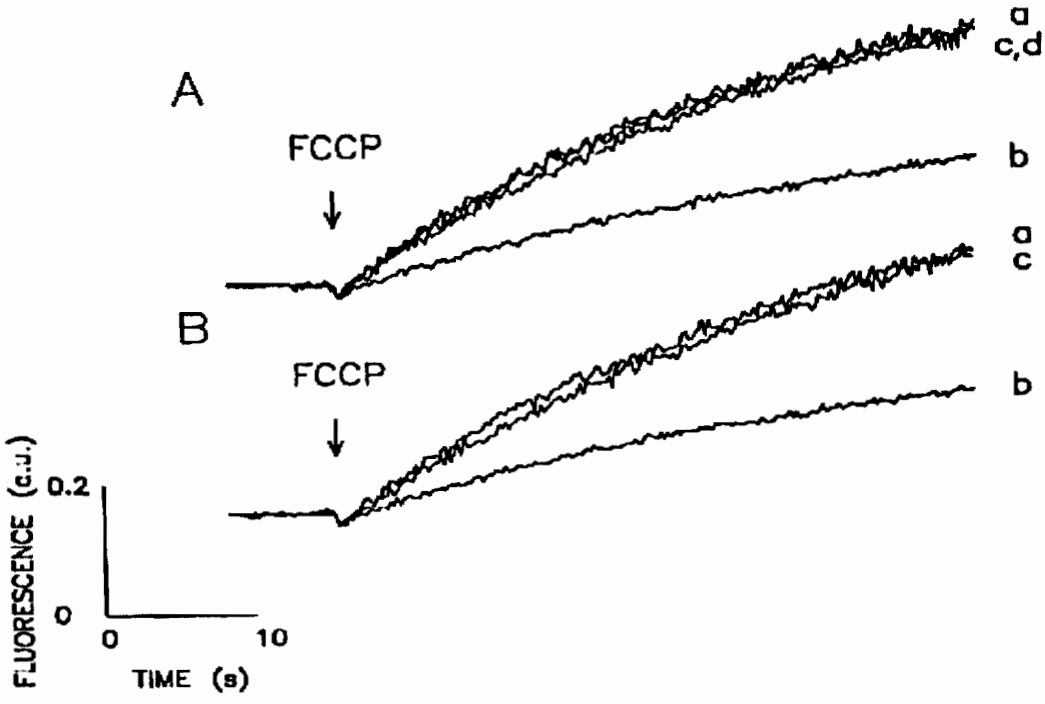

Figure 2.5 Activation of the palmitoyl-CoA-inhibited mitoK$_{ATP}$ by GTP, cromakalim and diazoxide. Shown are PBFI fluorescence traces from proteoliposomes reconstituted with purified mitoK$_{ATP}$. Increasing fluorescence reflects increasing intraliposomal [K^+] due to K^+ transport. Electrophoretic K^+ influx was initiated by adding 1 μM FCCP to KCl assay medium at 10 s. (**A**) Reversal of palmitoyl-CoA inhibition by cromakalim and diazoxide. *Trace a*, assay medium contained 1 mM Mg^{2+} and no palmitoyl CoA; *trace b*, assay medium contained 1 mM Mg^{2+} and 1 μM palmitoyl-CoA; *traces c, d,* assay medium contained Mg^{2+} and palmitoyl-CoA as in trace b, and 20 μM cromakalim *(c)* or 10 μM diazoxide *(d)*. (**B**) Reversal of palmitoyl-CoA inhibition by GTP. *Trace a*, assay medium contained 1 mM Mg^{2+} and no palmitoyl-CoA; *trace b*, assay medium contained 1 mM Mg^{2+} and 1 μM palmitoyl-CoA; *trace c*, assay medium contained Mg^{2+} and palmitoyl-CoA as in trace b, and 1 mM GTP.

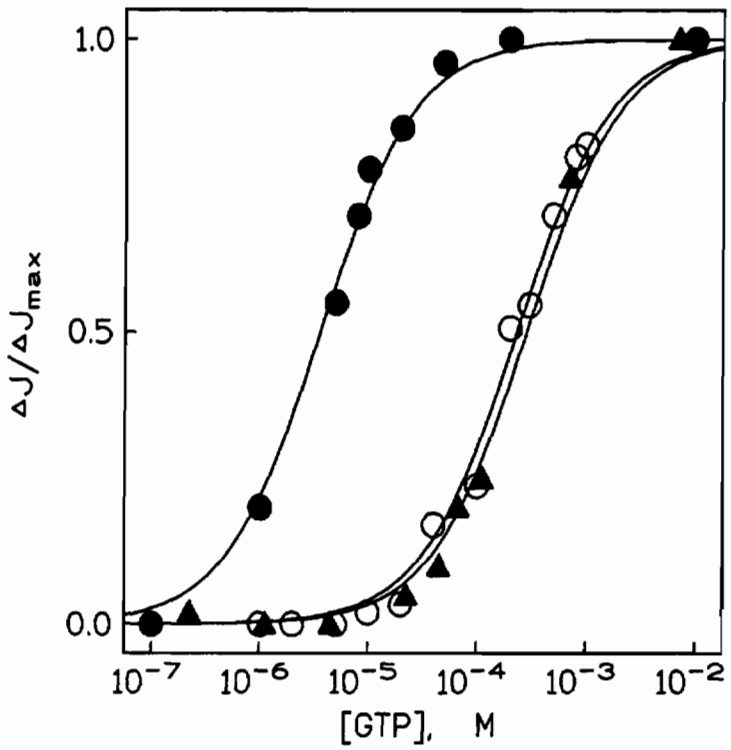

Figure 2.6 GTP activation of K^+ flux in the presence of ATP and/or palmitoyl-CoA. The relative ATP- or palmitoyl-CoA-sensitive K^+ uptake, $\Delta J/\Delta J_{max}$, into liposomes reconstituted with mitoK_{ATP} is plotted versus concentration of GTP. Assay medium contained 1 mM Mg^{2+} and either 0.5 mM ATP or 1 μM palmitoyl-CoA. The channel's open state, ΔJ_{max}, was obtained as the difference between control fluxes in the absence or presence of inhibitors. ΔJ is the difference between fluxes in the presence or absence of GTP. The $K_{1/2}$ values for GTP activation were 4 μM (●) in ATP, 232 μM (○) in palmitoyl-CoA, and 283 μM (▲) in 0.5 mM ATP and 1 μM palmitoyl-CoA.

CoA esters. Inhibition of mitoK$_{ATP}$ by long-chain acyl-CoA esters with high affinity is consistent with a proposed signaling role of this channel in regulating β-oxidation of fatty acids (75). Inhibition by these ligands exhibits an absolute requirement for Mg^{2+} ions, and Mg^{2+} reduces the apparent affinity for glibenclamide in inhibiting K^+ flux through mitoK$_{ATP}$ (68). These findings suggest that Mg^{2+} interacts separately with the mitoK$_{ATP}$ complex, because acyl-CoA esters and glibenclamide are not Mg^{2+} chelators. It is noteworthy that ADP and acyl-CoA esters, which are chemical analogues, exert opposite effects on K$_{ATP}$ channels from mitochondria and plasma membranes. They inhibit mitoK$_{ATP}$ (68, this chapter), but they activate the plasma membrane K$_{ATP}$ channels of pancreatic β-cells (113).

Inhibition by adenine nucleotides or acyl-CoA esters can be fully overcome by GTP and GDP, and by the pharmacological agents known as K^+ channel openers (70, this chapter). Guanine nucleotide activation is competitive with ATP, with kinetics indicating two nucleotide binding sites. The effects on the $K_{1/2}$ for ATP inhibition (Fig. 2.3) suggest both high-affinity and low-affinity GTP sites.

It is characteristic of all K$_{ATP}$ channels that the $K_{1/2}$ values for ATP inhibition are roughly two orders of magnitude lower than normal cytosolic [ATP]. We now show that the $K_{1/2}$ values for GTP reversal of ATP inhibition of mitoK$_{ATP}$ are two orders of magnitude less than normal cytosolic [GTP]. These results can, however, be rationalized by the simple consideration that the nucleotide binding sites will be occupied *in situ* by high-affinity ligands other than ATP. The data suggest that ATP cannot inhibit mitoK$_{ATP}$ in the presence of physiological [GTP], raising the possibility that ATP is *not* a physiological regulator of mitoK$_{ATP}$. On the other hand, when long-chain acyl-CoA esters and GTP are present together, as in the experiments of Fig. 2.6, their $K_{1/2}$ values fall within their respective physiological ranges. We infer from our results that the nucleotide binding sites on mitoK$_{ATP}$ are fully occupied by GTP or long-chain acyl-CoA esters under physiological conditions, and that the fraction of open channels is determined by the balance between these regulators.

2.3.2 Mitochondrial volume is controlled by the potassium cycle

The mitochondrial K^+ cycle consists of electrophoretic K^+ uptake and electroneutral K^+ efflux across the inner membrane. Any *net* K^+ flux will be accompanied by electroneutral flux of anions and osmotically obligated water (73). Because matrix [K^+] is about 180 mM, net K^+ transport will have little effect on the matrix *concentration* of K^+, but it will have a profound effect on matrix volume. Thus, the redox energy consumed by the K^+ cycle is the cost of regulating matrix volume (73). The K^+ cycle is mediated by two highly regulated processes. Efflux is mediated by the K^+/H^+ antiporter, whose existence was predicted by Mitchell (76) and first demonstrated by Garlid (114) nearly 20 years later. Influx is mediated by the mitochondrial K_{ATP} channel (mitoK_{ATP}), which was described by Inoue et al. (65) and Paucek et al. (68).

A primary role of regulated K^+/H^+ antiport is to compensate for unregulated K^+ leak into the matrix, driven by the high voltages required for oxidative phosphorylation. *Uncompensated* K^+ uptake amounting to as little as 10% of proton pumping would double matrix volume within 1–2 minutes (115). The K^+/H^+ antiporter is inhibited by matrix Mg^{2+} ($K_i \approx 300\ \mu M$) as well as by matrix protons, and the concentrations of these inhibitors decrease with uptake of K^+ salts, causing compensatory activation of K^+ efflux (73). Thus, the K^+/H^+ antiporter is responsible for *volume homeostasis* and is essential for maintaining vesicular integrity in the face of high ionic traffic across the inner membrane.

The discovery of mitoK_{ATP} has profound new implications for mitochondrial physiology, because the existence of a regulated K^+ influx pathway permits *volume regulation*. For example, opening of mitoK_{ATP} will transiently shift the balance between K^+ uniport and K^+/H^+ antiport until the antiport catches up with the higher rate of K^+ influx. This will cause transient swelling to a higher steady-state volume that will persist for as long as mitoK_{ATP} remains open. Such a "regulated interplay" between K^+ uniport and K^+/H^+ antiport was correctly postulated many years ago by Brierley (116).

2.3.3 Matrix volume regulates electron transport

Fatty acids are the fuel for thermogenesis by brown adipose tissue mitochondria, and their rate of oxidation is strictly controlled by matrix volume (78). A thorough characterization of this phenomenon by Halestrap (80) has demonstrated that increasing matrix volume, over the narrow range thought to obtain *in vivo*, greatly stimulates activity of the respiratory chain in both heart and liver mitochondria. β-oxidation of fatty acids is particularly sensitive to matrix volume. The site of activation has been localized to membrane enzymes that feed electrons to ubiquinone. The molecular mechanism is not known, but may involve a stretch receptor. Matrix volume changes have been observed *in vivo* during respiratory stimulation secondary to hormonal activation of liver (80) and brown adipose tissue (82).

A role for mitoK_{ATP} in regulating cellular bioenergetics has been suggested by Halestrap (83), Szewczyk et al. (84), and Garlid (75), and the exquisite sensitivity of mitoK_{ATP} to long-chain acyl-CoA esters dovetails nicely with this hypothesis. A plausible scenario is that mitoK_{ATP} will open in the glucose-depleted state, where long-chain acyl-CoA esters are low. The resulting matrix expansion will activate β-oxidation and direct energy to support gluconeogenesis in liver, increased mechanical work in heart and skeletal muscle, and thermogenesis in brown adipose tissue. Conversely, elevated long-chain acyl-CoA esters in the fed state may inhibit mitoK_{ATP}, and, together with inhibition of CPT-1 (117), promote diversion of energy to fatty acid esterification in hepatocytes, adipocytes, and pancreatic β-cells, and to glycolysis in heart and skeletal muscle.

Chapter 3

THE MITOCHONDRIAL K_{ATP} CHANNEL AS A RECEPTOR FOR POTASSIUM CHANNEL OPENERS AND INHIBITORS*

K^+ channel openers (KCOs) activate ATP-inhibited K_{ATP} channels. As described in several excellent reviews (118–120), members of this drug family exhibit a rich and clinically important pharmacology. Thus, cell membrane K_{ATP} channels (cellK_{ATP}) in different tissues are considered to mediate the hypotensive and diabetogenic effects of diazoxide (14) and the cardioprotective effects of cromakalim and its derivatives (30). It is important to determine whether these drugs also act on mitochondrial K_{ATP} channels (mitoK_{ATP}) in their therapeutic range.

In the first reports of the actions of KCOs in mitochondria, Belyaeva et al. (121) and Szewczyk et al. (122) observed stimulation of K^+ uptake by KCOs in respiring mitochondria. RP66471 was the most potent KCO studied ($K_{1/2}$ = 50 μM), whereas P1060 and diazoxide were only weakly active at 700 μM. Because these concentrations are much higher than $K_{1/2}$ values observed with cellK_{ATP} (118), these

---

* This material has been published in this or similar form in *The Journal of Biological Chemistry* and is used here with permission of the American Society for Biochemistry and Molecular Biology:

Garlid, K. D., Paucek, P., Yarov-Yarovoy, V., Sun, X., and Schindler, P. (1996) The mitochondrial K_{ATP} Channel as a Receptor for Potassium Channel Openers. *J. Biol. Chem.* **271**, 8796–8799.

Sections 3.2.4 and 3.2.5 and Figures 3.5 and 3.6 are reprinted with permission from Waverly, Williams & Wilkins · Urban & Schwartzenberg.

Garlid, K. D., Paucek, P., Yarov-Yarovoy, V., Murray, H. N., Darbenzio, R. B., D'Alonzo, A. J., Lodge, N. J., Smith, M. A., and Grover, G. J. (1997) Cardioprotective effect of diazoxide and its interaction with mitochondrial ATP-sensitive potassium channels: possible mechanism of cardioprotection. *Circ. Res.* **81**, 1072–1082.

results appear to imply that mitochondrial actions of KCOs are not pharmacologically important.

We now report that diazoxide, cromakalim, and two experimental benzopyran derivatives are very potent activators of K^+ flux through ATP-inhibited mitoK_{ATP}, with $K_{1/2}$ values similar to those observed for cellK_{ATP}. Activation of K^+ flux by KCOs was observed in both intact mitochondria and proteoliposomes containing reconstituted mitoK_{ATP}. No effect was observed on uninhibited K^+ flux, which likely explains the low potencies observed by previous workers (121, 122) in assays that did not include Mg^{2+} and ATP. We also found that mitoK_{ATP} and cellK_{ATP} from beef heart differed strongly in their sensitivity to diazoxide, indicating distinct receptor subtypes among K_{ATP} channels from the same cell. The opening effect of diazoxide on mitoK_{ATP} was abolished by K_{ATP} channel blockers such as glibenclamide and 5-hydroxydecanoate. Our results indicate that mitoK_{ATP} may be an important intracellular receptor for K^+ channel openers, and they raise the possibility that mitoK_{ATP} is the site of cardioprotective action of KCOs.

3.1 Materials and Methods

3.1.1 Isolation of rat liver mitochondria

Rat liver mitochondria were isolated using the protocol described in Chapter 2 with the following modifications: isolation medium for the first two low-speed spins contained 250 mM sucrose, 5 mM K-EDTA, 2 mM K-TES, pH 6.7, and 0.5 mg BSA/ml, and for the following high-speed spins contained 250 mM sucrose, 0.5 mM K-EGTA, 2 mM K-TES, pH 6.7. The mitochondria were resuspended to 100 mg protein/ml in 250 mM sucrose and stored on ice for light-scattering experiments or stored at -70°C for subsequent preparation of submitochondrial particles.

3.1.2 Isolation of rat heart mitochondria

Rat heart mitochondria were isolated using the protocol described by Matlib et al. (123).

3.1.3 Preparation of submitochondrial particles from rat liver mitochondria

Submitochondrial particles (SMPs) were prepared using the protocol described in Chapter 2 with the following modifications: SMP preparation medium contained 250 mM sucrose, 10 mM K-HEPES, pH 7.4, and 1 mM K-EDTA. The resulting pellet was resuspended in 250 mM sucrose at a protein concentration of 50 mg/ml and stored at -70°C until ready to use.

3.1.4 Preparation of submitochondrial particles and guanidine-treated inner mitochondrial membrane vesicles from rat heart mitochondria

Submitochondrial particles (SMPs) and guanidine-treated inner mitochondrial membrane vesicles (3xGMs) were prepared using the protocols described in Chapter 2.

3.1.5 Assays of K^+ flux in proteoliposomes containing reconstituted mitoK_{ATP} isolated from rat liver and rat heart mitochondria

MitoK_{ATP} from rat liver or rat heart was purified and reconstituted into proteoliposomes exactly as described in Chapter 2.

3.1.6 Assays of K^+ flux in proteoliposomes containing reconstituted cellK_{ATP} isolated from beef heart sarcolemmal vesicles

Sarcolemmal vesicles were prepared from the left ventricular muscle of fresh beef heart according to a modification (124) of the method of Jones and Besch (125). The sarcolemmal K_{ATP} channel was solubilized, purified, and reconstituted into proteoliposomes exactly as described in Chapter 2 for mitoK_{ATP}, except that cellK_{ATP} activity was found in the 100 mM KCl fraction (126). Internal and external media were as described for mitoK_{ATP}, except that Na^+ was substituted for TEA^+ ion, because TEA^+ inhibits K^+ flux through cellK_{ATP}. Assays of cardiac cellK_{ATP} were carried out as described for mitoK_{ATP}.

3.1.7 Assays of K^+ flux in intact rat liver mitochondria

Electrophoretic uptake of K^+ or TEA^+ into respiring mitochondria is driven by the high membrane potential and is accompanied by electroneutral uptake of acetate and succinate. Uptake of salts and water results in osmotic swelling of mitochondria and a consequent decrease in light scattered by the mitochondrial suspension. Under proper conditions, the light scattering variable, β, is linearly related to volume, and $d\beta/dt$ is proportional to the rate of cation uptake (105, 127). β normalizes reciprocal absorbance (A^{-1}) for mitochondrial concentration, P (mg/ml):

$$\beta \equiv (P/P_s)*(A^{-1} - a)$$

where P_s (= 1 mg/ml) is introduced to make β a scaled, dimensionless quantity, and a is a machine constant equal to 0.25 with our apparatus. Absorbance is measured at 520 nm and sampled at 0.6-s intervals with a Brinkmann PC 700 probe colorimeter connected via an analog/digital converter to a computer for conversion to A^{-1}, real-time plotting, and data storage. A linear regression routine is used to obtain rates, $d\beta/dt$ (min^{-1}), from the traces.

The standard assay medium for light scattering studies is described in ref. 128. It contains either K^+ or TEA^+ salts of chloride (45 mM), succinate (3 mM), acetate (25.4 mM), TES (5 mM), and EGTA (0.1 mM), pH 7.4. 1 mM $MgCl_2$ was added where indicated. Media were supplemented with rotenone (2 μg/mg) and cytochrome *c* (10 μM) and maintained at 25°C. Endogenous cytochrome *c* is mobilized in salt medium and may diffuse away when the outer membrane is ruptured by matrix swelling (129). Under the conditions tested, cytochrome *c* in fact had little or no effect on mitoK_{ATP}-dependent K^+ flux; however, any reduction of respiration would cause a hidden artifactual reduction of K^+ flux, so cytochrome *c* was added to all media. The instrument was zeroed before each run; consequently there was no interference from cytochrome *c* absorbance.

Stock mitochondria were added to the assay medium in a final concentration of 0.1 mg protein/ml. The mitochondria used in these studies exhibited respiratory control ratios of 4:6.

3.1.8 Materials

PBFI was purchased from Molecular Probes Inc. (Eugene, OR). Two benzopyranyl derivatives, EMD57970 and EMD60480, were provided by E. Merck (Darmstadt, Germany). 5-HD was obtained from Research Biochemicals Inc. All other chemicals and reagents were obtained from Sigma Chemical Co. (St. Louis, MO).

3.2 Results

3.2.1 Activation of K^+ flux through reconstituted mitoK_{ATP} by K^+ channel openers

Fig. 3.1 contains dose–response curves for KCO stimulation of K^+ flux in vesicles reconstituted with mitoK_{ATP}. Drug assays were carried out in media containing 3 mM Mg^{2+} and 0.5 mM ATP, which fully inhibits mitoK_{ATP} ($K_{1/2}$(ATP) $\approx$ 22 μM). The drugs tested were potent activators of K^+ flux, restoring ATP-inhibited flux to, but not beyond, control rates measured in the absence of ATP.

Observed $K_{1/2}$ values (mean and S.D.) were 1.05 $\pm$ 0.06 μM for cromakalim (n = 5), 0.37 $\pm$ 0.03 μM for diazoxide (n = 4), 6.1 $\pm$ 1.3 nM for EMD60480 (n = 2), and 6.20 $\pm$ 0.02 nM for EMD57970 (n = 2). As shown in the inset to Fig. 3.1, cromakalim and diazoxide exhibited indistinguishable Hill slopes of 2.0 $\pm$ 0.5, and the benzopyranyl derivatives yielded Hill slopes of 3.5 $\pm$ 0.3. Hill slopes greater than 1.0 may reflect a tetrameric structure of the channel, as observed with other K^+ channels (130), or the existence of multiple binding sites on a regulatory ATP binding cassette, as has been proposed for the sulfonylurea receptor of the pancreatic β-cell (52).

We also measured KCOs activation of K^+ flux in proteoliposomes reconstituted with mitoK_{ATP} purified from beef heart mitochondria. The observed $K_{1/2}$ values from two experiments were 1 μM for cromakalim and 0.4 μM for diazoxide. These results extend a previous observation that cardiac and hepatic mitoK_{ATP} behave very similarly.

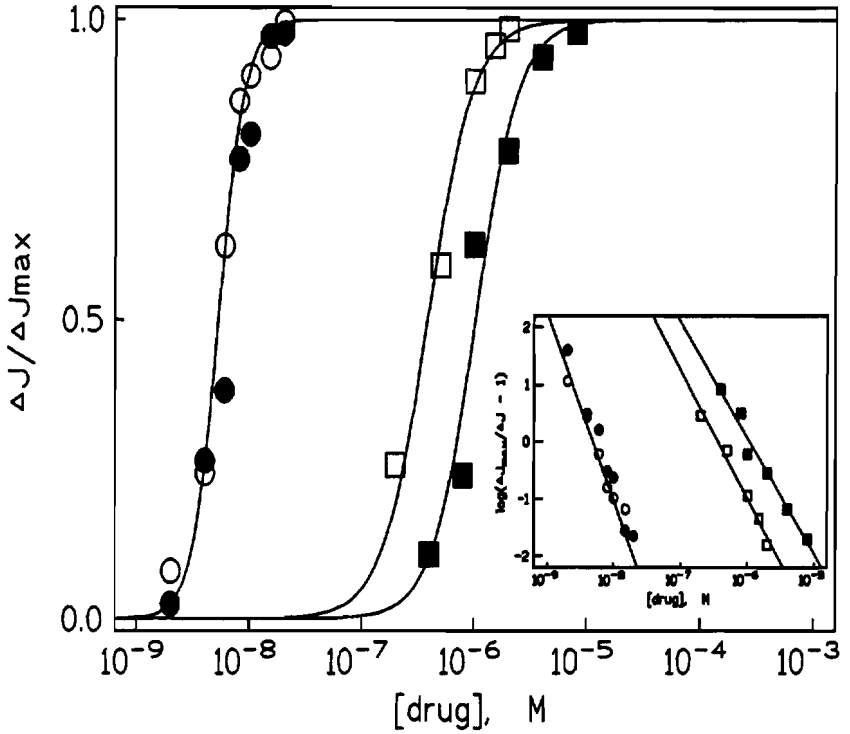

Figure 3.1 Activation of K^+ flux by K^+ channel openers in liposomes reconstituted with mitoK_{ATP}. Figure contains dose-response curves and Hill plots (inset) for activation of K^+ flux through mitoK_{ATP} by four KCOs: EMD60480 (○), EMD57970 (●), diazoxide (□), and cromakalim (■). ΔJ_{max} is the maximum ATP-sensitive K^+ flux, i.e., the difference between control fluxes in the absence and presence of saturating ATP (0.5 mM). ΔJ is the difference between fluxes in the presence or absence of the drug, both measured in the presence of 0.5 mM ATP. In nine separate preparations, ΔJ_{max} ranged between 400 and 600 μM/s, similar to values previously reported using these protocols (68). Observed $K_{1/2}$ values and Hill slopes are given in the text.

We stress that these drugs stimulated K^+ flux only when K^+ flux was inhibited by Mg^{2+} and ATP. Control (uninhibited) K^+ flux is observed in media containing Mg^{2+} alone, ATP alone, and lacking both Mg^{2+} and ATP (68). In each of these conditions, KCOs had no effect on control K^+ flux at doses up to 30-fold higher than their respective $K_{1/2}$ values.

3.2.2 Activation of K^+ flux through reconstituted cardiac plasma membrane K_{ATP} by K^+ channel openers

The high potency of diazoxide for cardiac mitoK_{ATP} was somewhat surprising and suggested a pharmacological distinction from cardiac cellK_{ATP}, which is relatively insensitive to diazoxide (131). Accordingly, we evaluated the effects of the same set of KCOs on cellK_{ATP} reconstituted from cardiac sarcolemmal vesicles (126, 132). Fig. 3.2 contains dose–response curves for KCO stimulation of K^+ flux in proteoliposomes reconstituted with cardiac cellK_{ATP}. These assays were carried out in media containing 2 mM ATP ($K_{1/2}$ = 0.5 mM). Each of the drugs restored ATP-inhibited K^+ flux to control rates measured in the absence of ATP. As was the case with mitoK_{ATP}, these KCOs had no effect on the control rate in the absence of ATP. Observed $K_{1/2}$ values and Hill slopes (in parentheses) for opening the plasma membrane K_{ATP} channel were 3.7 nM (1.1) for EMD57970, 22 nM (1.2) for EMD60480, 17 μM (1.1) for cromakalim, and 855 μM (0.9) for diazoxide. Similar values were obtained in a separate preparation. The $K_{1/2}$ values for the benzopyranyl derivatives are reasonably similar to those observed for mitoK_{ATP}; however, the $K_{1/2}$ value for diazoxide is about 2000-fold higher. In contradistinction to the finding with mitoK_{ATP}, the Hill slopes for activation of cellK_{ATP} were indistinguishable from 1 for all of the KCOs tested.

3.2.3 Activation of ATP-sensitive K^+ flux in intact mitochondria by K^+ channel openers

The preceding results appear to conflict with previous work (121, 122) showing very low potencies for KCO activation of K^+ flux in mitochondria. Accordingly, it was important to determine whether the high potencies observed in Fig. 3.1 are also observed *in situ*.

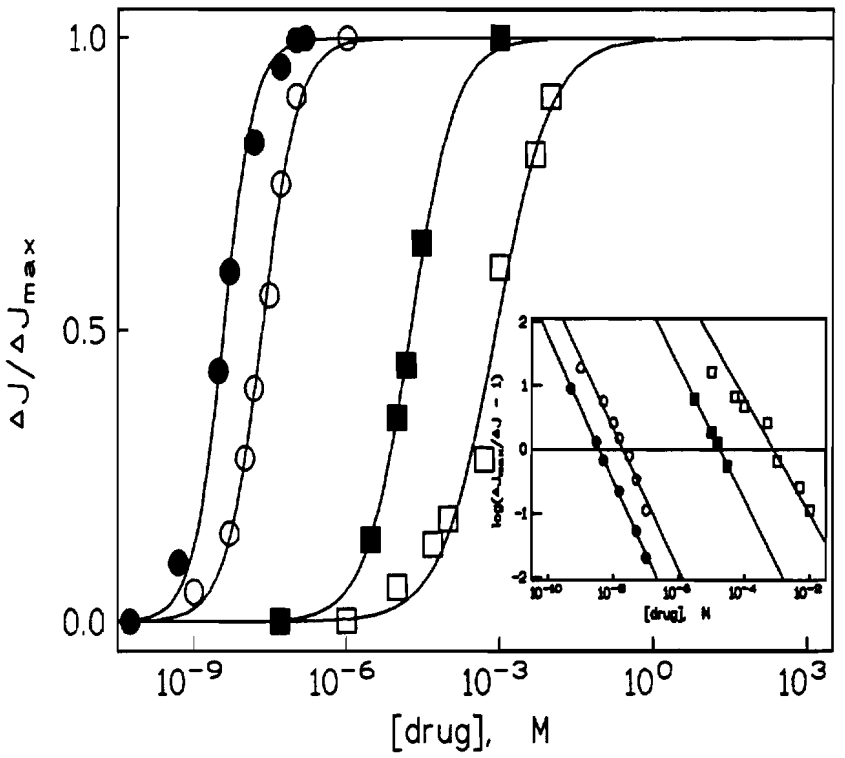

Figure 3.2 Activation of K^+ flux by K^+ channel openers in liposomes reconstituted with cardiac sarcolemmal K_{ATP} channels (cellK_{ATP}). Figure contains dose-response curves and Hill plots (inset) for activation of K^+ flux through cellK_{ATP} by four KCOs: EMD57970 (●), EMD60480 (○), cromakalim (■), and diazoxide (□). ΔJ_{max} and ΔJ are defined as in Fig. 3.1, but with reference to rates in 2 mM ATP. Observed $K_{1/2}$ values and Hill slopes are given in the text. Duplicate experiments on an independent preparation yielded similar results.

Fig. 3.3 contains representative light-scattering traces from rat liver mitochondria respiring on ascorbate-TMPD. Swelling in K^+ salts (*trace a*) was sharply inhibited by addition of 100 μM ATP (down arrow to *trace b*) to levels close to those observed in TEA^+ salts (*trace c*). In agreement with previous results (124), higher [ATP] had no further effect in K^+ medium, and ATP had no effect on TEA^+ flux (not shown). When 20 μM cromakalim was included in the assay medium containing 100 μM ATP, ATP inhibition was prevented (up arrow to *trace d*, Fig. 3.3). In the *absence* of ATP, cromakalim had no effect on the control rate up to 100 μM, the highest dose tested. When cromakalim was added during the inhibited state, ATP inhibition was reversed (not shown).

Fig. 3.4 contains dose–response curves for activation of K^+ flux by diazoxide, cromakalim, and EMD60480 in mitochondria. Activation was measured relative to rates in the presence of 100 μM ATP and 1 mM Mg^{2+}, conditions in which the $K_{1/2}$ for ATP inhibition is 2–3 μM (128). The estimated $K_{1/2}$ values were 2.3 μM for diazoxide, 6.3 μM for cromakalim, and 5.4 nM for EMD60480.

As in proteoliposomes, these drugs stimulated K^+ flux only when K^+ flux was inhibited by Mg^{2+} and ATP. In doses 20-fold higher than their respective $K_{1/2}$ values, these KCOs had no effect on flux through the uninhibited channel. This effect was verified in media containing Mg^{2+} alone, ATP alone, and lacking both Mg^{2+} and ATP.

3.2.4 Effect of diazoxide on reconstituted bovine heart mitochondrial and sarcolemmal K_{ATP} activity

Fig. 3.5 contains the diazoxide (Fig. 3.5A) and cromakalim (Fig. 3.5B) concentration-response curves for stimulation of K^+ flux in vesicles reconstituted with K_{ATP} purified from bovine heart mitochondria (solid circles, Fig. 3.5) and sarcolemma (open circles, Fig. 3.5). Cromakalim was a potent activator of K^+ flux in both preparations (Fig. 3.5B). Observed $K_{1/2}$ values for cromakalim were 1.6 $\pm$ 0.1 μmol/L (n = 5) for mitochondrial K_{ATP} and 18 $\pm$ 2 μmol/L (n = 3) for sarcolemmal K_{ATP}. The reconstituted K_{ATP} from the two resources responded differently to diazoxide. Observed $K_{1/2}$ values for diazoxide were 0.80 $\pm$ 0.03 μmol/L (n = 4) for mitochondrial K_{ATP} and 840 $\pm$ 25 μmol/L (n = 3) for sarcolemmal K_{ATP}. In both

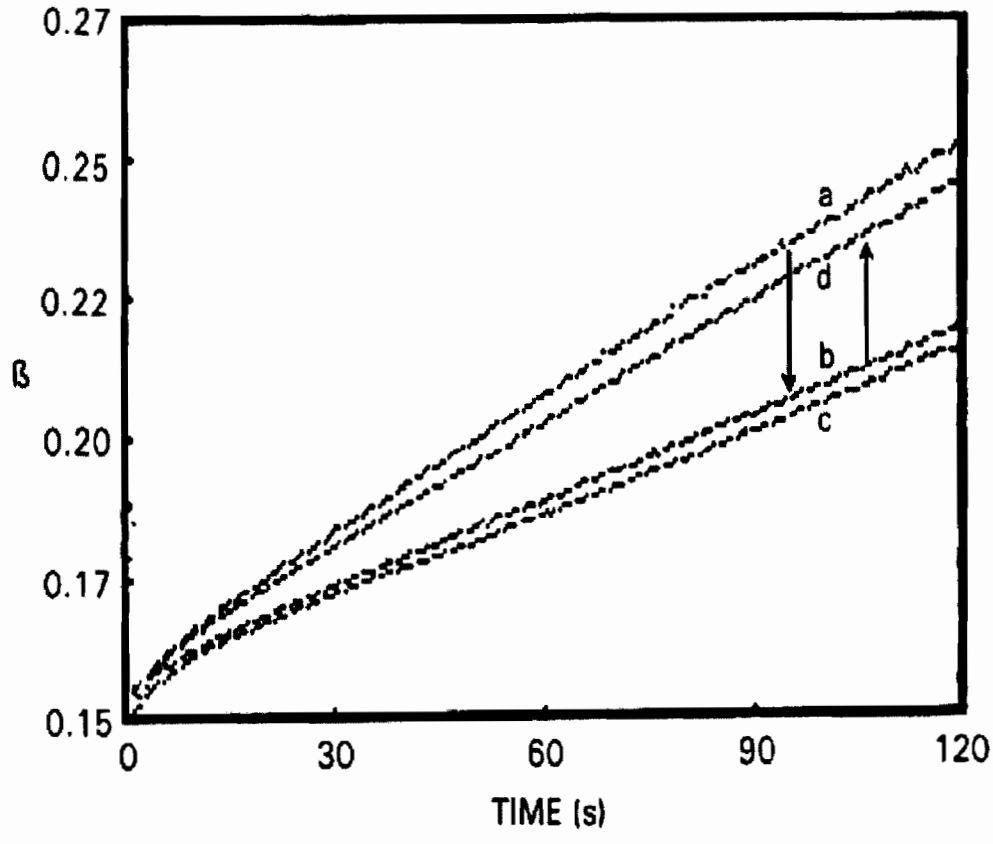

Figure 3.3 Activation of K^+ flux by cromakalim in intact mitochondria. Light-scattering kinetics for mitochondria suspended in K^+ media (see Section 3.1). *Trace a*, K^+ medium without ATP or cromakalim. *Trace b*, K^+ medium containing 0.1 mM ATP. *Trace c*, TEA^+ medium without ATP. *Trace d*, K^+ medium with 0.1 mM ATP and 20 μM cromakalim. The down arrow from *trace a* to *trace b* shows the inhibitory effect of ATP on swelling kinetics, and the up arrow from *trace b* to *trace d* shows the opening effect of cromakalim. Ascorbate-TMPD was used as the respiratory substrate, entirely similar results were obtained with succinate.

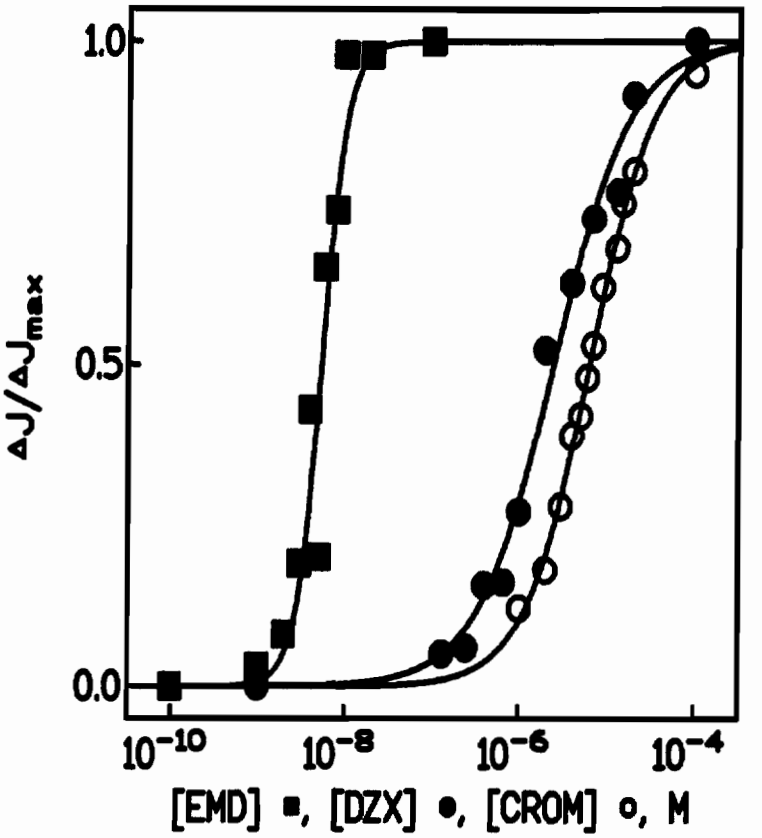

Figure 3.4 Dose-response curves for activation of K^+ flux in intact mitochondria. Relative ATP-sensitive K^+ uptake into respiring rat liver mitochondria, $\Delta J/\Delta J_{max}$, is plotted versus drug concentration. ΔJ_{max} and ΔJ are defined as in Fig. 3.1. The dose-response curves reflect activation by EMD60480 (■), diazoxide (●), and cromakalim (○). Assay medium for ΔJ contained 1 mM Mg^{2+} and 0.1 mM ATP, which maximally inhibited K^+ uniport in mitochondria (124), and ascorbate-TMPD as respiratory substrates. The $K_{1/2}$ values reported in the text are means of two independent experiments. For each drug, duplicate $K_{1/2}$ values were within 5% of each other.

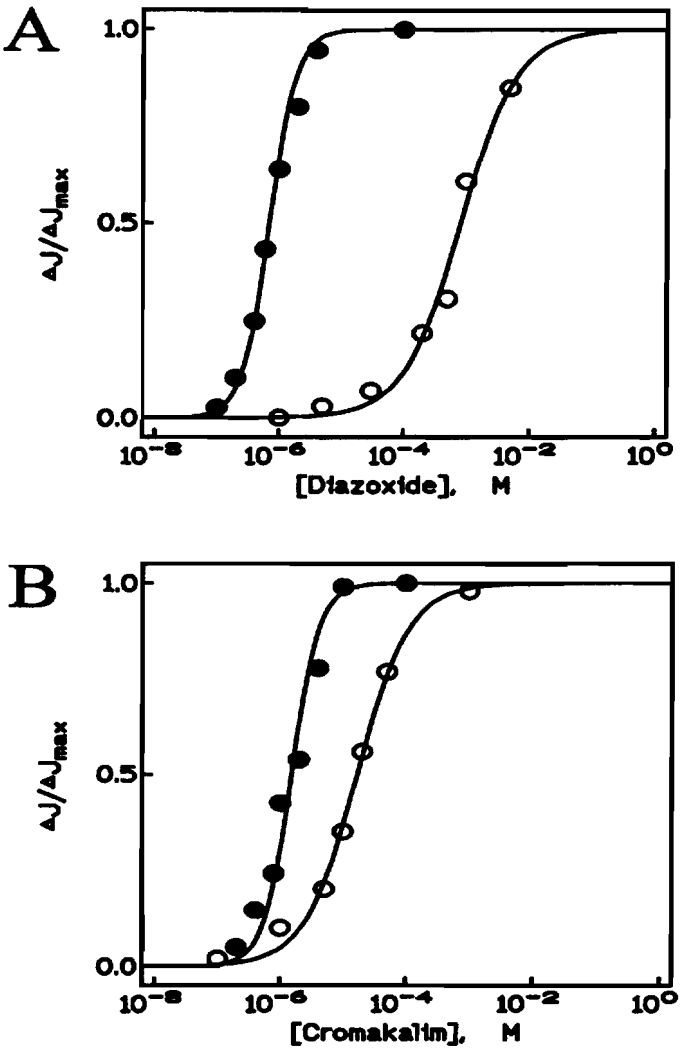

Figure 3.5 Activation of K^+ flux by diazoxide or cromakalim in K_{ATP} channels from bovine heart mitochondria and sarcolemma. Relative K^+ flux, ($\Delta J/\Delta J_{max}$) is plotted vs concentration of drug added to the assay. Reconstituted K_{ATP} channels were first inhibited with ATP; then K^+ flux was activated by K_{ATP} opener. The figure contains relative fluxes from cardiac mitochondrial K_{ATP} channels (●) and sarcolemmal K_{ATP} channels (○) in response to diazoxide (***panel A***) or cromakalim (***panel B***). ΔJ_{max} is the difference between control fluxes in the presence and absence of ATP, and ΔJ is the difference between fluxes in the presence and absence of drug, with both fluxes measured in the presence of 1 mmol/L Mg^{2+} and 0.5 mmol/L ATP for mitochondrial K_{ATP} and in the presence of 2 mmol/L ATP for sarcolemmal K_{ATP}. Fluxes were obtained from linear regression of initial rates of K^+ uptake. Observed $K_{1/2}$ values for cromakalim were 1.6 ± 0.1 μmol/L for mitochondrial K_{ATP} and 18 ± 2 μmol/L for sarcolemmal K_{ATP}. The reconstituted K_{ATP} from the two resources responded differently to diazoxide. Observed $K_{1/2}$ values for diazoxide were 0.80 ± 0.03 μmol/L for mitochondrial K_{ATP} and 840 ± 25 μmol/L for sarcolemmal K_{ATP}.

preparations, K_{ATP} openers activated K^+ flux only when it was inhibited by ATP. Therefore, mitochondrial K_{ATP} is $\approx$1000-fold more sensitive to diazoxide than sarcolemmal channels. These data confirm previously published work from this laboratory (70). Also compared with cromakalim, diazoxide is $\approx$50-fold less potent at activating sarcolemmal K_{ATP}, which is consistent with the findings seen with whole-cell currents.

3.2.5 Effect of diazoxide and cromakalim on rat heart mitochondrial K_{ATP}: effect of K_{ATP} blockade

Since the ischemia studies were performed in isolated rat hearts, we also determined the effect of diazoxide on rat cardiac mitochondrial K_{ATP}. As shown in Fig. 3.6A, diazoxide and cromakalim are potent activators of the ATP-inhibited mitochondrial K_{ATP} from rat heart. Observed $K_{1/2}$ values were 0.49 $\pm$ 0.05 μmol/L for diazoxide (n = 3) and 1.1 $\pm$ 0.1 μmol/L for cromakalim (n = 3). These values are similar to those previously obtained with reconstituted mitochondrial K_{ATP} from rat liver and bovine heart (70).

To mimic the in situ pharmacological experiments, we included MgATP, diazoxide (10 μmol/L), and glibenclamide or 5-HD in the assay medium and varied the inhibitor concentration. As demonstrated in Fig. 3.6B, K^+ flux through the diazoxide-opened channel was inhibited by low concentrations of glibenclamide ($K_{1/2}$, 56 nmol/L) and 5-HD ($K_{1/2}$, 83 μmol/L). Similar results were obtained in two experiments using 10 μmol/L cromakalim, with glibenclamide inhibiting with $K_{1/2}$ of 92 nmol/L and 5-HD inhibiting with $K_{1/2}$ of 31 μmol/L. In the absence of ATP and K^+ channel openers, glibenclamide inhibited K^+ flux with $K_{1/2}$ of 40 nmol/L, whereas 5-HD had no effect up to 500 μmol/L, the highest concentration tested.

3.3 Discussion

This is the first report showing that KCOs activate mitoK_{ATP} over the same dose range as they activate cellK_{ATP}. This finding was observed in mitochondria and in proteoliposomes reconstituted with mitoK_{ATP} and raises the possibility that mitoK_{ATP} may be activated by KCOs *in vivo*. Kinetic parameters differed between intact

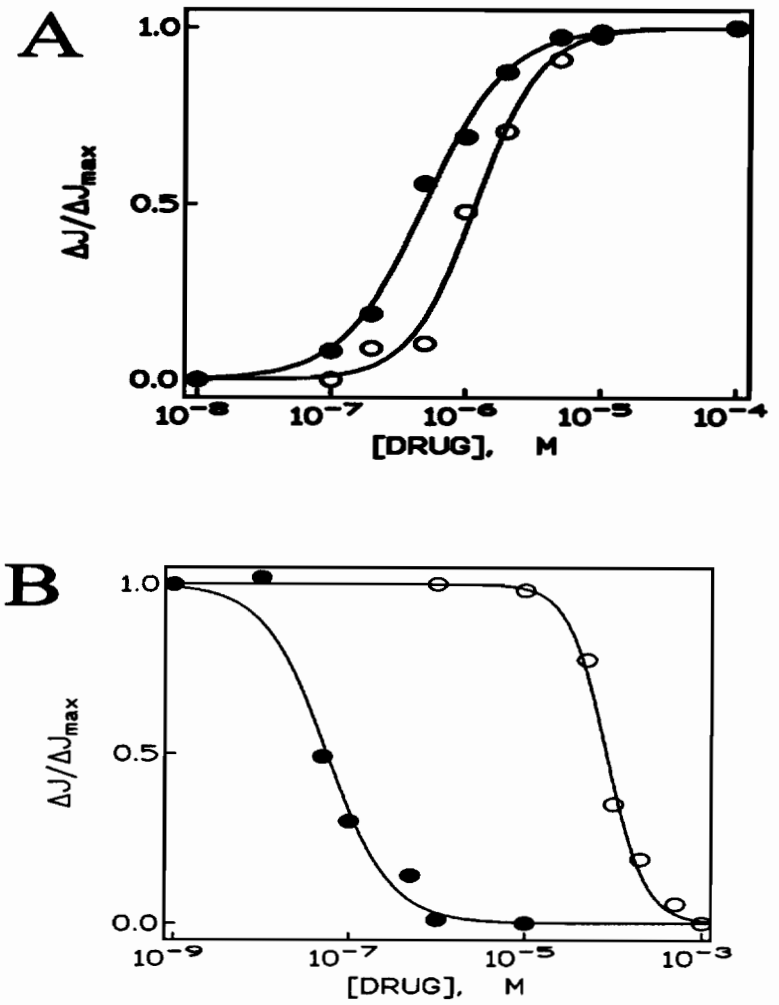

Figure 3.6 A, Activation of the reconstituted rat heart mitochondrial K_{ATP} channel by diazoxide and cromakalim. ***Panel A*** contains concentration-response curves for activation of K^+ flux through mitochondrial K_{ATP} by diazoxide (●) or cromakalim (○). Assay medium contained 1 mmol/L Mg^{2+} , 0.5 mmol/L ATP, and the indicated concentrations of K_{ATP} opener. Normalized K^+ flux ($\Delta J/\Delta J_{max}$) is plotted vs concentration of the drug added to the assay medium. ΔJ is the difference between fluxes in the presence and absence of drug, both measured in the presence in the presence of MgATP. ΔJ_{max} is the difference between control fluxes in the presence and absence of MgATP. B, Glibenclamide and 5-HD reversed the opening effect of diazoxide on the reconstituted rat heart mitochondrial K_{ATP}. ***Panel B*** contains concentration-response curves for inhibition of K^+ flux through mitochondrial K_{ATP} by glibenclamide (●) or 5-HD (○). Assay medium contained 1 mmol/L Mg^{2+} , 0.5 mmol/L ATP, 10 μmol/L diazoxide, and indicated concentrations of glibenclemide and 5-HD. Normalized K^+ flux is plotted vs concentration of the inhibitor added to the assay medium. Results are typical of two experiments with each inhibitor.

mitochondria and the reconstituted preparations. As previously reported (128), the $K_{1/2}$ for ATP inhibition is lower in mitochondria (2–3 μM) than in proteoliposomes (20–25 μM). We now show that the $K_{1/2}$ values for diazoxide and cromakalim are about 6-fold higher in mitochondria than in liposomes. On the other hand, the $K_{1/2}$ for EMD60480 is about the same in the two preparations. These differences may reflect regulatory complexity in intact mitochondria, which is lost upon extraction and reconstitution.

In the dose ranges studied, KCOs had no effect on K^+ flux when Mg^{2+} and/or ATP were omitted from the assay medium. The lack of effect of KCOs on the open channel is also characteristic of cellK_{ATP} (133). The finding that KCOs in low doses have no effect on the uninhibited channel is also consistent with the results of Belyaeva et al. (121) and Szewczyk et al. (122), who did not include Mg^{2+} and ATP in the assay medium used for their studies.

3.3.1 Physiological consequences of opening and closing mitoK_{ATP}

Opening of mitoK_{ATP} will shift the balance between K^+ uniport and K^+/H^+ antiport, causing transient net K^+ uptake and matrix swelling to a higher steady-state volume (73). Halestrap (80) has established that increasing matrix volume over a fairly narrow range greatly activates electron transport at the point where electrons feed into ubiquinone, and he has suggested (83) that this sequence may be triggered by opening of mitoK_{ATP}. Thus, opening of mitoK_{ATP} may be a *necessary* component of the cellular signals calling, for example, for higher ATP production to support increased work in heart or for faster β oxidation of fatty acids to support thermogenesis in brown adipose tissue. Conversely, blocking mitoK_{ATP} may interfere with the cell's response to these signals.

3.3.2 MitoK_{ATP} as a pharmacological receptor

Recognition of mitoK_{ATP} as an intracellular receptor for KCOs adds a new dimension to the KCO pharmacology, which has heretofore focused exclusively on plasma membrane K_{ATP} channels. Pharmacological regulation of K_{ATP} channels has many important, tissue-dependent consequences (118–120); however, the receptors for these effects have not yet been identified, and a mitochondrial contribution cannot be

excluded. The role of K_{ATP} channels in pancreatic β-cells is a case in point. Flatt et al. (134) have recently shown that Ca^{2+}-dependent insulin release from electropermeabilized β-cells is stimulated by glyburide and inhibited by diazoxide. Because plasma membrane K_{ATP} channels are inoperative in the permeabilized cell, these effects point to an intracellular receptor for these agents (134).

A particularly exciting development in heart is the finding by Grover and colleagues (30, 31) and others (46, 135) that KCOs are cardioprotective during experimental ischemia. KCO-treated hearts maintained higher ATP levels and exhibited reduced infarct size and enhanced post-ischemic recovery upon reperfusion. All of these effects were blocked by glyburide, which is contraindicated in patients susceptible to cardiac ischemia. Preconditioning, in which a period of brief ischemia reperfusion protects the heart against subsequent ischemic damage (136), was also blocked by glyburide (137). These pharmacological effects point to a role of K_{ATP} channels in myocardial protection; but, again, the receptor for these effects has not been identified, and a mitochondrial site of action cannot be excluded (31).

Exploration of this possibility is aided by the existence of receptor subtypes among K_{ATP} channels (118). For example, cromakalim is a potent activator of cellK_{ATP} from heart and vascular smooth muscle (137) but has a minimal effect on insulin secretion (13, 14). Diazoxide is a potent vasodilator (14) and also reduces insulin secretion (10) but has little effect on cardiac cellK_{ATP} (131). This raises the question whether mitoK_{ATP} and cellK_{ATP} from the *same* cell differ pharmacologically. Accordingly, we have compared drug sensitivities of cardiac mitoK_{ATP} and cellK_{ATP} reconstituted from beef heart. These experiments yielded the following preliminary results:

(i) MitoK_{ATP} from heart and liver do not differ significantly in their drug sensitivities ($K_{1/2}$ values).

(ii) Cardiac mitoK_{ATP} and cardiac cellK_{ATP} exhibit similar sensitivities to benzopyran derivatives.

(iii) Cardiac mitoK_{ATP} is about 2000 times more sensitive to diazoxide than cardiac cellK_{ATP}.

The low sensitivity of reconstituted cardiac cellK_{ATP} to diazoxide is entirely consistent with previous reports (131).

5-HD has been shown to abolish cardioprotective effects of diazoxide, but did not abolish the action potential duration shortening or vasodilator effects of KCOs (89). Cardiac cellK_{ATP} is blocked by glyburide but not by 5-HD (89). In this report, we demonstrated that 5-HD inhibited the ability of diazoxide to open reconstituted mitoK_{ATP}. These data, taken together with the fact that diazoxide is a specific opener of cardiac mitoK_{ATP}, but not cardiac cellK_{ATP}, strongly suggest an important role of mitoK_{ATP} in mediating cardioprotective effects of KCOs.

Chapter 4

THE NUCLEOTIDE REGULATORY SITES ON THE MITOCHONDRIAL K_{ATP} CHANNEL FACE THE CYTOSOL*

In previous work (68–70, 75, 128), we showed that the mitochondrial K_{ATP} channel (mitoK_{ATP}) is inhibited with high affinity by adenine nucleotides, long-chain acyl-CoA esters, and glyburide. Inhibition by ATP and palmitoyl-CoA is reversed with high affinity by guanine nucleotides and K^+ channel openers such as cromakalim and diazoxide. The rich variety of its regulation suggests that mitoK_{ATP} has an important physiological function, but the nature of this function remains to be established.

It is clear that opening of mitoK_{ATP} will shift the balance between K^+ uptake and efflux and thereby increase the steady-state volume of mitochondria (73, 75). Substrate oxidation, in turn, is tightly controlled by matrix volume, a phenomenon that was first reported in 1948 by Lehninger and Kennedy (77). The volume effect can be summarized as follows: contracted mitochondria oxidize substrates slowly and fatty acids hardly at all; whereas mildly expanded mitochondria oxidize all substrates at rapid rates. Volume activation of electron transport has been demonstrated in liver, heart, and brown adipose tissue mitochondria (78–80, 83). Volume changes secondary to hormonal stimulation of liver (80) and brown adipose tissue (82) have also been observed in the intact cell. It was demonstrated conclusively by Nicholls et al. (78) that regulation of oxidation is mediated strictly by changes in matrix volume, independently of the means used to change volume.

---

* This material has been published in this or similar form in *Biochimica Biophysica Acta* and is used here with permission of Elsevier Science.

Yarov-Yarovoy, V., Paucek, P., Jaburek, M., and Garlid, K. D. (1997) The nucleotide regulatory sites on the mitochondrial K_{ATP} channel face the cytosol. *Biochim. Biophys. Acta* **1321**, 128–136.

In view of these findings, the working hypothesis that volume regulation by mitoK$_{ATP}$ plays a central role in cell signaling pathways calling for activation of electron transport and stimulation of fatty acid oxidation (69, 70, 75, 83, 138) is entirely sound. Nevertheless, the hypothesis remains to be proven. A crucial issue in its evaluation is knowing *where* the nucleotide regulatory sites reside. Do they face the matrix, as suggested by Inoue (65) and Halestrap (83), or do they face the cytosol?

We addressed these questions using three techniques:

(i) Measurement of K^+ flux in liposomes reconstituted with purified mitoK$_{ATP}$.

(ii) Measurement of electrical activity in BLM containing purified mitoK$_{ATP}$.

(iii) Measurement of K^+ flux in intact mitochondria using light scattering.

The reconstitutions provided us with a very useful handle on the problem. We found that mitoK$_{ATP}$ is 90% oriented inward or outward with respect to ATP access, depending on the presence or absence of Mg^{2+} in the reconstitution buffer. This enabled us to demonstrate that mitoK$_{ATP}$ is unipolar with respect to regulation by Mg^{2+}, ATP, GTP, and palmitoyl-CoA and that all of these ligands react on the side of the protein facing the cytosol.

4.1 Materials and Methods

4.1.1. Assays of K^+ flux in proteoliposomes containing reconstituted mitoK$_{ATP}$ isolated from rat liver mitochondria

Purification and reconstitution of mitoK$_{ATP}$ followed the protocols described in Chapter 2.

4.1.2. Assays of K^+ flux in intact rat liver mitochondria

Light-scattering studies followed protocols described in Chapter 3.

4.1.3 Electrophysiology of mitoK$_{ATP}$ in the bilayer lipid membrane

Stock vesicles containing mitoK$_{ATP}$ were incorporated into BLM using protocols described by Cuppoletti et al. (139). A lipid solution was painted across the

aperture (0.9×10^{-3} cm^2) in a clean, dry chamber (140). The lipid was a 3:1 (w/w) mixture of 1-palmitoyl-2-oleoyl-*sn*-glycero-3-[phospho-L-serine] (POPS) and 1-palmitoyl-2-oleyl-*sn*-glycero-3-phosphoethanolamine (POPE), 40 mg/ml in *n*-decane (Sigma). The bilayer was formed under gradient conditions with 150 mM KCl on the *cis*-side and 50 mM KCl on the trans-side. Both solutions contained 20 mM Tris-HCl buffer, pH 7.2. Proteoliposomes loaded with 150 mM KCl were painted over the *cis*-side of the aperture using a fire-polished glass micropipette. Fusion was induced by addition of 5 mM $CaCl_2$ to the *cis*-side of the chamber and by application of ± 100 mV across the membrane. Experimental data were collected using an amplifier (Dagan model 8900, Minneapolis, MN) connected on-line with an IBM PC and storage oscilloscope (model 549, Tektronix Inc.). Membrane conductivity was determined using standard voltage-clamp methodology.

4.1.4 Materials

The sources of chemicals and drugs used were the same as described in Chapter 2.

4.2 Results

4.2.1 Activation of the inhibited K_{ATP} channel by Mg^{2+} chelation

Inhibition of K^+ flux through mitoK_{ATP} by ATP, ADP, and palmitoyl-CoA requires the presence of Mg^{2+} ions (68, 69). To fully exploit this behavior, it was necessary to show that removal of Mg^{2+} is sufficient to reverse ATP inhibition. The traces shown in Fig. 4.1 demonstrate that the fully inhibited channel can be activated by Mg^{2+} removal. Normal K^+ flux was observed in the presence of ATP without Mg^{2+} (Fig. 4.1, *trace a*) and was strongly inhibited by addition of Mg^{2+} to the assay medium (Fig. 4.1, *trace b*). K^+ flux was restored by the addition of EDTA during the assay (Fig. 4.1, *trace c*). Palmitoyl-CoA inhibition of K^+ flux was also reversed by chelation after inhibition had occurred (data not shown).

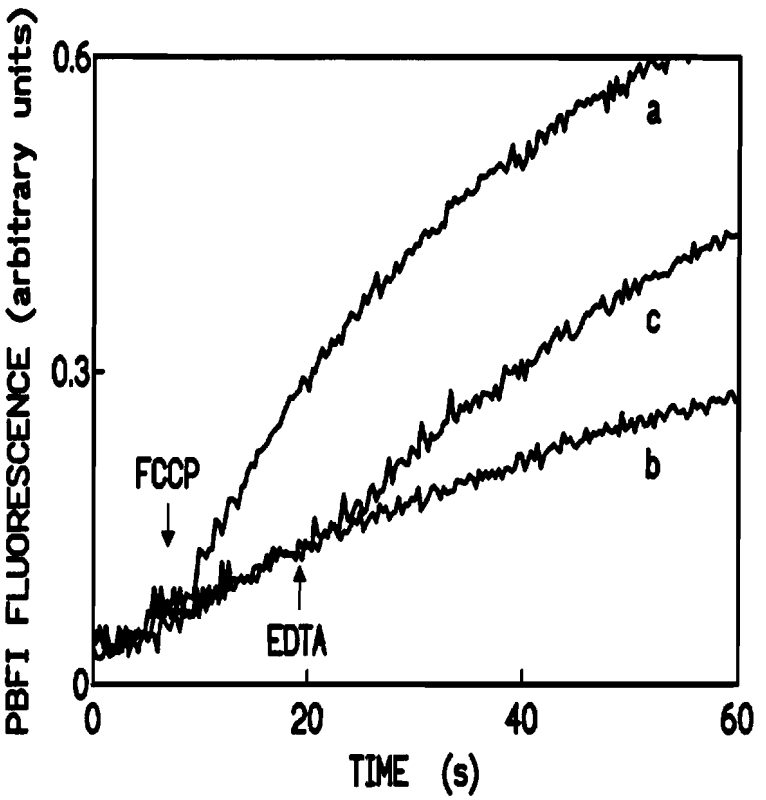

Figure 4.1 Activation of the ATP-inhibited mitoK$_{ATP}$ by Mg^{2+} removal. Shown are PBFI fluorescence traces from liposomes reconstituted with purified mitoK$_{ATP}$. Increasing PBFI fluorescence reflects increasing intraliposomal [K^+] due to K^+ transport. Electrophoretic K^+ influx was initiated by adding 1 μM FCCP to KCl assay medium at 10 s. *Trace a*, assay medium contained 0.5 mM ATP and no Mg^{2+}. *Trace b*, assay medium contained 3 mM Mg^{2+} and 0.5 mM ATP. *Trace c*, assay medium contained Mg^{2+} and ATP, as in trace b, and TEA-EDTA (10 mM, with pH adjusted to leave final assay pH unaffected) was added at 20 s. Proteoliposomes were reconstituted in internal medium containing EDTA.

4.2.2 Inhibition of reconstituted mitoK$_{ATP}$ by intraliposomal and extraliposomal ATP

The three sets of traces in Fig. 4.2 illustrate the basic finding that the composition of reconstitution buffer strongly affects ATP inhibition of K^+ flux through mitoK$_{ATP}$. Different reconstitution buffers (*internal media*) were used for each set of traces. For the data in Fig. 4.2A, standard reconstitution buffer containing EDTA was used. For the data in Fig. 4.2B, reconstitution buffer contained ATP (0.5 mM), Mg^{2+} (3 mM), and no EDTA. For the data in Fig. 4.2C, reconstitution buffer contained Mg^{2+} (3 mM) and no ATP or EDTA. We emphasize that ATP and Mg^{2+} were added *prior* to detergent removal and liposome formation.

The results in Fig. 4.2A (EDTA vesicles) demonstrate 90% inhibition of K^+ flux by external MgATP (Fig. 4.2A, *trace d*) relative to control (Fig. 4.2A, *trace a*). ATP did not inhibit K^+ flux in the absence of Mg^{2+} (Fig. 4.2A, *trace c*). These results, including the requirement for Mg^{2+}, confirm previous findings (68).

The results in Fig. 4.2B (MgATP vesicles) demonstrate that the presence of ATP and Mg^{2+} in the reconstitution buffer had a profound effect on the response of mitoK$_{ATP}$. Almost no K^+ flux was observed when assayed in medium lacking ATP and Mg^{2+} (Fig. 4.2B, *trace a*). K^+ flux was restored when MgATP vesicles were exposed to 0.5 μM 4-Br-A23187 in an assay medium containing 5 mM EDTA to remove intraliposomal Mg^{2+} (Fig. 4.2B, *trace b*). K^+ flux was again inhibited when 4-Br-A23187 was added to assay medium containing 3 mM Mg^{2+} and no EDTA (Fig. 4.2B, *trace c*). These results show that K^+ flux in MgATP vesicles is 90% inhibited by internal MgATP.

The results in Fig. 4.2C (Mg vesicles) demonstrate that the presence of Mg^{2+} alone in the reconstitution buffer also had a profound, but different, effect on the response of mitoK$_{ATP}$. Normal K^+ flux was observed in EDTA-containing medium (Fig. 4.2C, *trace a*) and was not affected by external ATP in the absence of Mg^{2+} (Fig. 4.2C, *trace c*). Furthermore, external ATP plus Mg^{2+}, which inhibited K^+ flux by 90% in EDTA vesicles, had almost no effect on K^+ flux in Mg vesicles (Fig. 4.2C, *trace d*).

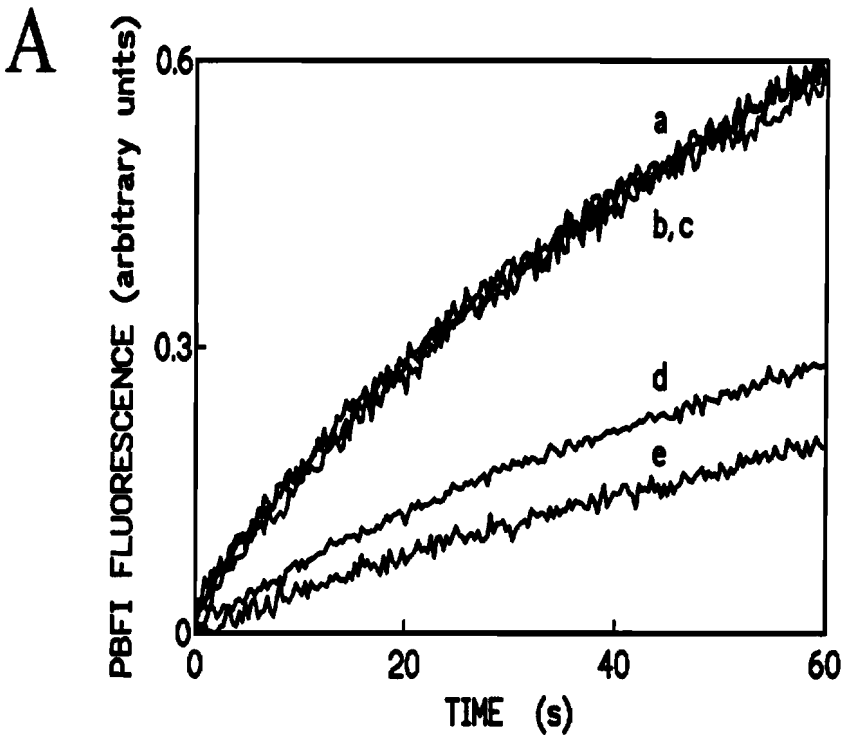

Figure 4.2 The effects of reconstitution buffer composition on behavior of reconstituted mitoK_{ATP}. Each panel contains PBFI fluorescence traces from liposomes reconstituted with purified mitoK_{ATP} in different internal media. K^+ influx is reflected in increasing PBFI fluorescence.

Panel A: EDTA vesicles. Vesicles were reconstituted in standard internal medium containing 1 mM EDTA and assayed in external medium, as described in Section 4.1. *Trace a*, assay medium contained no Mg^{2+} and no ATP. *Trace b*, assay medium contained 3 mM Mg^{2+} and no ATP. *Trace c*, assay medium contained no Mg^{2+} and 0.5 mM ATP. *Trace d*, assay medium contained 3 mM Mg^{2+} and 0.5 mM ATP. *Trace e*, assay medium as used for trace a, but FCCP was omitted (baseline).

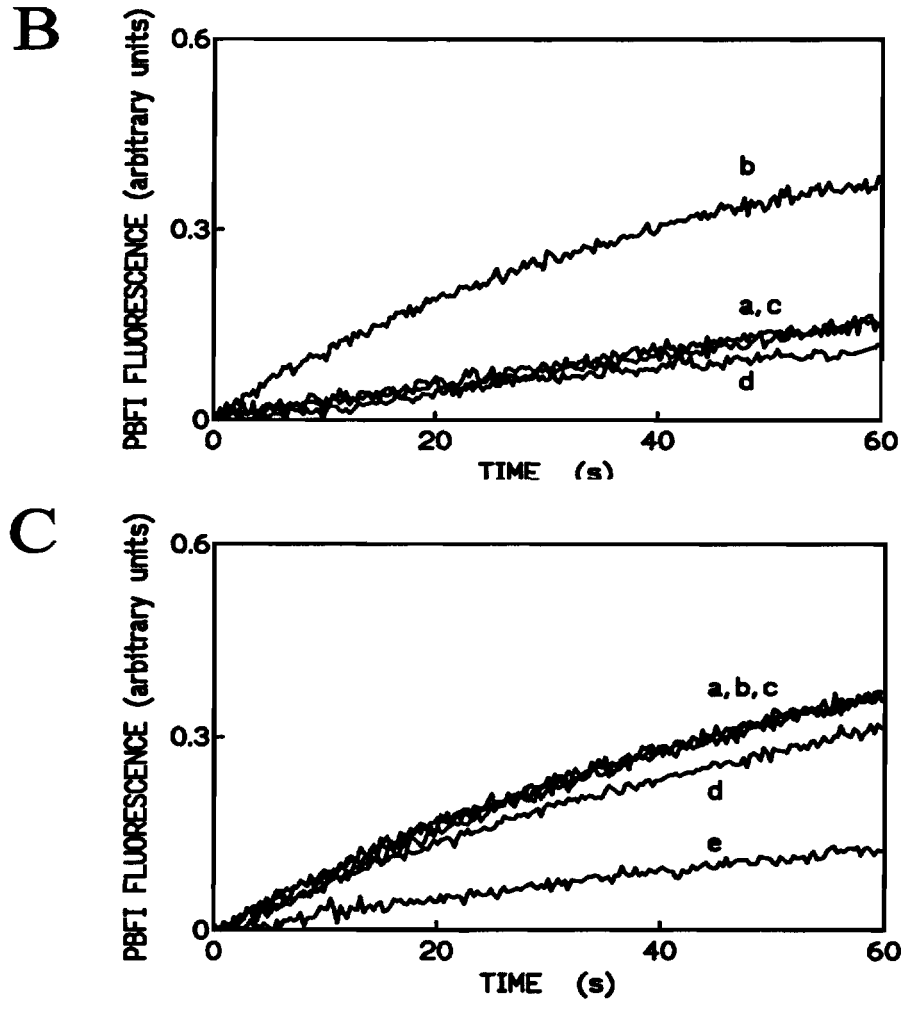

Figure 4.2 The effects of reconstitution buffer composition on behavior of reconstituted mitoK$_{ATP}$. Each panel contains PBFI fluorescence traces from liposomes reconstituted with purified mitoK$_{ATP}$ in different internal media. K^+ influx is reflected in increasing PBFI fluorescence.

Panel B: MgATP vesicles. Vesicles were reconstituted in standard internal medium containing 0.5 mM ATP, 3 mM Mg^{2+}, and no EDTA. *Trace a*, assay medium contained no Mg^{2+} and no ATP. *Trace b*, assay medium as used for trace a, plus 0.5 μM 4-Br-A23187 and 5 mM EDTA. *Trace c*, assay medium contained 3 mM Mg^{2+}, 0.5 μM 4-Br-A23187, and no EDTA or ATP. *Trace d*, assay medium as used for trace b, but FCCP was omitted (baseline).

Panel C: Mg vesicles. Vesicles were reconstituted in standard internal medium containing 3 mM Mg^{2+} and no EDTA or ATP. *Trace a*, assay medium contained no Mg^{2+} and no ATP. *Trace b*, assay medium contained 3 mM Mg^{2+} and no ATP. *Trace c*, assay medium contained no Mg^{2+} and 0.5 mM ATP. *Trace d*, assay medium contained 3 mM Mg^{2+} and 0.5 mM ATP. *Trace e*, assay medium as used for trace a, but FCCP was omitted (baseline).

4.2.3 The polarity of reconstituted mitoK$_{ATP}$

The findings contained in Fig. 4.2 are consistent with two interpretations which cannot be distinguished unequivocally by the preceding experiments. Either the channel has bipolar nucleotide regulatory sites, or its orientation in the liposomal membrane is reversed by the presence of Mg^{2+} or ATP during liposome formation. Special protocols were devised to distinguish between these alternatives.

We prepared MgATP vesicles in which K^+ flux was 90% inhibited in the absence of external ATP, as was demonstrated in Fig. 4.2B. We preincubated these liposomes in 1 mM EDTA with a low dose of 4-Br-A23187 that was (i) sufficient to remove Mg^{2+} in the *concentrated* suspension, but (ii) insufficient to catalyze Mg^{2+} flux after 130-fold dilution into the assay medium. The test of the first requirement is to show that the A23187 pretreatment was sufficient to activate K^+ flux. The test of the second requirement is to show that adding Mg^{2+} to the assay medium does not re-inhibit K^+ flux, because final [A23187] is too low to catalyze Mg^{2+} uptake.

Both criteria were satisfied by preincubation with 0.5 μM 4-Br-A23187. Pretreatment fully activated K^+ flux (Fig. 4.3, *trace a*) by comparison to control with high 4-Br-A23187 added to the assay medium (see Fig. 4.2B, *trace b*). Furthermore, K^+ flux was not inhibited when assayed in 3 mM Mg^{2+} (Fig. 4.3, *trace b*), showing that dilution of A23187 rendered it ineffective over the time period studied. Results of the test experiment are shown in *trace c* of Fig. 4.3. These Mg^{2+}-depleted MgATP vesicles were inhibited only 10% by external ATP and Mg^{2+}. When the assay medium contained Mg^{2+} and 0.5 μM 4-Br-A23187, K^+ flux was inhibited 85% by internal MgATP (Fig. 4.3, *trace d*). This result was obtained with three separate reconstitutions.

The experiments shown in Figs. 4.2 and 4.3 establish that composition of the reconstitution buffer determines mitoK$_{ATP}$ orientation, that ATP acts only on one side of mitoK$_{ATP}$, and that ATP and Mg^{2+} act on the same side. These statements also apply to GTP and palmitoyl-CoA. External GTP activates the ATP-inhibited mitoK$_{ATP}$ when added to EDTA vesicles on the same side as ATP (69), whereas external GTP has no effect on the inhibited K^+ flux observed in MgATP vesicles (see Fig. 4.8). Similarly, palmitoyl-CoA was unable to inhibit K^+ flux in Mg vesicles

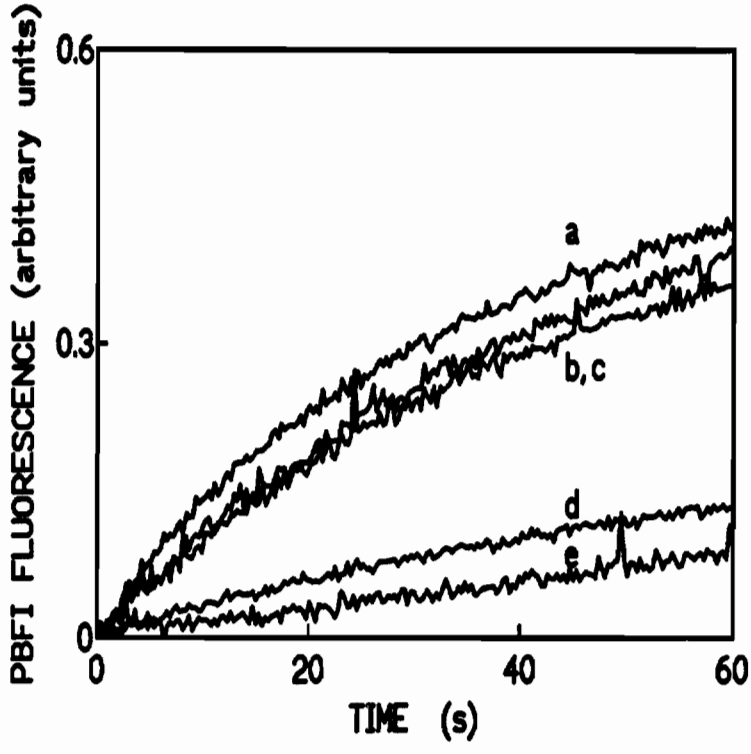

Figure 4.3 Demonstration that ATP inhibition of mitoK$_{ATP}$ is unipolar. Figure contains PBFI fluorescence traces from liposomes reconstituted with purified mitoK$_{ATP}$ in internal medium containing 3 mM Mg^{2+} and 0.5 mM ATP, as described in legend to Fig. 4.2B. These liposomes were preincubated at 4°C for 5 min with 0.5 μM 4-Br-A23187 and 1 mM EDTA, then diluted 130-fold into the assay media. *Trace a*, K^+ flux was activated by pretreatment to remove intraliposomal Mg^{2+}. Assay medium contained no Mg^{2+} and no ATP. *Trace b*, residual 4-Br-A23187 is inadequate to restore inhibition by internal ATP. Assay medium contained 3 mM Mg^{2+} and no ATP. *Trace c*, K^+ flux in MgATP vesicles cannot be inhibited by external MgATP; therefore, the nucleotide binding sites are intraliposomal. Assay medium contained 3 mM Mg^{2+} and 0.5 mM ATP. *Trace d*, assay medium contained 0.5 μM 4-Br-A23187 and 3 mM Mg^{2+}. *Trace e*, control. Assay medium as used for trace a, but FCCP was omitted.

(data not shown), indicating that palmitoyl-CoA could not gain access to the internalized binding sites.

4.2.4 Polarity of mitoK$_{ATP}$ following incorporation in BLM

Fig. 4.4 contains a typical single channel record from BLM after fusion with liposomes containing purified mitoK$_{ATP}$. (The same liposomes exhibited ATP-sensitive K^+ flux.) In the experiment shown in Fig. 4.4, both chambers contained 150 mM KCl and 5 mM Ca^{2+}, and ATP was added to the chamber *trans* to the direction of K^+ flux driven by 100 mV. ATP blocked the current almost completely. On the other hand, when ATP was added to the opposite chamber, there was no inhibition (not shown). We observed this asymmetry in over ten experiments. These results provide independent evidence for the contention that mitoK$_{ATP}$ is asymmetric with respect to ATP inhibition.

4.2.5 Orientation of mitoK$_{ATP}$ in intact mitochondria

The preceding experiments set the stage for determining the side on which nucleotides and Mg^{2+} interact with mitoK$_{ATP}$ *in situ*. The traces in Fig. 4.5 demonstrate progressive inhibition of respiration-induced K^+ uptake by increasing doses of palmitoyl CoA. Like ATP, palmitoyl-CoA was without effect in the absence of Mg^{2+} (data not shown). Fig. 4.6 contains dose–response curves for inhibition by palmitoyl-CoA and ATP in the presence of 1 mM Mg^{2+}. The $K_{1/2}$ for palmitoyl-CoA in intact mitochondria is about 262 nM ($n_H \approx 3.8$), very similar to the value for inhibition of K^+ flux through reconstituted mitoK$_{ATP}$ [69]. The $K_{1/2}$ for ATP is about 2.5 μM ($n_H \approx 1$). The finding that externally added palmitoyl-CoA and ATP inhibit ATP-sensitive K^+ flux is consistent with interaction with external sites on mitoK$_{ATP}$.

Fig. 4.7 contains dose–response curves for activation of K^+ flux in mitochondria by GTP. Assay media also contained 100 μM ATP and 1 mM Mg^{2+}, which completely inhibit K^+ flux through mitoK$_{ATP}$ in intact mitochondria. GTP restored K^+ flux to fully active rates with $K_{1/2} = 4.6$ μM ($n_H \approx 1$), similar to values observed with reconstituted mitoK$_{ATP}$ (69). Since mitochondria contain no transport systems for GTP, this result shows that GTP is acting on the cytosolic face of mitoK$_{ATP}$.

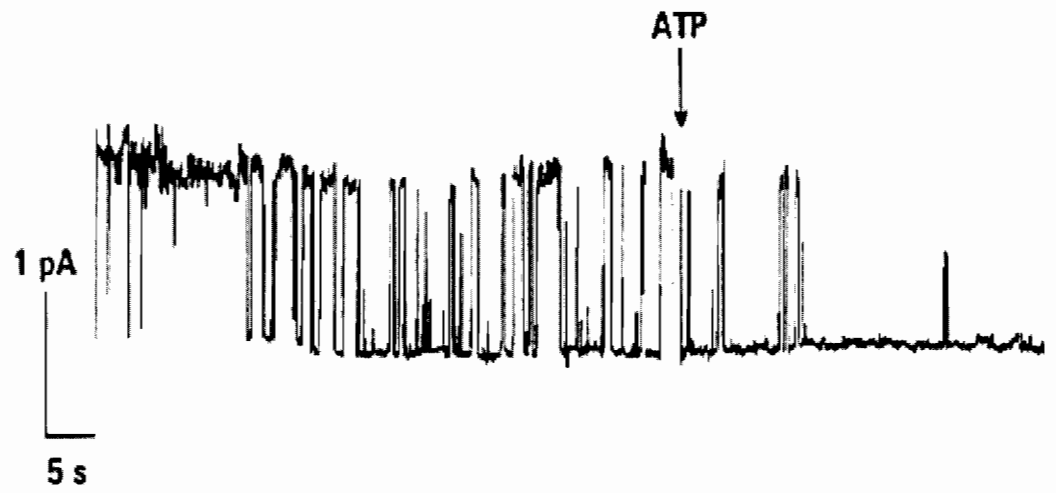

Figure 4.4 ATP-sensitive single channel currents from purified mitoK_{ATP} incorporated in lipid bilayer membranes. Figure contains a single channel record (1.6 pA in 150/150 mM KCl, +100 mV) from BLM after fusion with liposomes containing purified mitoK_{ATP}. 1 mM ATP was added to the *trans* side of the membrane. ATP also inhibited K^+ current when the potential was reversed, but no effect was observed when ATP was added to the *cis* side of the membrane. Similar results were obtained in ten bilayer experiments. Media contained 150 mM KCl, 5 mM Ca^{2+} and 20 mM Tris-HCl (pH 7.2) on both sides of the chamber.

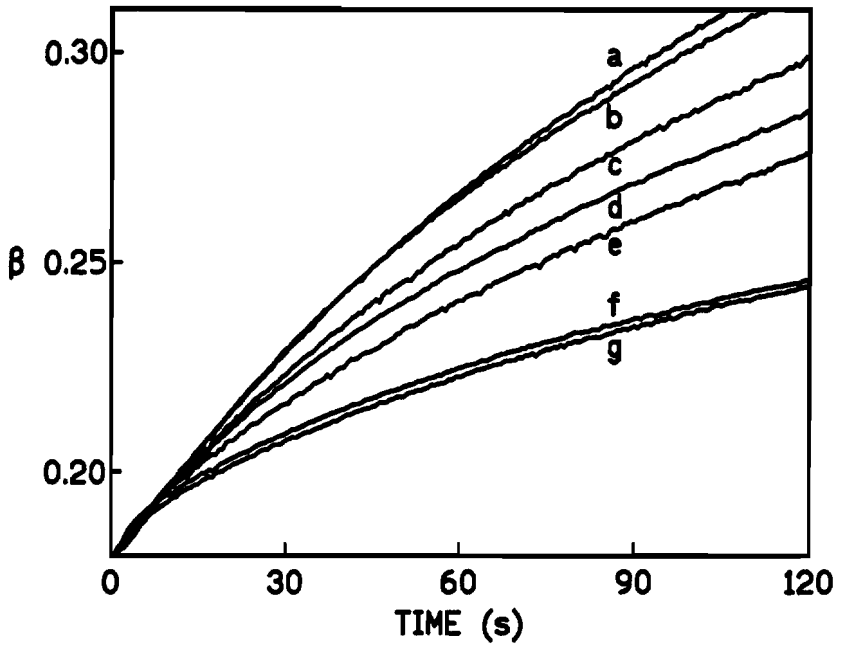

Figure 4.5 Palmitoyl-CoA inhibits K^+ flux in intact mitochondria. Light-scattering kinetics for mitochondria suspended in K^+ media are shown (see Section 4.1). *Trace a*, control trace in assay medium containing 1 mM Mg^{2+} and no ATP. *Traces b, c, d, e, and f*, assay medium containing 1 mM Mg^{2+} and 133, 200, 250, 300, and 2000 nM of palmitoyl-CoA, respectively. *Trace g*, maximally inhibited K^+ flux in assay medium containing 1 mM Mg^{2+} and 0.1 mM ATP. Palmitoyl-CoA inhibited K^+ flux to the level observed in the presence of saturating ATP. Palmitoyl-CoA had no effect if Mg^{2+} was absent from assay medium. These results are representative of three experiments. Ascorbate/TMPD was used as substrate.

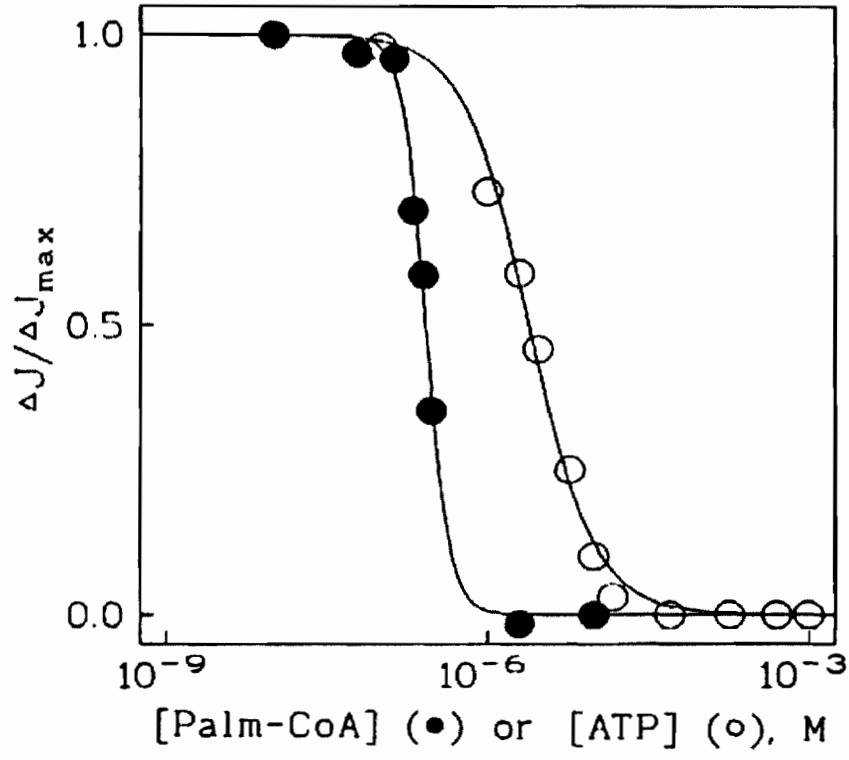

Figure 4.6 Dose–response curves for inhibition of K^+ flux in mitochondria by palmitoyl-CoA and ATP. Relative ATP-sensitive K^+ uptake into respiring rat liver mitochondria, $\Delta J/\Delta J_{max}$, is plotted versus concentrations of palmitoyl-CoA (●) or ATP (○), in the presence of 1 mM Mg^{2+}. ΔJ_{max} is the maximum ATP-sensitive K^+ flux (i.e., the difference between control fluxes in the absence and presence of saturating ATP). ΔJ is the difference between fluxes in the presence and absence of palmitoyl-CoA or ATP. $K_{1/2}$ values and Hill coefficients are given in the text.

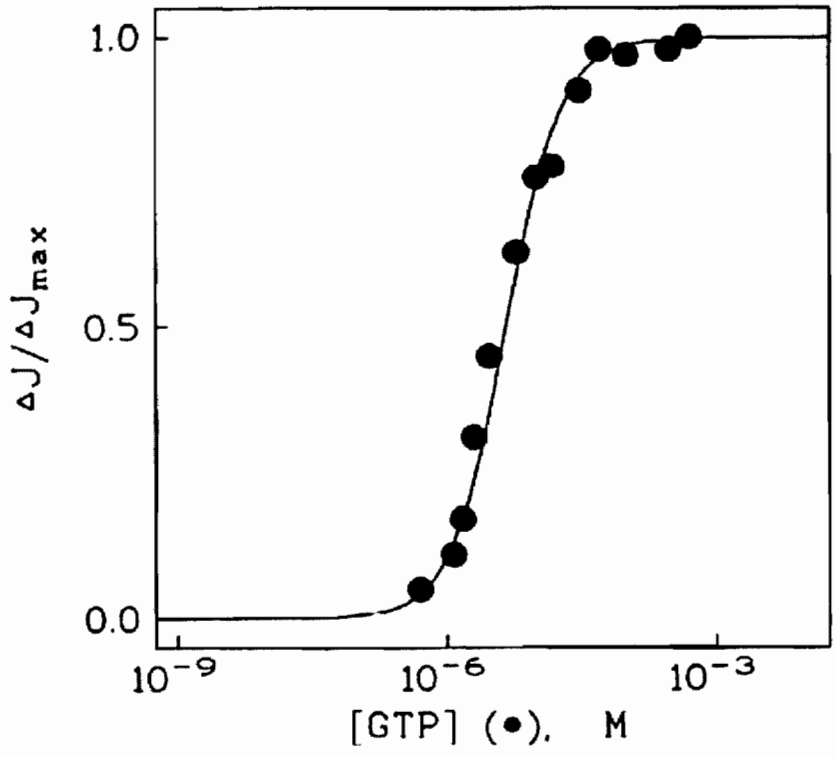

Figure 4.7 Dose–response curves for activation of ATP-inhibited K^+ flux in mitochondria by GTP. Relative ATP-sensitive K^+ uptake into respiring rat liver mitochondria, $\Delta J/\Delta J_{max}$, is plotted versus concentrations of GTP (●) in the presence of 1 mM Mg^{2+}. ΔJ_{max} is defined in Fig. 4.6. ΔJ is the difference between fluxes in the presence and absence of GTP, with both fluxes being measured in 0.1 mM ATP. $K_{1/2}$ value and Hill coefficient are given in text.

The K^+ channel opener, cromakalim, was previously shown to restore K^+ flux from the fully inhibited state in MgATP to control rates observed in the absence of MgATP (70). In additional experiments (not shown), we observed that neither cromakalim nor GTP activated K^+ flux *beyond* control rates, whether or not mitoK_{ATP} was inhibited by palmitoyl CoA or ATP. Cromakalim is a membrane permeant drug (see Fig. 4.8); consequently, this result shows that mitoK_{ATP} is *fully* asymmetric in intact mitochondria and does not have nucleotide regulatory sites facing in both directions.

4.2.6 Accessibility of the internalized mitoK_{ATP} receptor to K^+ channel openers

The experiments in Fig. 4.8 were carried out in MgATP vesicles, in which the nucleotide-binding sites are oriented inward. These preparations were assayed for the ability of GTP, cromakalim, and diazoxide to activate the inhibited channels. As can be seen from the figure, the K^+ channel openers fully activated the channel, whereas GTP was without its normal activating effect. The $K_{1/2}$ values for cromakalim (1.7 μM) and diazoxide (0.6 μM) are very close to the values obtained in preparations with outward orientation (70). Thus, these hydrophobic drugs can activate from either side of the membrane, whereas the impermeant GTP cannot.

4.3 Discussion

MitoK_{ATP} is exquisitely sensitive to metabolites, including adenine nucleotides (inhibitors), long-chain acyl-CoA esters (inhibitors), and guanine nucleotides (activators) (68, 69). Metabolite inhibition exhibits an absolute requirement for Mg^{2+} ions, which appear to react independently with the receptor (69). *In vivo*, these ligands exist on both sides of the inner membrane, and no experiments have heretofore been performed to determine which pool regulates mitoK_{ATP}. The cell physiology of mitoK_{ATP} regulation is a new and important area of investigation. To establish whether the mitoK_{ATP} receptor sites face the cytosol or the mitochondrial matrix is a prerequisite for such studies.

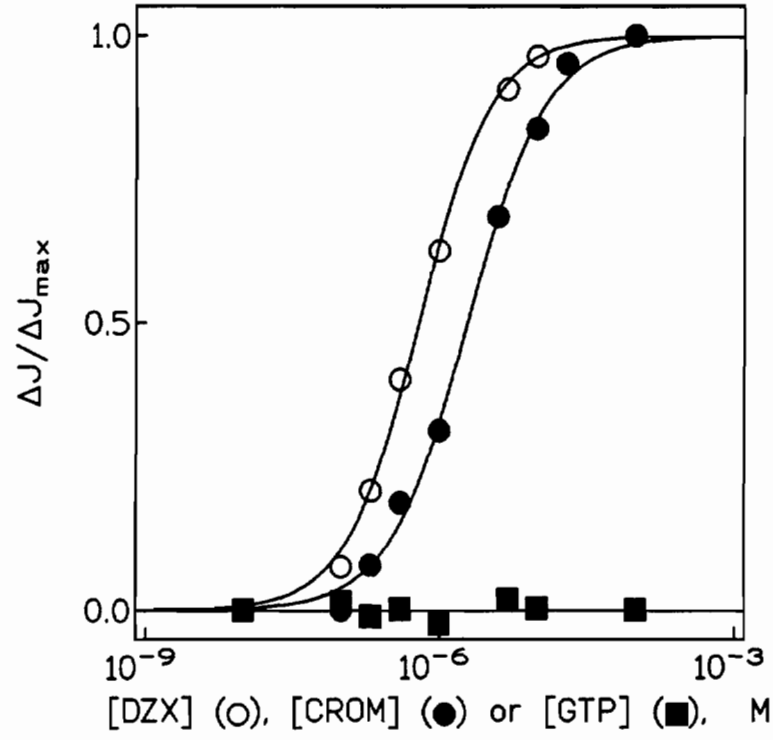

Figure 4.8 Effects of K^+ channel openers and GTP on inward-oriented mitoK_{ATP} (MgATP vesicles). The relative ATP-sensitive K^+ uptake into liposomes reconstituted with mitoK_{ATP}, $\Delta J/\Delta J_{max}$, is plotted versus concentration of GTP (■), cromakalim (●) and diazoxide (○), which were added to the KCl assay medium. Vesicles were reconstituted in internal medium containing 3 mM Mg^{2+} and 0.5 mM ATP without EDTA, which induces an inward orientation of the nucleotide receptors. Two experiments yielded essentially the same results. ΔJ_{max} is the difference between control fluxes in the activated (0.5 μM 4-Br-A23187 and 5 mM EDTA added to assay) and inhibited (no additions) states of MgATP vesicles. ΔJ is the difference between fluxes in the presence or absence of drug or GTP.

Our experiments yielded an unambiguous answer to this question with results that may be summarized as follows:

(i) In proteoliposomes, orientation of mitoK$_{ATP}$ is determined by the composition of the reconstitution buffer. The ATP regulatory sites were oriented outward when reconstituted in EDTA medium and inward when reconstituted in the presence of Mg^{2+}. It is interesting that we previously observed a similar orienting effect of Mg^{2+} ions on the reconstituted K^+/H^+ antiporter (141). We also showed in liposomes that nucleotides, palmitoyl CoA, and Mg^{2+} ions regulate from one and the same side of the channel.

(ii) In BLM, mitoK$_{ATP}$ is also unipolar, with ATP inhibition being seen from only one side.

(iii) In intact mitochondria, nucleotide regulatory sites on mitoK$_{ATP}$ are accessible from the *external* medium. Thus, external GTP maximally activates, and external palmitoyl-CoA maximally inhibits, mitoK$_{ATP}$ under conditions in which these ligands are not transported across the inner membrane.

Taken together, our results establish the topology of mitoK$_{ATP}$ as it exists in the inner membrane of intact mitochondria: the regulatory domains face the *cytosol* or, more specifically, the intermembrane space between inner and outer mitochondrial membranes. This conclusion does not exclude the possibility that other ligands may regulate from the matrix side, but none has yet been identified.

This result conflicts with the conclusion of Inoue et al. (65) that mitoK$_{ATP}$ is inhibited by ATP added to the *matrix* side of the membrane. In those experiments, patch clamp was applied to fused giant mitoplasts that had undergone severe osmotic swelling and exposure to 20 mM Ca^{2+}. No experiments were undertaken to establish the sidedness of the fused mitoplasts. A possible explanation for the discrepancy is that the membranes were inverted during this fusion process as occurs, for example, with submitochondrial particles. This discrepancy must be resolved by future experiments.

Cromakalim and diazoxide are able to activate the ATP-inhibited mitoK$_{ATP}$ in either orientation, with the regulatory sites facing inward (Fig. 4.8), or outward (70). Thus, the intracellular location of the mitoK$_{ATP}$ receptor does not prevent access by

hydrophobic drugs, such as K^+ channel openers and glyburide *in vivo*. This important pharmacological point supports our hypothesis (70) that mitoK_{ATP} may be a receptor for the cardioprotective actions of K^+ channel openers.

Chapter 5

PHOTOAFFINITY LABELING AND PURIFICATION OF MitoSUR, THE SULFONYLUREA RECEPTOR OF THE MITOCHONDRIAL K_{ATP} CHANNEL*

The ATP-sensitive K^+ channel of mitochondria (mitoK_{ATP}) regulates the volume of the matrix and the intermembrane space (75). MitoK_{ATP} has gained new importance with the discovery that it is the receptor for the protective actions of K^+ channel openers in ischemia–reperfusion injury (76), a result that has been confirmed by Liu et al. (93). Although the mechanism of cardioprotection is unknown, it presumably involves endogenous regulation of mitoK_{ATP} (142).

MitoK_{ATP} is highly regulated and closely resembles plasma membrane K_{ATP} channels (cellK_{ATP}) in its physiological and pharmacological properties (68). Thus, mitoK_{ATP} is regulated by ATP, GTP, long-chain acyl-CoA esters, K^+ channel openers, glyburide, and 5-hydroxydecanoate (68–72, 75, 142). CellK_{ATP} channels are regulated by a separate sulfonylurea receptor (50, 51, 55, 56). Based on the observation that two proteins are found in the highly purified, reconstitutively active mitoK_{ATP} fraction, we have suggested that mitoK_{ATP} is also a heteromultimer, consisting of an inwardly rectifying K^+ channel (mitoKIR) and a sulfonylurea receptor (mitoSUR) (75).

To test this hypothesis, we photolabeled inner membrane proteins with the fluorescent analogue of glyburide, FL-glyburide. Only one inner membrane protein was specifically labeled, and it migrated at 63 kD on SDS-PAGE. We also raised

---

* This material will be published in this or similar form in *The Journal of Biological Chemistry* and is used here with permission of the American Society for Biochemistry and Molecular Biology.

Paucek, P., Yarov-Yarovoy, V., and Garlid, K. D. (1998) Photoaffinity labeling and purification of mitoSUR, the sulfonylurea receptor of the mitochondrial K_{ATP} channel. *J. Biol. Chem.*, in review.

polyclonal antibodies to a 55-kD protein band, which is also associated with mitoK$_{ATP}$ activity (68). The antibodies inhibited K^+ flux when added to proteoliposomes containing partially purified mitoK$_{ATP}$, but they did not react with the 63-kD protein. We conclude that mitoK$_{ATP}$ functions as a multimeric complex consisting of a 63-kD mitoSUR and a 55-kD mitoKIR.

5.1 Materials and Methods

5.1.1 Purification of guanidine-treated membranes (3xGMs) from rat liver mitochondria

Guanidine-treated inner mitochondrial membrane vesicles were prepared as described in Chapter 2.

5.1.2 Purification, reconstitution, and assay of mitoK$_{ATP}$

Purification, reconstitution, and assay of mitoK$_{ATP}$ followed protocols described in Chapter 2. The fraction eluted between 200 and 300 mM KCl was reconstitutively active (68, 110) and is hereafter designated the active DEAE fraction.

For further purification, the active DEAE fraction was loaded onto a 1-ml ATP-affinity column (immobilized on cross-linked 4% beaded agarose, from Sigma) that had been equilibrated with Mg-column buffer (column buffer containing 1 mM Mg^{2+}). The column was sequentially washed with 2 bed volumes each of Mg-column buffer containing 0 mM NaCl, 500 mM NaCl, 20 mM ATP, and 1% SDS. The fraction eluted with 20 mM ATP was reconstitutively active and is hereafter designated the active ATP fraction.

5.1.3 Purification of anti-55-kD protein polyclonal antibodies

The 55-kD protein from rat liver mitochondria was extracted by ethanol (143) and purified as described previously (68). 10–20 μg were injected into each of two rabbits at 3–4-week intervals, using established procedures (144). The 55-kD protein was used to immunopurify the antibodies, according to the method of Smith and

Fisher (145). The resulting polyclonal antibodies were monospecific, as shown by western blot (see Results).

5.1.4 FL-glyburide labeling of 3xGMs

1 ml of the 3xG membrane stock suspension was incubated for 120 min at room temperature with 100 nM FL-glyburide, in the presence or absence of 1 μM unlabeled glyburide. The reaction mixture was then UV-irradiated for 2 min at 4°C by a 15 W high-intensity mercury lamp at a distance of 5 cm. Proteins were then extracted and purified on a DEAE-cellulose column, exactly as described above. Each eluted fraction was analyzed for FL-glyburide fluorescence using an excitation wavelength of 493 nm (1-nm slit) and an emission wavelength of 515 nm (8-nm slit).

5.1.5 FL-glyburide labeling of Triton-solubilized proteins

The active DEAE and ATP fractions, containing Triton-solubilized proteins, were also used for FL-glyburide labeling. Fractions were incubated for 60 min at 25°C with 50 nM FL-glyburide, in the presence or absence of 1 μM unlabeled glyburide and/or the following compounds: 20 mM ATP, 1 mM Mg^{2+}, 1 mM EDTA, and 100 μM cromakalim. The reaction mixture was UV-irradiated as described above. Each sample was precipitated by the method of Wessel and Flugge (146), dissolved in 50 mM Tris-HCl, pH 6.8, containing 5% SDS, then diluted 20 times with 50 mM Tris-HCl, pH 6.8, and analyzed directly for fluorescence as described above.

5.1.6 [^{125}I]-Azidoglyburide labeling of 3xGMs

3xG membrane stock suspension (1 ml) was supplemented with 0.1 mM PMSF and incubated for 30 min at room temperature with 5 nM [^{125}I]-azidoglyburide in the presence or absence of 1 μM unlabeled glyburide. Samples were irradiated in a UV-crosslinker at 254 nm at 0.6 J/cm^2 at room temperature. Proteins were extracted and purified as described above, except that a 2-ml DEAE-cellulose column was used. Each fraction was precipitated, dissolved in 5% SDS sample buffer, and subjected to

SDS-PAGE (147). After staining with Coomassie Brilliant Blue R-250 (148), the gels were vacuum dried at 80°C and autoradiographed.

5.1.7 8-Azido-[α-^{32}P]ATP labeling of 3xGMs

3xG membrane stock suspension (1 ml) was incubated overnight at 4°C with 2 μM 8-azido-[α-^{32}P]ATP in the presence or absence of 1 mM unlabeled ATP. Samples were irradiated, extracted, and purified as described above. Fractions were precipitated and electrophoresed for autoradiograms, as described above.

5.1.8 Preparative electrophoresis

The fraction containing specific glyburide labeling was loaded onto an 8-cm cylindrical sieving SDS-PAGE matrix of a Model 491 Prep Cell (Bio-Rad) and run at 40 mA constant current for 8–12 h. As the individual proteins migrated from the gel, they were collected by a constant flow of elution buffer (0.1% SDS, 192 mM glycine, and 25 mM Tris) through an elution frit to a fraction collector. Eluted fractions (800 μl each) were then analyzed for FL-glyburide fluorescence, as described above.

5.1.9 Materials

FL-glyburide was from Molecular Probes, Inc. (Eugene, OR). Electrophoresis reagents were purchased from Bio-Rad (Hercules, CA). 8-azido-[α-^{32}P]ATP was from ICN (Costa Mesa, CA). [^{125}I]-Azidoglyburide was the kind gift of Dr. Joseph Bryan. All other chemicals were obtained from Sigma Chemical (St. Louis, MO) unless otherwise indicated.

5.2 Results

5.2.1 Purification of the mitochondrial K_{ATP} channel

The active DEAE fraction, described in Section 5.1, was desalted and loaded onto a second DEAE-cellulose column and eluted with a shallow, linear KCl gradient. Two predominant protein bands, migrating at 55 kD and 63 kD, can be seen in lanes 4–7 of the SDS-PAGE in Fig. 5.1A. The active DEAE fraction was further purified

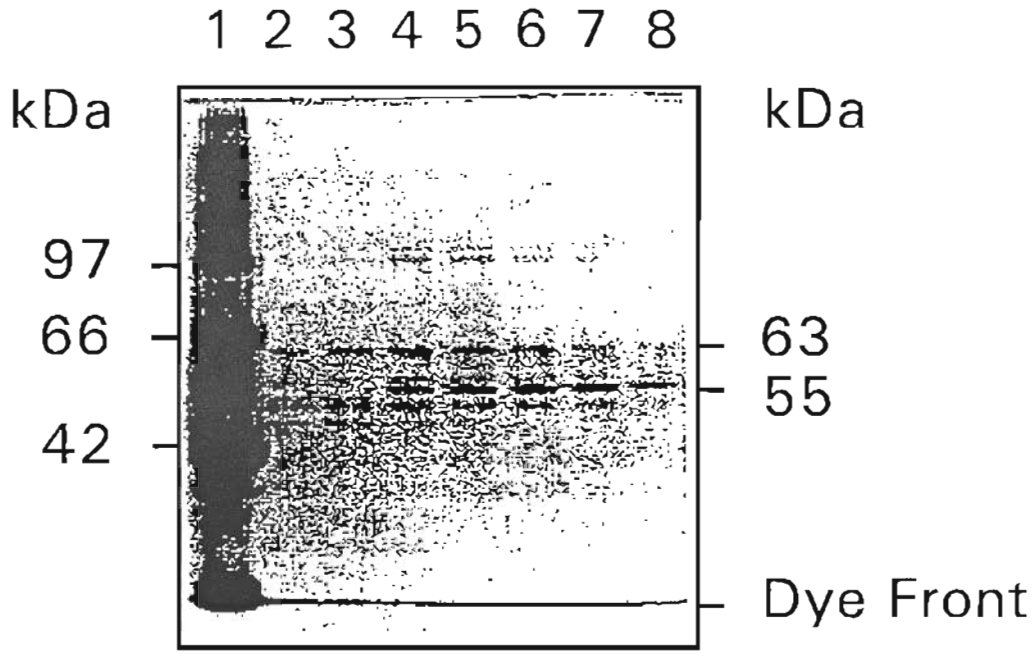

Figure 5.1 Purification of the mitochondrial K_{ATP} channel.

Panel A: Silver-stained gels from 7.5% SDS-PAGE of fractions eluted from a DEAE-cellulose column. Numbers on the left indicate positions of the molecular weight standards. *Lane 1*, molecular weight standards; *lanes 2–8*, fractions eluted with a linear KCl gradient ranging from 200 to 350 mM KCl.

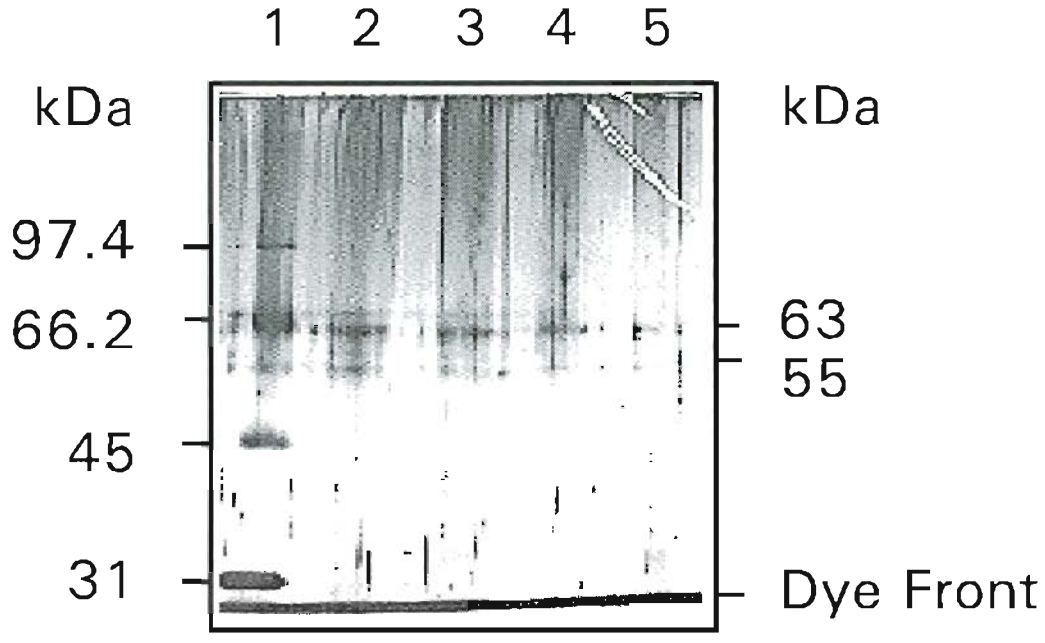

Figure 5.1 Purification of the mitochondrial K_{ATP} channel.

Panel B: Silver-stained gels from 10% SDS-PAGE of fractions eluted from an ATP-affinity column. *Lane 1*, molecular weight standards; *lanes 2–5*, fractions eluted by 20 mM ATP.

on an ATP-affinity column. The resulting active ATP fraction, described in Section 5.1, also contained two major bands at 55 kD and 63 kD (Fig. 5.1B). When either of these fractions was reconstituted into liposomes, K^+ flux was inhibited by ATP and glyburide, as previously shown (68).

5.2.2 Anti-55-kD polyclonal antibodies

A typical western blot analysis is shown in Fig. 5.2A. The anti-55-kD antibodies, raised against rat liver protein, recognized a 55-kD protein purified from both beef heart (Fig. 5.2A, lane 1) and rat liver (Fig. 5.2A, lane 4) mitochondria. Significantly, these antibodies did not react with the 63-kD protein, which was also present in this fraction.

The polyclonal antibodies inhibited K^+ flux in proteoliposomes reconstituted with the active DEAE fraction from either beef heart or rat liver mitochondria (Fig. 5.2B). As a negative control, we used proteoliposomes reconstituted with the beef heart sarcolemmal K_{ATP} channel (71). The antibodies had no effect on K^+ flux in this system (data not shown). Inhibition of K^+ flux by anti-55-kD polyclonal antibodies was not associated with any loss of PBFI fluorescence signal, indicating no effect of the antibodies on the liposomes.

5.2.3 Labeling of mitochondrial membrane vesicles by [^{125}I]-azidoglyburide and 8-azido-[α-^{32}P]ATP

Fig. 5.3A, contains an autoradiogram of the purified active DEAE fraction following labeling of membrane vesicles with [^{125}I]-azidoglyburide in the absence (Fig. 5.3A, *lane a*) or presence (Fig. 5.3A, *lane b*) of unlabeled glyburide. Only the active fraction exhibited specific [^{125}I]-azidoglyburide labeling of 63-, 55-, and 33-kD proteins, i.e., labeling that was abolished by 1 μM unlabeled glyburide. Fig. 5.4 shows that a similar result was obtained when 8-azido-[α-^{32}P]ATP was used to photolabel inner mitochondrial membrane vesicles in the absence (Fig. 5.4A, *lane a*) or presence (Fig. 5.4A, *lane b*) of 1 mM unlabeled ATP.

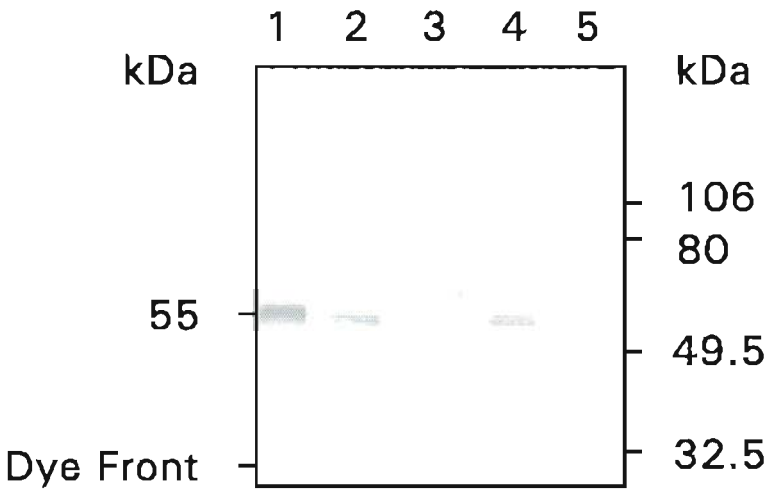

Figure 5.2 Inhibition of K^+ flux by anti-55-kD polyclonal antibodies.

Panel A: Western blots. Beef heart and rat liver mitochondrial proteins were subjected to 10% SDS-PAGE, transferred onto nitrocellulose, and analyzed by western blot with anti-55-kD polyclonal antibodies. Numbers on the right indicate positions of the molecular weight standards. *Lane 1*, active DEAE fraction from beef heart mitochondria; *lane 2*, total protein extract of inner membrane vesicles purified from beef heart mitochondria; *lane 3*, prestained molecular weight standards; *lane 4*, active DEAE fraction from rat liver mitochondria; *lane 5*, total protein extract of inner membrane vesicles purified from rat liver mitochondria.

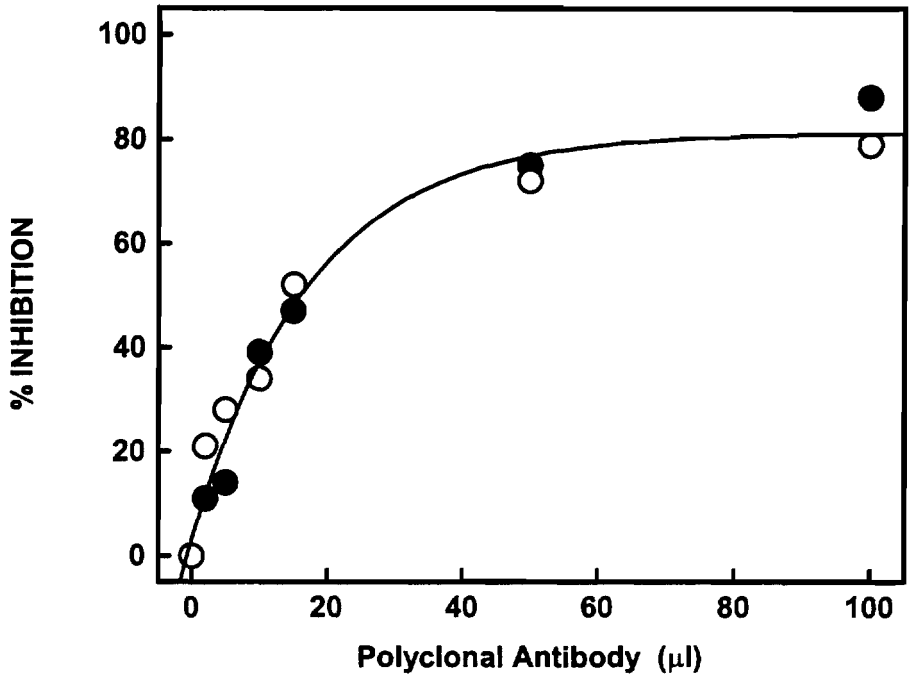

Figure 5.2 Inhibition of K^+ flux by anti-55-kD polyclonal antibodies.

Panel B: Inhibition of K^+ flux. Dose-response curves for inhibition of K^+ flux in proteoliposomes reconstituted with the active DEAE fraction. Antibodies were diluted $1:10^4$ and pre-incubated for 60 min with proteoliposomes reconstituted with mitoK_{ATP} from beef heart mitochondria (●) and rat liver mitochondria (○).

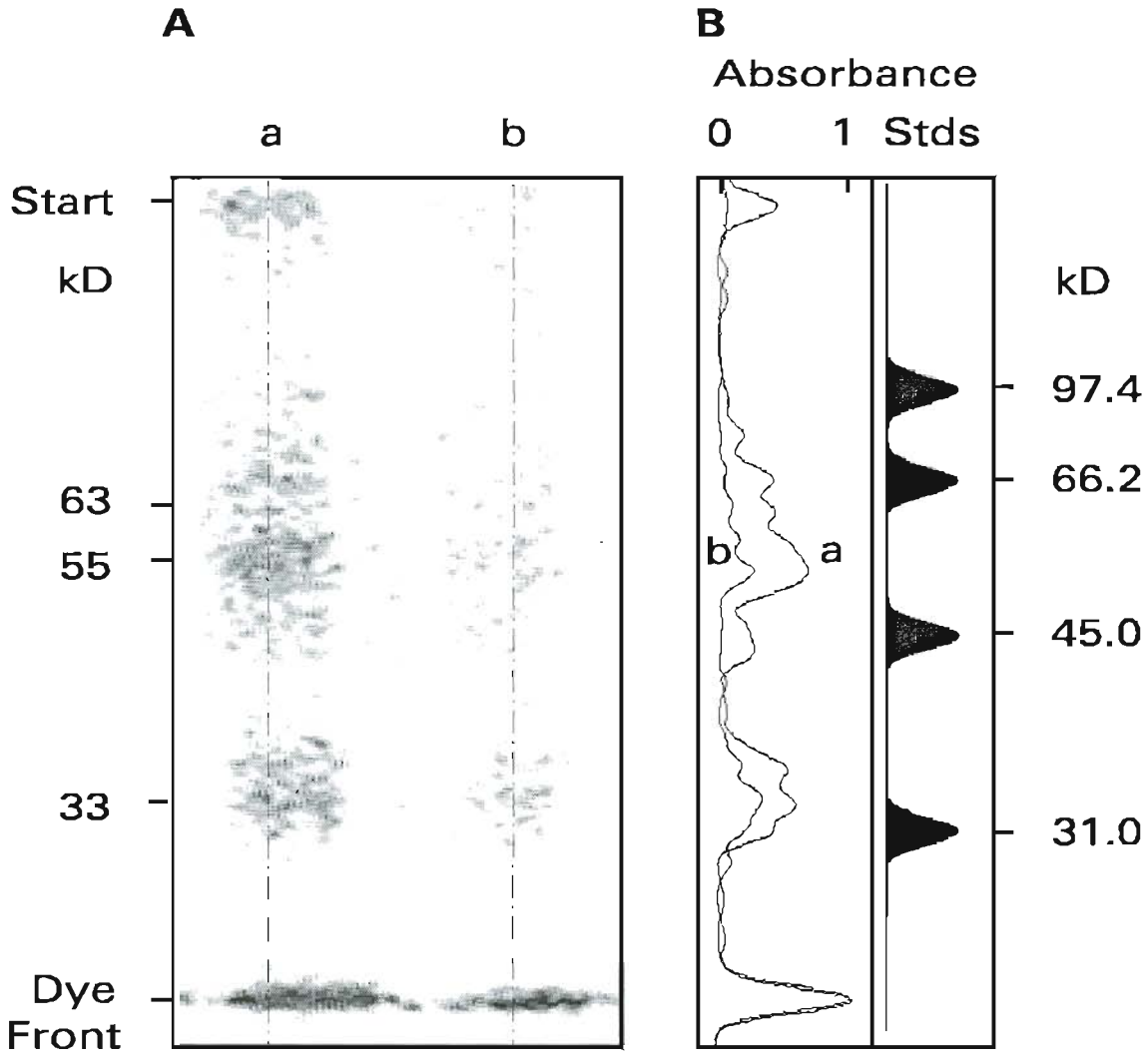

Figure 5.3 Autoradiograms following labeling of vesicles with [^{125}I]-azidoglyburide. After labeling, the active DEAE fraction was obtained for autoradiography, as described in Section 5.1.

Panel A: Autoradiograms: *Lane a*, fraction from a preparation labeled with [^{125}I]-azidoglyburide only. *Lane b*, fraction from a preparation labeled with [^{125}I]-azidoglyburide in the presence of 1 μM unlabeled glyburide.

Panel B: Absorbance readings of lanes a and b from panel A. Numbers on the right indicate position of the molecular weight standards.

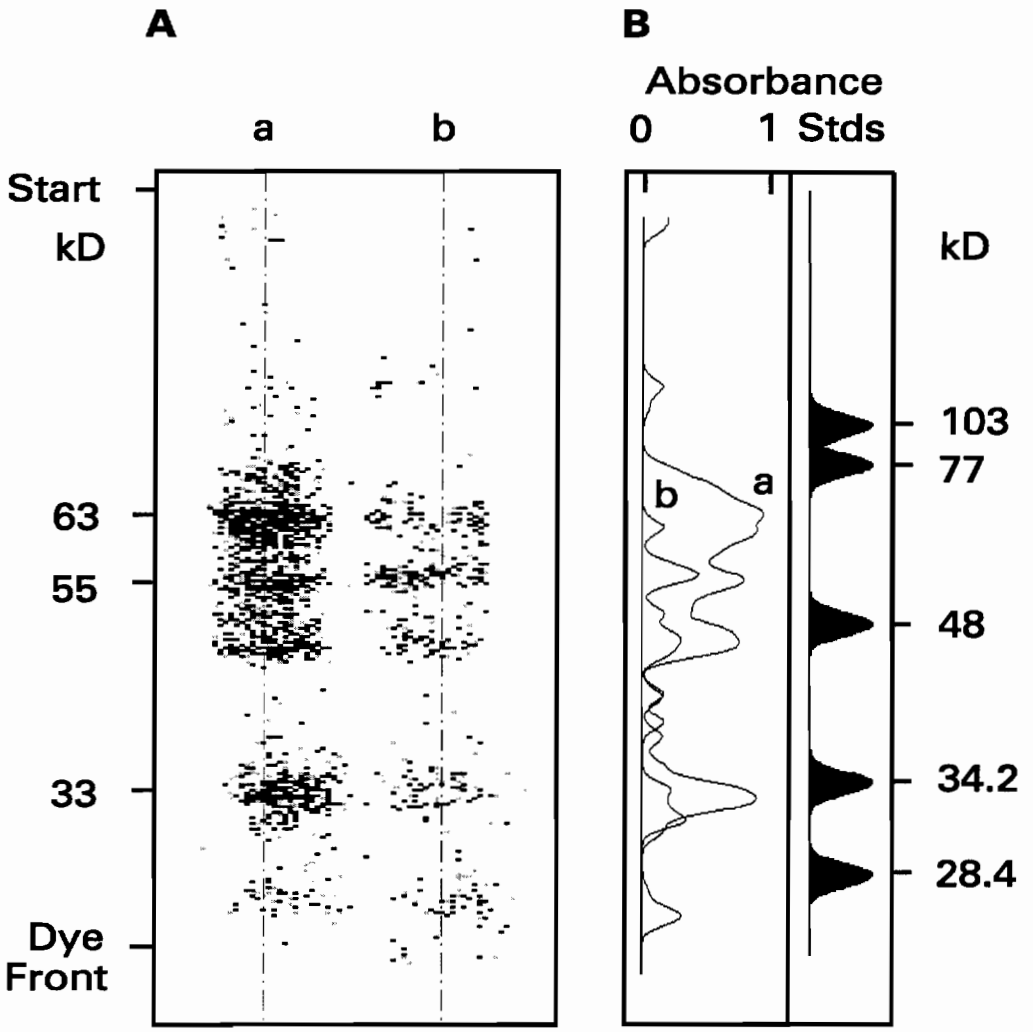

Figure 5.4 Autoradiograms following labeling of vesicles with 8-azido-[α-^{32}P]ATP. After labeling, the active DEAE fraction was obtained for autoradiography, as described in Section 5.1.

Panel A: Autoradiograms: *Lane a*, fraction from preparation labeled with 8-azido-[α-^{32}P]ATP only. *Lane b*, fraction from preparation labeled with azido-[α-^{32}P]ATP in the presence of 1 mM unlabeled ATP.

Panel B: Absorbance readings of lanes a and b from panel A. Numbers on the right indicate positions of the molecular weight standards.

5.2.4 Labeling of mitochondrial membrane vesicles by FL-glyburide

The glyburide molecule is intrinsically photoreactive and can be used directly as a photoaffinity probe (149). Fig. 5.5 contains fluorescence data obtained from all DEAE column fractions. While all fractions contained non-specifically labeled proteins, only the reconstitutively active DEAE fraction, fraction 4, exhibited specific labeling, defined as FL-glyburide fluorescence that was significantly reduced by 1 μM unlabeled glyburide. An estimate of specific binding affinity of the fraction for FL-glyburide is contained in Fig. 5.6. The $K_{1/2}$ value for FL-glyburide binding was 13 nM with a Hill slope of 1.0.

5.2.5 Identification of the protein specifically labeled with FL-glyburide

We separated the proteins in the active DEAE fraction using preparative SDS-PAGE and analyzed each eluted fraction directly in the spectrofluorometer. Good separation was achieved by this protocol, as demonstrated in Fig. 5.7A. Fig. 5.7B contains FL-glyburide fluorescence data for the fractions portrayed in Fig. 5.7A. Prep-Cell fraction number 19 (corresponding to Fig. 5.7A, lane 6) exhibited the highest fluorescence signal and also contained the 63-kD protein. The fluorescent signal from the same fraction of a preparation labeled in the presence of 1 μM unlabeled glyburide was reduced by about 70% (data not shown). This result is representative of three separate experiments.

5.2.6 Direct labeling of the active ATP fraction by FL-glyburide

The active ATP fraction, containing protein–detergent micelles, was labeled by FL-glyburide. A weak specific signal was observed in the control sample (Fig. 5.8, bars 1 and 2). We considered the possibility that glyburide binding was blocked by Mg^{2+} and ATP in the sample, and noted that glyburide *inhibition* requires the presence of Mg^{2+}, ATP, and a K^+ channel opener (72). Accordingly, we added 100 μM cromakalim directly to the detergent-solubilized fraction. Following this addition, we observed strong labeling that was blocked by 1 μM glyburide (Fig. 5.8, bars 3 and 4). This result is fully consistent with previous observations on the requirements for glyburide inhibition (72). The result also indicates that ATP and Mg^{2+} prevents FL-glyburide binding to mitoK_{ATP}.

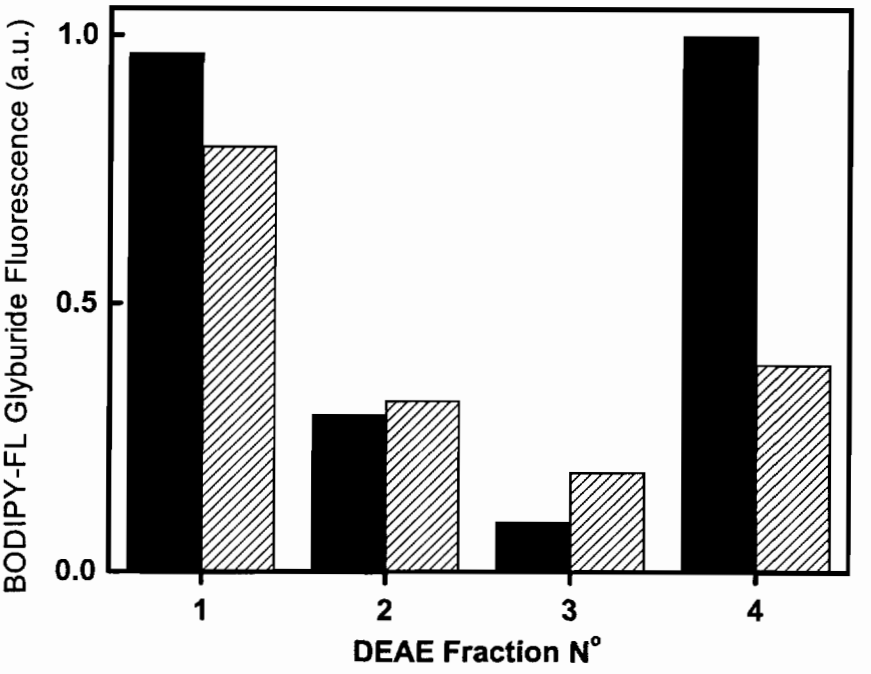

Figure 5.5 Fluorescence profile of DEAE-cellulose column fractions following labeling of vesicles with FL-glyburide. The figure shows the fluorescence intensity of fractions eluted from the DEAE column. Solid bars represent data from preparations labeled with FL-glyburide only. Shaded bars represent data from the preparation labeled with FL-glyburide in the presence of 1 μM unlabeled glyburide. *Fraction 1*, column flow-through, which contains residual unreacted FL-glyburide; *fractions 2, 3, and 4* were eluted by 0, 200, and 300 mM KCl, respectively. The intensity of the emission signal at 515 nm was measured for each eluted sample.

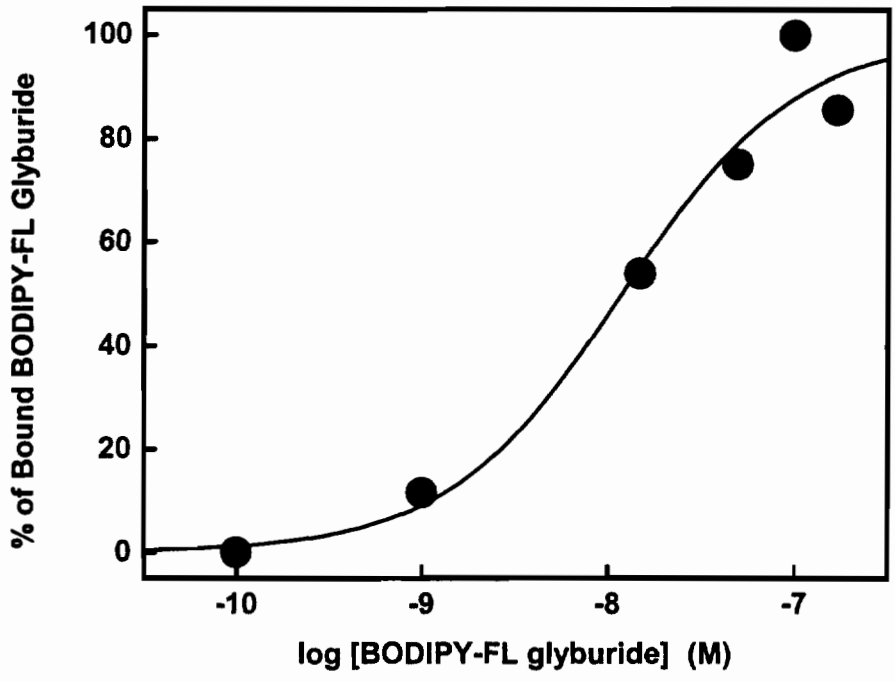

Figure 5.6 Concentration dependence of FL-glyburide labeling. Bound FL-glyburide was measured as fluorescence intensity and expressed as percent of maximum fluorescence observed at 100 nM total FL-glyburide. Membrane vesicles were incubated with 0.1, 1, 15, 50, 100, and 170 nM FL-glyburide for 2 h at room temperature, then UV-irradiated, extracted, and purified as described in Section 5.1. Background fluorescence was determined in parallel on samples incubated with 50 nM FL-glyburide in the presence of 1 μM unlabeled glyburide. The active DEAE fraction from each preparation was analyzed on the spectrofluorometer for FL-glyburide fluorescence.

Figure 5.7 Identification of mitoSUR. The DEAE eluate containing FL-glyburide-labeled protein was further purified by preparative gel electrophoresis on the Prep-Cell.

Panel A: SDS-PAGE of Prep-Cell fractions. A 10% gel was loaded with selected fractions eluted from the Prep-Cell in the molecular weight range of 30–100 kD and silver stained.

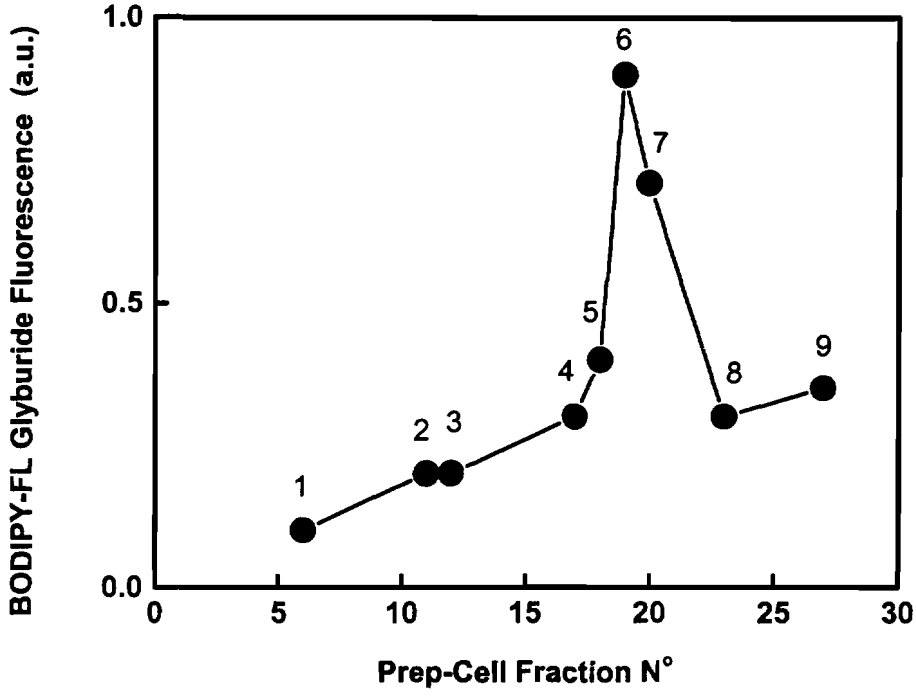

Figure 5.7 Identification of mitoSUR. The DEAE eluate containing FL-glyburide-labeled protein was further purified by preparative gel electrophoresis on the Prep-Cell.

Panel B: FL-glyburide fluorescence of Prep-Cell fractions. The fractions shown in Fig. 5.7A were analyzed for fluorescence in the spectrofluorometer, and the intensity of the emission signal at 515 nm is plotted versus the Prep-Cell fraction number. The fluorescence of fraction 19 identifies mitoSUR as the 63-kD protein.

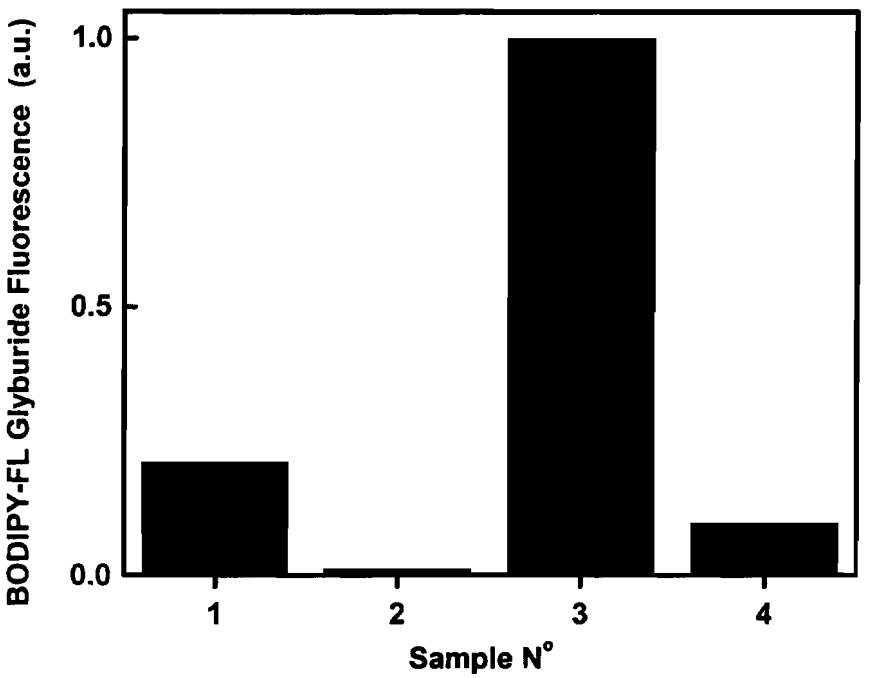

Figure 5.8 Direct FL-glyburide labeling of an active ATP fraction. The bars represent FL-glyburide fluorescence following labeling of the active ATP fraction. Note that the untreated eluate contained 20 mM ATP. In addition to 50 nM FL-glyburide, the samples contained the following: *Bar 1*, no additions; *bar 2*, same as bar 1 plus 1 μM unlabeled glyburide; *bar 3*, 100 μM cromakalim and 1 mM Mg^{2+}; *bar 4*, same as bar 3 plus 1 μM unlabeled glyburide.

5.2.7 Direct labeling of the active DEAE fraction by FL-glyburide

To confirm this conclusion, we also labeled the active DEAE fraction with FL-glyburide. This fraction exhibits specific labeling when EDTA is included in the buffer (Fig. 5.9, bars 1 and 2). 1 mM Mg^{2+} attenuated the labeling (Fig. 5.9, bar 3), consistent with the observation that Mg^{2+} reduces glyburide inhibition of mitoK_{ATP} (68).

No specific labeling was observed when ATP alone was added to the fraction (Fig. 5.9, bars 4 and 5), and ATP plus Mg^{2+} also blocked labeling (Fig. 5.9, bar 6). When 100 μM cromakalim was added with ATP and Mg^{2+}, specific labeling was again observed (Fig. 5.9, bars 7 and 8), confirming the results with the ATP column eluate.

5.2.8 Estimation of the yield of the 63-kD mitoSUR

Comparative densitometry was used to estimate the amount of 63-kD protein recovered in the Prep-Cell eluate. A representative experiment is contained in Fig. 5.10. The results of two such experiments indicate that the inner membrane vesicles contain about 29 ng (460 fmol) of 63-kD protein per mg of inner membrane protein. A rough estimate of the amount per mg of *total mitochondrial protein* can be made by assuming that purified vesicles concentrate integral membrane proteins about five-fold. Thus, rat liver mitochondria contain about 90 fmol of 63-kD protein/mg mitochondrial protein.

5.3 Discussion

MitoK_{ATP} exhibits three regulatory features that distinguish it from cellK_{ATP}:

(i) Divalent cations are absolutely required for inhibition of mitoK_{ATP} by ATP and long-chain acyl-CoA esters (68, 69).

(ii) Long-chain acyl-CoA esters and ADP, which are analogues, inhibit mitoK_{ATP} (68, 69) and activate cellK_{ATP} (113).

(iii) MitoK_{ATP} is highly sensitive to the K^+ channel opener, diazoxide, with $K_{1/2}$ values in the submicromolar range, whereas most plasma membrane K_{ATP} are sensitive in the 100–1000 μM range (70, 71).

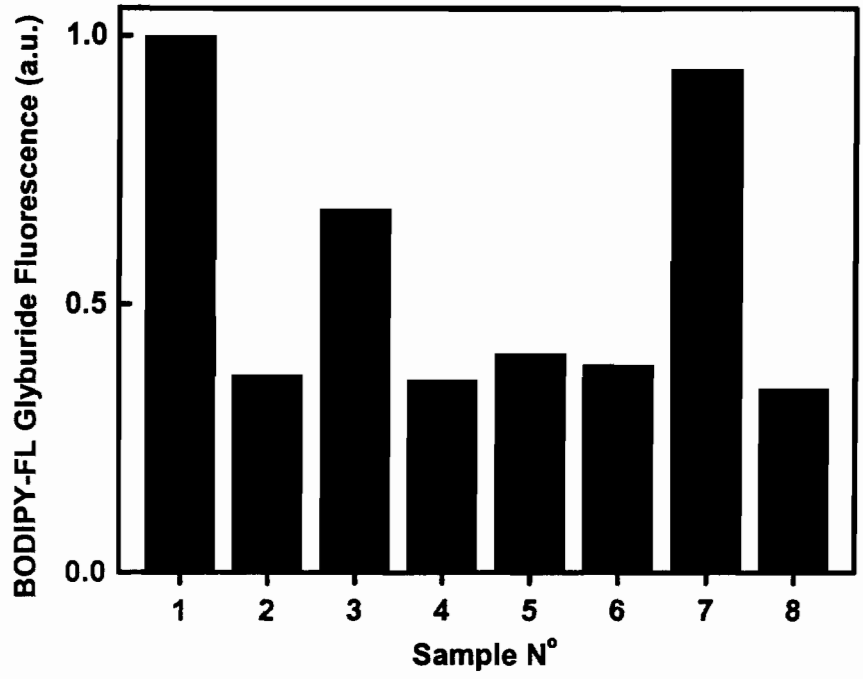

Figure 5.9 Direct FL-glyburide labeling of the active DEAE fraction. The bars represent FL-glyburide fluorescence following labeling of the active DEAE fraction. Note that the untreated eluate contains 1 mM EDTA. In addition to 50 nM FL-glyburide, the samples contained the following: *Bar 1*, no additions; *bar 2*, 1 μM unlabeled glyburide; *bar 3*, 1 mM Mg^{2+}; *bar* 4, 20 mM ATP and 1 mM EDTA; *bar 5*, same as bar 4 plus 1 μM unlabeled glyburide; *bar 6*, 20 mM ATP and 1 mM Mg^{2+}; *bar 7*, 100 μM cromakalim, 20 mM ATP, and 1 mM Mg^{2+}; *bar 8*, same as bar 7 plus 1 μM unlabeled glyburide.

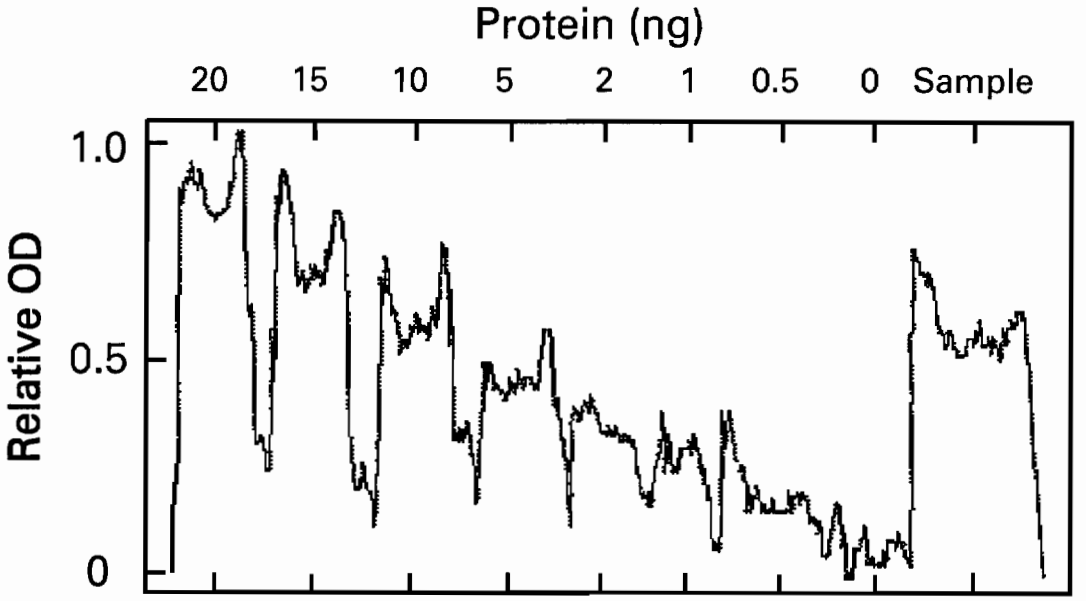

Figure 5.10 Estimation of the yield of purified mitoSUR. Figure contains relative OD of protein bands after SDS-PAGE. Fumarase was used as the protein standard and compared with the 63-kD protein eluted from the Prep-Cell. OD was measured by a video densitometer and analyzed using BIOMED software (Biomed Instruments). Inner membrane vesicles containing 10 mg of protein were extracted and fractionated on a DEAE column, and the active DEAE fraction was applied to the Prep-Cell. In this experiment, the 40-μl aliquot from two combined 800-μl Prep-Cell fractions contained about 7 ng protein, or 280 ng total. In a second experiment, the Prep-Cell eluate contained about 300 ng of 63-kD protein. Assuming 100% recovery, the inner membrane vesicles contain about 29 ng mitoSUR/mg total protein, or 460 fmol/mg of protein.

It is likely, based on recent characterization of cell SUR isoforms (50, 51, 55, 56), that these distinctions reside within the regulatory domains of mitoK_{ATP}.

Because the subunit structure of mitoK_{ATP} is unknown, we set out to test the hypothesis (75) that mitoK_{ATP} functions as a heteromultimer consisting of an inward rectifying K^+ channel, mitoKIR, and a sulfonylurea receptor, mitoSUR. If mitoK_{ATP} is a heteromultimer, the subunits must remain associated during detergent extraction and isolation, because reconstituted mitoK_{ATP} retains regulation by sulfonylureas and nucleotides. One indication that this is so is provided by the gels in Figs. 5.1A and 5.1B, which demonstrate that both the active DEAE fraction and the active ATP fraction contain a 55- and a 63-kD protein.

There is considerable evidence for identifying mitoKIR with the 55-kD protein. This protein was first purified by Mironova (143) using an unusual ethanol extraction technique. It exhibits typical channel activity when incorporated into bilayer lipid membranes (103), and the unitary conductance of the channel, 10 pS in symmetrical 100 mM KCl, agrees with the patch clamp studies of Inoue et al. (65). Our anti-55-kD antibodies were raised to protein purified by Mironova's ethanol extraction protocols. The antibodies recognize the band in the highly purified, reconstitutively active DEAE fraction, and they inhibit K^+ flux when incubated with proteoliposomes reconstituted with mitoK_{ATP}, as shown in Fig. 5.2.

Our data establish that the active fraction contains a high-affinity sulfonylurea-binding protein, designated mitoSUR. For the purpose of this study, specific FL-glyburide binding was defined as that displaced by 1 μM unlabeled glyburide. Only one inner membrane protein, at 63 kD, meets this criterion. Identification of the 63-kD protein with mitoSUR is based on a variety of studies, including labeling of vesicles, followed by purification (Fig. 5.5) and direct labeling of fractions containing detergent micelles of the proteins (Figs. 5.8 and 5.9). The apparent affinity of mitoSUR for FL-glyburide is about 13 nM (Fig. 5.6). This is roughly comparable to the inhibitory potency in liposomes (68) but considerably less than the $K_{1/2}$ for glyburide inhibition of mitoK_{ATP}, which is about 1 μM. Aside from extensive non-specific binding to proteins in intact mitochondria, we have no explanation at present for this discrepancy.

The most remarkable aspect of this study is the observation that inhibition of FL-glyburide binding by ATP can be reversed simply by adding cromakalim to the micellar mixture (Figs. 5.8 and 5.9). This is an exact parallel with the observation that glyburide does not inhibit mitoK_{ATP} in intact mitochondria unless Mg^{2+}, ATP, and a K^+ channel opener are also present in the assay (72). Our results demonstrate that ATP, or ATP + Mg^{2+}, prevents glyburide binding and that binding is restored by cromakalim.

Azidoglyburide and 8-azido-ATP labeled three bands at 63, 55, and 33 kD (Figs. 5.3 and 5.4). A similar result was obtained with plasma membrane K_{ATP}, in which both the 38-kD protein (Kir6.2) and the 140-kD protein (SUR1) were labeled by ^{125}I-azidoglyburide (150, 151). As reported here, the co-photolabeling was only observed with the azido derivative and was not observed with ^{125}I-glyburide, which only labeled the 140-kD protein (58). The explanation for co-labeling (152) is that the azido group can attach to other proteins if they are in close proximity to the glyburide-binding site. We have not identified the 33-kD protein that is also co-labeled in mitochondria; however, it may be the adenine nucleotide translocator, which is present in very high amounts in the inner mitochondrial membrane. The 33-kD protein is not found in the reconstitutively active fraction.

The amount of mitoSUR in mitochondria, estimated at 90 fmol/mg of protein, can be compared with an independent estimate obtained by dividing the molar turnover rate by V_{max}. At 25°C, the V_{max} of K^+ influx through mitoK_{ATP} is about 150 nmol/mg · min. Incidentally, the sum of K^+ influx from mitoK_{ATP} and K^+ leak (about 50 nmol/mg · min at 180 mV (153), must be less than the V_{max} for the K^+/H^+ antiporter, and indeed, the latter value is about 350 nmol/mg · min (154). The turnover is given directly by the conductance (10 pS) and is about 10^8 mol K^+/mol channel · min. These values yield an estimate of 1.5 fmol channel/mg of protein. If the channel is tetrameric and is open 25% of the time during V_{max} measurements, the estimate becomes 24 fmol channel/mg, which is in reasonable agreement with the direct measurement of mitoSUR.

Our finding that mitoSUR has a much lower molecular weight than SUR1 may be of interest from an evolutionary standpoint. SUR1 is related to the ATP-binding

cassette (ABC) superfamily (53, 155). Individual domains of ABC transporters are commonly expressed as separate polypeptides in prokaryotes, whereas they are often fused into a single polypeptide in eukaryotes (156).

We recently established that the regulatory domains of mitoK_{ATP} face outward, toward the intermembrane space (84). Thus, mitoK_{ATP} and cellK_{ATP}, which are regulated by the same ligands, appear to be accessible to the same pool of cytosolic regulatory metabolites. It should be noted, however, that the outer membrane is an important barrier for nucleotides and that voltage-dependent anion channels (VDAC) may be involved in regulating their distributions between intermembrane and cytosolic spaces (157).

5.4 Summary

Purified mitoK_{ATP} consists of two proteins. We raised antibodies to the 55-kD protein, and they inhibited K^+ flux in liposomes containing mitoK_{ATP} from heart and liver. The 63-kD, but not the 55-kD, protein was specifically labeled by FL-glyburide. Accordingly, we provisionally identify the 55-kD protein as mitoKIR, the inward-rectifying K^+ channel of mitoK_{ATP}, and the 63-kD protein as mitoSUR, the regulatory sulfonylurea receptor subunit.

Chapter 6
SUMMARY OF RESULTS

Physiological and pharmacological properties of mitoK$_{ATP}$ have been characterized in this study. The data presented in Chapter 2 demonstrate that K^+ flux through the MgATP-inhibited channel is restored to full activity by GTP or GDP. Neither of the guanine nucleotides has any effect on the channel activity in the absence of MgATP. Palmitoyl-CoA and oleoyl-CoA inhibit mitoK$_{ATP}$ with high potency, and this inhibition is also reversed by GTP and potassium channel openers, such as diazoxide and cromakalim. Inhibition by long-chain acyl-CoA esters, like inhibition by MgATP, exhibits an absolute requirement for Mg^{2+} ions. Thus, GTP and long-chain acyl-CoA esters may be the physiological regulators of mitoK$_{ATP}$, and we hypothesize that mitoK$_{ATP}$ may play an important role *in vivo* in regulating fatty acid oxidation.

The data presented in Chapter 3 demonstrate that diazoxide, cromakalim, and two experimental cromakalim derivatives are very potent activators of K^+ flux through mitoK$_{ATP}$. Cardiac mitoK$_{ATP}$ is 2000-fold more sensitive to diazoxide than cardiac cellK$_{ATP}$, indicating that two distinct receptor subtypes coexist within the myocyte. 5-HD inhibits diazoxide-activated K^+ flux through mitoK$_{ATP}$. These results indicate that mitoK$_{ATP}$ may be an important intracellular receptor for KCOs and inhibitors. These data also raise the possibility that mitoK$_{ATP}$ is the site of action of cardioprotective effects of KCOs. This hypothesis is now supported by other investigators (93, 94).

Chapter 4 is a supplement to Chapter 2 in that it clarifies the topological location of nucleotide regulatory sites on mitoK$_{ATP}$. Electrophysiological experiments in bilayer lipid membranes containing purified mitoK$_{ATP}$ showed that K^+ current through the channel is blocked asymmetrically by ATP. K^+ flux experiments using

proteoliposomes containing purified mitoK_{ATP} showed that mitoK_{ATP} is unipolar with respect to regulation by Mg^{2+}, ATP, GTP, and palmitoyl-CoA and that all of these ligands react on the same pole of the protein. K^+ flux experiments in respiring rat liver mitochondria showed that mitoK_{ATP} was inhibited by palmitoyl-CoA and activated by GTP when these ligands were added to the external medium. Given that the inner mitochondrial membrane is impermeant to these ligands and that mitoK_{ATP} is unipolar with respect to nucleotide regulation, it follows that the regulatory sites on mitoK_{ATP} face the cytosol.

Chapter 5 reports photoaffinity labeling and purification of mitoSUR, the sulfonylurea receptor of mitoK_{ATP}. A fluorescent analog of glyburide, BODIPY-FL glyburide, has been used to photolabel the inner mitochondrial membrane vesicles. This novel probe was specifically photoincorporated by ultraviolet irradiation into a peptide with a molecular weight of 63 kD. This protein co-purified with 55-kD protein in the same fraction when eluted from the DEAE-cellulose column with 300 mM KCl. When this fraction was reconstituted into liposomes, K^+ flux was inhibited with high affinity by ATP, glyburide, and polyclonal antibodies raised to 55-kD protein. Based on these results, we hypothesized that mitoK_{ATP} is heteromultimer consisting of the 63-kD protein as a regulatory sulfonylurea receptor and the 55-kD protein as an inward-rectifying K^+ channel (mitoKIR).

Future research will focus on microsequencing, cloning, and expression of mitoKIR and mitoSUR. Investigation of native and mutagenized mitoKIR and mitoSUR would help to elucidate the molecular mechanisms involved in regulation of mitoK_{ATP}. Further studies should be conducted to test the hypotheses that mitoK_{ATP} is involved in regulation of cellular bioenergetics and also in cardioprotection against myocardial ischemia.

REFERENCES

1. Noma, A. (1983) ATP-regulated K^+ channels in cardiac muscle. *Nature* **305**, 147–148.

2. Cook, D. L., and Hales, C. N. (1984) Intracellular ATP directly blocks K^+ channels in pancreatic β-cells. *Nature* **311**, 271–273.

3. Ashcroft, F. M., Harrison, D. E., and Ashcroft, S. J. H. (1984) Glucose induces closure of single potassium channels in isolated rat pancreatic β-cells. *Nature* **312**, 446–448.

4. Spruce, A. E., Standen, N. B., and Standfield, P. R. (1985) Voltage-dependent ATP-sensitive potassium channels of skeletal muscle membrane. *Nature* **316**, 736–738.

5. Standen, N. B., Quayle, J. M., Davis, N. W., Brayden, J. E., Huang, Y., and Nelson, M. T. (1989) Hyperpolarizing vasodilators activate ATP-sensitive K^+ channels in arterial smooth muscle. *Science* **245**, 177–180.

6. Ashford, M. L. J., Sturgess, N. C., Trout, N. J., Gardner, N. J., and Hales, C. N. (1988) Adenosine-5′-triphosphate-sensitive ion channels in neonatal rat cultured central neurons. *Pflügers Arch.* **412**, 297–304.

7. Ashcroft, S. J. H., and Ashcroft, F. M. (1990) Properties and function of ATP-sensitive K-channels. *Cell. Signaling* **2**, 197–214.

8. Terzic, A., Jahangir, A., and Kurachi, Y. (1995) Cardiac ATP-sensitive K^+ channels: regulation by intracellular nucleotides and K^+ channel-opening drugs. *Am. J. Physiol.* **269**, C525–C545.

9. Nelson, M. T., and Quayle, J. M. (1995) Physiological roles and properties of potassium channels in arterial smooth muscle. *Am. J. Physiol.* **268**, C799–C822.

10. Trube, G., Rorsman, P., and Ohno-Shosaku, T. (1986) Opposite effect of tolbutamide and diazoxide on the ATP-dependent K^+ channel in mouse pancreatic β-cells. *Pflügers Arch.* **407**, 493–499.

11. Dunne, M. J., and Petersen, O. H. (1986) GTP and GDP activation of K^+ channels that can be inhibited by ATP. *Pflügers Arch.* **407**, 564–565.

12. Weiss, J. N., Venkatesh, N., and Lamp, S. T. (1992) ATP-sensitive K^+ channels and cellular K^+ loss in hypoxic and ischemic mammalian ventricle. *J. Physiol. Lond.* **447**, 649–673.

13. Lazdunski, M. (1994) ATP-sensitive potassium channels: an overview. *J. Cardiovasc. Pharmacol.* **24**, S1–S5.

14. Quast, U., and Cook, N. S. (1989) *In vitro* and *in vivo* comparison of two K^+ channel openers, diazoxide and cromakalim and their inhibition by glibenclamide. *J. Pharmacol. Exp. Ther.* **250**, 261–271.

15. Trube, G., and Hescheler, J. (1984) Inward-rectifying channels in isolated patches of the heart cell membrane: ATP-dependence and comparison with cell-attached patches. *Pflügers Arch.* **401**, 178–184.

16. Findlay, I. (1986) ATP maintains ATP-inhibited channels in an operational state. *Pflügers Arch.* **407**, 238–240.

17. Ohno-Shosaku, T., Zünkler, B. J., and Trube, G. (1987) Dual effects of ATP on K^+ currents of mouse pancreatic β-cells. *Pflügers Arch.* **408**, 133–138.

18. Takano, M., Qin, D., and Noma, A. (1990) ATP-dependent decay and recovery of K^+ channels in guinea pig cardiac myocytes. *Am. J. Physiol.* **258**, H45–H50.

19. Gribble, F. M., Tucker, S. J., Haug, T., and Ashcroft, F. M. (1998) MgATP activates the β-cell K_{ATP} channel by interaction with its SUR1 subunit. *Proc. Natl. Acad. Sci. U.S.A.* **95**, 7185–7190.

20. Misler, S., Falke, L. C., Gillis, K., and McDaniel, M. L. (1986) A metabolite-regulated potassium channel in rat pancreatic β-cells. *Proc. Natl. Acad. Sci. U.S.A.* **83**, 7119–7123.

21. Kakei, M., Kelly, R. P., Ashcroft, S. J., and Ashcroft, F. M. (1986) The ATP-sensitivity of K^+ channels in rat pancreatic β-cells is modulated by ADP. *FEBS Lett.* **208**, 63–66.

22. Lederer, W. J., and Nichols, C. G. (1989) Nucleotide modulation of the activity of rat heart ATP-sensitive K^+ channels in isolated membrane patches. *J. Physiol. (Lond.)* **419**, 193–213.

23. Ribalet, B., Eddlestone, G. T., and Ciani, S. (1988) Metabolic regulation of the K(ATP) and a maxi-K(V) channel in the insulin-secreting RINm5F cell. *J. Gen. Physiol.* **92**, 219–237.

24. Dunne, M. J., and Petersen, O. H. (1986) Intracellular ADP activates K^+ channels that are inhibited by ATP in an insulin-secreting cell line. *FEBS Lett.* **208**, 59–62.

25. Findlay, I. (1988) Effects of ADP upon the ATP-sensitive K^+ channel in rat ventricular myocytes. *J. Membr. Biol.* **101**, 83–92.

26. Findlay, I. (1987) The effects of magnesium upon adenosine triphosphate-sensitive potassium channels in a rat insulin-secreting cell line. *J. Physiol. (Lond.)* **391**, 611–629.

27. Tung, R. T., and Kurachi, Y. (1991) On the mechanism of nucleotide diphosphate activation of the ATP-sensitive K^+ channel in ventricular cell of guinea-pig. *J. Physiol. (Lond.)* **437**, 239–256.

28. Hamilton, T. C., and Weston, A. H. (1989) Cromakalim, nicorandil and pinacidil: novel drugs which open potassium channels in smooth muscle. *Gen. Pharmacol.* **20**, 1–9.

29. Grover, G. J., Sleph, P. G., and Dzwonezvk S. (1990) Pharmacological profile of cromakalim in the treatment of myocardial ischemia in isolated rat hearts and anesthetized dogs. *J. Cardiovasc. Pharmacol.* **16**, 853–864.

30. Grover, G. J., McCullough, J. R., Henry, D. E., Conder, M. L., and Sleph, P. G. (1989) Anti-ischemic effects of the potassium channel activators pinacidil and cromakalim and the reversal of these effects with the potassium channel blocker glyburide. *J. Pharmacol. Exp. Ther.* **251**, 98–104.

31. Grover, G. J. (1994) Protective effects of ATP-sensitive potassium-channel openers in experimental myocardial ischemia. *J. Cardiovasc. Pharmacol.* **24**, S18–S27.

32. Gross, G. J., and Auchampach, J. A. (1992) Blockade of ATP-sensitive potassium channels prevents myocardial preconditioning in dogs. *Circ. Res.* **70**, 223–233.

33. Nichols, C. G., and Lederer, W. J. (1991) Adenosine triphosphate-sensitive potassium channels in the cardiovascular system. *Am. J. Physiol.* **261**, H1675–1686.

34. Garrino, M. G., Plant, T. D., and Henquin, J. C. (1989) Effects of putative activators of K^+ channels in mouse pancreatic β-cells. *Br. J. Pharmacol.* **98**, 957–965.

35. Zunkler, B. J., Lenzen, S., Manner, K., Panten, U., and Trube, G. (1988) Concentration-dependent effects of tolbutamide, meglitinide, glipizide, glibenclamide and diazoxide on ATP-regulated K^+ currents in pancreatic β-cells. *Naunyn. Schmiedebergs. Arch. Pharmacol.* **337**, 225–230.

36. Misler, S., Gee, W. M., Gillis, K. D., Scharp, D. W., and Falke, L. C. (1989) Metabolite-regulated ATP-sensitive K^+ channel in human pancreatic islet cells. *Diabetes* **38**, 422–427.

37. Henquin, J. C., and Meissner, H. P. (1982) Opposite effects of tolbutamide and diazoxide on $^{86}Rb^+$ fluxes and membrane potential in pancreatic β-cells. *Biochem. Pharmacol.* **31**, 1407–1415.

38. Dunne, M. J., and Petersen, O. H. (1991) Potassium selective ion channels in insulin-secreting cells: pharmacology and their role in stimulus-secretion coupling. *Biochim. Biophys. Acta* **1071**, 67–82.

39. Nelson, D. A., Aguilar-Bryan, L., and Bryan, J. (1992) Specificity of photolabeling of β-cell membrane proteins with an ^{125}I-labeled glyburide analog. *J. Biol. Chem.* **267**, 14928–14933.

40. Nichols, C. G., Ripoll, C., and Lederer, W. J. (1991) ATP-sensitive potassium channel modulation of the guinea pig ventricular action potential and contraction. *Circ. Res.* **68**, 280–287.

41. Nelson, M. T., and Quayle, J. M. (1995) Physiological roles and properties of potassium channels in arterial smooth muscle. *Am. J. Physiol.* **268**, C799–C822.

42. Beech, D. J., Zhang, H., Nakao, K., and Bolton, T. B. (1993) K channel activation by nucleotide diphosphates and its inhibition by glibenclamide in vascular smooth muscle cells. *Br. J. Pharmacol.* **110**, 573–582.

43. Bonev, A. D., and Nelson, M. T. (1993) ATP-sensitive potassium channels in smooth muscle cells from guinea pig urinary bladder. *Am. J. Physiol.* **264**, C1190–C1200.

44. Fosset, M., De Weille, J. R., Green, R. D., Schmid-Antomarchi, H., and Lazdunski, M. (1988) Antidiabetic sulfonylureas control action potential properties in heart cells via high affinity receptors that are linked to ATP-dependent K^+ channels. *J. Biol. Chem.* **263**, 7933–7936.

45. Findlay, I. (1992) Inhibition of ATP-sensitive K^+ channels in cardiac muscle by the sulphonylurea drug glibenclamide. *J. Pharmacol. Exp. Ther.* **261**, 540–545.

46. Gross, G. J., and Auchampach, J. A. (1992) Role of ATP-dependent potassium channels in myocardial ischemia. *Cardiovasc. Res.* **26**, 1011–1016.

47. Kanton, P. F., Coetzee, W. A., Dennis, S. C., and Opie, L. H. (1987) Effects of glibenclamide on ischemic arrhythmias. *Circulation* **76**, 17.

48. Inagaki, N., Tsuura, Y., Namba, N., Masuda, K., Gonoi, T., Horie, M., Seino, Y., Mizuta, M., and Seino, S. (1995) Cloning and functional characterization of a novel ATP-sensitive potassium channel ubiquitously expressed in rat tissues, including pancreatic islets, pituitary, skeletal muscle, and heart. *J. Biol. Chem.* **270**, 5691–5694.

49. Nichols, C. G., and Lopatin, A. N. (1997) Inward rectifier potassium channels. *Annu. Rev. Physiol.* **59**, 171–191.

50. Inagaki, N., Gonoi, T., Clement, J. P., IV, Wang, C.-Z., Aguilar-Bryan, L., Bryan, J., and Seino, S. (1996) A family of sulfonylurea receptors determines the pharmacological properties of ATP-sensitive K^+ channels. *Neuron* **16**, 1011–1017.

51. Isomoto, S., Kondo, C., Yamada, M., Matsumoto, S., Higashiguchi, O., Horio, Y., Matsuzawa, Y., and Kurachi, Y. (1996) A novel sulfonylurea receptor forms with BIR (Kir6.2) a smooth muscle type ATP-sensitive K^+ channel. *J. Biol. Chem.* **271**, 24321–24324.

52. Aguilar-Bryan, L., Nichols, C. G., Wechsler, S. W., Clement, J. P., IV, Boyd, A. E., III, Gonzalez, G., Herrera-Sosa, H., Nguy, K., Bryan, J., and Nelson, D. A. (1995) Cloning of the β cell high-affinity sulfonylurea receptor: a regulator of insulin secretion. *Science* **268**, 423–426.

53. Higgins, C. F. (1995) The ABC of channel regulation. *Cell* **82**, 693–696.

54. Tusnady, G. E., Bakos, E., Varadi, A., and Sarkadi, B. (1997) Membrane topology distinguishes a subfamily of the ATP-binding cassette (ABC) transporters. *FEBS Lett.* **402**, 1–3.

55. Inagaki, N., Gonoi, T., Clement IV, J. P., Namba, N., Inazawa, J., Gonzalez, G., Aguilar-Bryan, L., Seino, S., and Bryan, J. (1995) Reconstitution of I_{KATP}: an inward rectifier subunit plus the sulfonylurea receptor. *Science* **270**, 1166–1170.

56. Sakura, H., Ammala, C., Smith, F. M., Gribble, F. M., and Ashcroft, F. M. (1995) Cloning and functional expression of the cDNA encoding a novel ATP-sensitive potassium channel subunit expressed in pancreatic β-cells, brain, heart, and skeletal muscle. *FEBS Lett.*, **377**, 338–344.

57. Tucker S. J., Gribble, F. M., Zhao C., Trapp, S., and Ashcroft, F. M. (1997) Truncation of Kir6.2 produces ATP-sensitive K^+ channels in the absence of the sulfonylurea receptor. *Nature* **387**, 179–183.

58. Aguilar-Bryan, L., Nelson, D. A., Vu, Q. A., Humphrey, M. B., and Boyd, A. E., III (1990) Photoaffinity labeling and partial purification of the β cell sulfonylurea receptor using a novel, biologically active glyburide analog. *J. Biol. Chem.* **265**, 8218–8224.

59. Thomas, P. M., Cote, G. J., Wohlik, N., Haddad, B., Mathew, P. M., Rabl, W., Aguilar-Bryan, L., Gagel, R. F., and Bryan, J. (1995) Mutations in the sulfonylurea receptor gene in familial persistent hyperinsulinemic hypoglycemia of infancy. *Science* **268**, 426–429.

60. Thomas, P. M., Wohllk, N., Huang, E., Kuhnle, U., Rabl, W., Gagel, R. F., and Cote, G. J. (1996) Inactivation of the first nucleotide-binding fold of the sulfonylurea receptor, and familial persistent hyperinsulinemic hypoglycemia of infancy. *Am. J. Hum. Genet.* **59**, 510–518.

61. Gribble, F. M., Tucker, S. J., and Ashcroft, F. M. (1997) The essential role of the Walker A motifs of SUR1 in K-ATP channel activation by Mg-ADP and diazoxide. *EMBO J.* **16**, 1145–1152.

62. Clement, J. P., IV, Kunjilwar, K., Gonzalez G., Schwanstecher, M., Panten, U., Aguilar-Bryan, L., and Bryan, J. (1997) Association and stoichiometry of K_{ATP} channel subunits. *Neuron* **18**, 827–838.

63. Inagaki, N., Gonoi, T., and Seino, S. (1997) Subunit stoichiometry of the pancreatic β-cell ATP-sensitive K^+ channel. *FEBS Lett.* **409**, 232–236.

64. Shyng, S., and Nichols, C. G. (1997) Octameric stoichiometry of the K_{ATP} channel complex. *J. Gen. Physiol.* **110**, 655–664.

65. Inoue, I., Nagase, H., Kishi, K., and Higuti, T. (1991) ATP-sensitive K^+ channel in the mitochondrial inner membrane. *Nature* **352**, 244–247.

66. Hegazy, M. G., Mahdi, F., Li, X., Gui, G., Mironova, G., Beavis, A. D., and Garlid, K. D. (1991) Purification and reconstitution of the rat liver mitochondrial K^+ uniporter. *Biophys. J.* **59**, 136A.

67. Gui, G., Hegazy, M. G., Mironova, G., Mahdi, F., Beavis, A., and Garlid, K. D. (1991) Purification and reconstitution of the mitochondrial K^+ channel. *J. Mol. Cell. Cardiol.* **23**, S78.

68. Paucek, P., Mironova, G., Mahdi, F., Beavis, A. D., Woldegiorgis, G., and Garlid, K. D. (1992) Reconstitution and partial purification of the glibenclamide-sensitive, ATP-dependent K^+ channel from rat liver and beef heart mitochondria. *J. Biol. Chem.* **267**, 26062–26069.

69. Paucek, P., Yarov-Yarovoy, V., Sun, X., and Garlid, K. D. (1996) Inhibition of the mitochondrial K_{ATP} channel by long-chain acyl-CoA esters and activation by guanine nucleotides. *J. Biol. Chem.* **271**, 32084–32088.

70. Garlid, K. D., Paucek, P., Yarov-Yarovoy, V., Sun, X., and Schindler, P. A. (1996) The mitochondrial K_{ATP} channel as a receptor for potassium channel openers. *J. Biol. Chem.* **271**, 8796–8799.

71. Garlid, K. D., Paucek, P., Yarov-Yarovoy, V., Murray, H. N., Darbenzio, R. B., D'Alonzo, A. J., Lodge, N. J., Smith, M. A., and Grover, G. J. (1997) Cardioprotective effect of diazoxide and its interaction with mitochondrial ATP-sensitive K^+ channels: possible mechanism of cardioprotection. *Circ.Res.* **81**, 1072–1082.

72. Jaburek, M., Yarov-Yarovoy, V., Paucek, P., and Garlid, K. D. (1998) State-dependent inhibition of the mitochondrial K_{ATP} channel by glyburide and 5-hydroxydecanoate. *J. Biol. Chem.* **273**, 13578–13582.

73. Garlid, K. D. (1988) Mitochondrial volume control. In *Integration of Mitochondrial Function* (Lemasters, J. J., Hackenbrock, C. R., Thurman, R. G., and Westerhoff, H. V., eds.), pp. 257–276, Plenum Publishing Corp., New York.

74. Garlid, K. D. (1980) On the mechanism of regulation of the mitochondrial K^+/H^+ exchanger. *J. Biol. Chem.* **255**, 11273–11279.

75. Garlid, K. D. (1996) Cation transport in mitochondria—the potassium cycle. *Biochim. Biophys. Acta* **1275**, 123–126.

76. Mitchell, P. (1961) Coupling of phosphorylation to electron and hydrogen transfer by a chemi-osmotic type of mechanism. *Nature* **191**, 144–148.

77. Lehninger, A. L., and Kennedy, E. P. (1948) The requirements of the fatty acid oxidase complex of rat liver. *J. Biol. Chem.* **173**, 753–771.

78. Nicholls, D. G., Grav, H. J., and Lindberg, O. (1972) Mitochondria from hamster brown adipose tissue. Regulation of respiration *in vitro* by variations of the matrix compartment. *Eur. J. Biochem.* **31**, 526–533.

79. Halestrap, A. P. (1987) The regulation of the oxidation of fatty acids and other substrates in rat heart mitochondria by changes in the matrix volume induced by osmotic strength, valinomycin and Ca^{2+}. *Biochem. J.* **244**, 159–164.

80. Halestrap, A. P. (1989) The regulation of the matrix volume of mammalian mitochondria *in vivo* and *in vitro* and its role in the control of mitochondrial metabolism. *Biochim. Biophys. Acta* **973**, 355–382.

81. Nicholls, D. G., and Lindberg, O. (1972) Inhibited respiration and ATPase activity of rat liver mitochondria under conditions of matrix condensation. *FEBS Lett.* **25**, 61–64.

82. Vallin, I. (1970) Norepinephrine response in brown adipose tissue from newborn rats. *Acta Zool.* **51**, 129–139.

83. Halestrap, A. P. (1994) Regulation of mitochondrial metabolism through changes in matrix volume. *Biochem. Soc. Trans.* **22**, 522–529.

84. Szewczyk, A., Mikolajek, B., Pikula, S., and Nalecz, M. (1993) ATP-sensitive K^+ channels in mitochondria. *Acta Biochim. Polon.* **40**, 329–336.

85. Yarov-Yarovoy, V., Paucek, P., Jabůrek, M., and Garlid, K. D. (1997) The nucleotide regulatory sites on the mitochondrial K_{ATP} channel face the cytosol. *Biochim. Biophys. Acta.* **1321**, 128–136.

86. Modriansky, M., Vassanelli, S., and Garlid, K. D. (1995) Palmitoyl-CoA is an allosteric inhibitor of proton transport through mitochondrial uncoupling protein. *Biophys. J.* **68**, A440.

87. Yellon, D. M., Baxter, G. F., Garcia-Dorado, D., Heusch, G., and Sumeray, M. S. (1998) Ischaemic preconditioning: present position and future directions. *Cardiovasc. Res.* **37**, 21–33.

88. Edwards, G., and Weston, A. H. (1993) The pharmacology of ATP-sensitive potassium channels. *Annu. Rev. Pharmacol. Toxicol.* **33**, 597–637.

89. McCullough, J. R., Normandin, D. E., Conder, M. L., Sleph, P. G., Dzwonczyk, S., and Grover, G. J. (1991) Specific block of the anti-ischemic actions of cromakalim by sodium 5-hydroxydecanoate. *Circ. Res.* **69**, 949–958.

90. Gross, G. J., Yao, Z., and Auchampach, J. A. (1994) Role of ATP-sensitive potassium channels in ischemic preconditioning. In *Ischemic Preconditioning: The Concepts of Endogenous Cardioprotection* (Przyklenk, K., Kloner, R. A., eds.) *Developments in Cardiovascular Medicine*, Vol. 148, pp. 125–135, Kluwer Academic Publishers, Boston, Mass.

91. Yao, Z., and Gross, G. J. (1994) Effects of the K_{ATP} channel opener bimakalim on coronary blood flow, monophasic action potential duration, and infarct size in dogs. *Circulation* **89**, 1769–1775.

92. Grover, G. J., D'Alonzo, A. J., Parham, C. S., and Darbenzio, R. B. (1995) Cardioprotection with the K_{ATP} opener cromakalim is not correlated with ischemic myocardial action potential duration. *J. Cardiovasc. Pharmacol.* **26**, 145–152.

93. Liu, Y., Sato, T., O'Rourke, B., and Marban, E. (1998) Mitochondrial ATP-dependent potassium channels: novel effectors of cardioprotection? *Circulation* **97**, 2463–2469.

94. Sato, T., O'Rourke, B., and Marban, E. (1998) Modulation of mitochondrial ATP-dependent K^+ channels by protein kinase C. *Circ. Res.* **83**, 110–114.

95. Liu, Y., Ytrehus, K., and Downey, J. M. (1998) Evidence that translocation of protein kinase C is a key event during ischemic preconditioning of rabbit myocardium. *J. Mol. Cell. Cardiol.* **26**, 661–668.

96. Speechly-Dick, M. E., Mocanu, M. M., and Yellon, D. M. (1994) Protein kinase C. Its role in ischemic preconditioning in the rat. *Circ. Res.* **75**, 586–590.

97. Ytrehus, K., Liu, Y., and Downey, J. M. (1994) Preconditioning protects ischemic rabbit heart by protein kinase C activation. *Am. J. Physiol.* **266**, H1145–H1152.

98. Downey, J. M., and Cohen, M. V. (1997) Signal transduction in ischemic preconditioning. *Adv. Exp. Med. Biol.* **430**, 39–55.

99. Garlid, K. D., Paucek, P., and Yarov-Yarovoy, V. (1996) Regulation of the mitochondrial K_{ATP} channel by palmitoyl-CoA, adenine and guanine nucleotides, and K^+ channel openers. *Biophys. J.* **70**, A311.

100. Paucek, P., Yarov-Yarovoy, V. and Garlid, K. D.(1997) Sulfonylurea receptor of the mitochondrial K_{ATP} channel. *Biophys. J.* **72**, A39.

101. Paucek, P., Yarov-Yarovoy, V., and Garlid, K. D. (1998) Photoaffinity labeling and purification of mitoSUR, the sulfonylurea receptor of the mitochondrial K_{ATP} channel. *J. Biol. Chem.*, submitted.

102. Szewczyk, A., Wojcik, G., Lobanov, N. A., and Nalecz, M. J. (1997) The mitochondrial sulfonylurea receptor: identification and characterization. *Biochem. Biophys. Res. Comm.* **230**, 611-615.

103. Mironova, G. D., Skarga, Yu. Yu., Grigoriev, S. M., Yarov-Yarovoy, V. M., Alexandrov, A. V., and Kolomytkin, O. V. (1996) The mitochondrial potassium channel from rat liver mitochondria. 1. Isolation, purification, and reconstitution in a bilayer lipid membrane. *Membr. Cell Biol.* **10**, 429-437.

104. Suzuki, M., Kotake, K., Fujikura, K., Inagaki, N., Suzuki, T., Gonoi, T., Seino, S., and Takata, K. (1997) Kir6.1: a possible subunit of ATP-sensitive K+ channels in mitochondria. *Biochem. Biophys. Res. Commun.* **241**, 693-697.

105. Beavis, A. D., Brannan, R. D., and Garlid, K. D. (1985) Swelling and contraction of the mitochondrial matrix: I. A structural interpretation of the relationship between light scattering and matrix volume. *J. Biol. Chem.* **260**, 13424-13433.

106. Brierley, G. P., Davis, M. H., and Jung, D. W. (1988) Intravesicular pH changes in submitochondrial particles induced by monovalent cations: relationship to the Na^+/H^+ and K^+/H^+ antiporters. *Arch. Biochem. Biophys.* **264**, 417-427.

107. McEnery, M. W., Hullihen, J. and Pedersen, P. L. (1989) F_o "proton channel" of rat liver mitochondria. Rapid purification of a functional complex and a study of its interaction with the unique probe diethylstilbestrol. *J. Biol. Chem.* **264**, 12029-12036.

108. Layne, E. (1957) Spectrophotometric and turbidimetric methods for measuring proteins. *Methods Enzymol.* **3**, 447-454.

109. Kaplan, R. S., and Pedersen, P. L. (1985) Determination of microgram quantities of protein in the presence of milligram levels of lipid with amido black 10B. *Anal. Biochem.* **150**, 97-104.

110. Garlid, K. D., Sun, X., Paucek, P., and Woldegiorgis, G. (1995) Mitochondrial cation transport systems. *Methods Enzymol.* **260**, 331-348.

111. Paucek, P., Yarov-Yarovoy, V., Sun, X., and Garlid, K. D. (1995) Physiological and pharmacological activators of the mitochondrial K_{ATP} channel. *Biophysics J.* **68**, A145.

112. Woldegiorgis, G., Lawrence, J., Ruoho, A., Duff, T., and Shrago, E. (1995) Photoaffinity labeling of mitochondrial proteins with 2-azido[32P]palmitoyl CoA. *FEBS Lett.* **364**, 143–146.

113. Larsson, O., Deeney, J. T., Bränström, R., Berggren, P.-O., and Corkey, B. E. (1996) Activation of the ATP-sensitive K^+ channel by long chain acyl-CoA. A role in modulation of pancreatic beta-cell glucose sensitivity. *J. Biol. Chem.* **271**, 10623–10626.

114. Garlid, K. D. (1978) Unmasking the mitochondrial K/H exchanger: swelling-induced K^+-loss. *Biochem. Biophys. Res. Commun.* **83,** 1450–1455.

115. Garlid, K. D. (1979) Unmasking the mitochondrial K/H exchanger: tetraethylammonium-induced K^+-loss. *Biochem. Biophys. Res. Commun.* **87,** 842–847.

116. Brierley, G. P. (1978) Ion transport by mitochondria. In *The Molecular Biology of Membranes* (Fleischer, S., Hatefi, Y., MacLennan, D. H., and Tzagaloff, A., eds.), pp. 295–308, Plenum Publishing Corp., New York.

117. Newgard, C. B., and McGarry, J. D. (1995) Metabolic coupling factors in pancreatic β-cell signal transduction. *Annu. Rev. Biochem.* **64,** 689–719.

118. Cook, N. S., and Quast, U. (1990) Potassium channel pharmacology. In *Potassium Channels* (Cook, N. S., ed.), pp. 181–231, Ellis Harwood Ltd., Chichester.

119. Escande, D., and Henry, H. (1993) Potassium channels as pharmacological targets in cardiovascular medicine. *Eur. Heart J.* **14,** 2–9.

120. McPherson, G. A. (1993) Current trends in the study of potassium channel openers. *Gen. Pharmacol.* **24,** 275–281.

121. Belyaeva, E. A., Szewczyk, A., Mikolajek, B., Nalecz, M. J., and Wojtczak, L. (1993) Demonstration of glibenclamide-sensitive K^+ fluxes in rat liver mitochondria. *Biochem. Mol. Biol. Int.* **31,** 493–500.

122. Szewczyk A., Wojcik, G., and Nalecz, M. J. (1995) Potassium channel opener, RP 66471, induces membrane depolarization of rat liver mitochondria. *Biochem. Biophys. Res. Commun.* **207,** 126–132.

123. Matlib, M. A., Rouslin, W., Vaghy, P. L., and Schwartz, A. (1984) Isolation of cardiac muscle mitochondria. *Methods Pharmacol.* **5**, 25–37.

124. Periyasamy, S. M., Kakar, S. S., Garlid, K. D., and Askari, A. (1990) Ion specificity of cardiac sarcolemmal Na^+/H^+ antiporter. *J. Biol. Chem.* **265,** 6035–6041.

125. Jones, L. R., and Besch, H. R., Jr. (1984) Isolation of canine cardiac sarcolemmal vesicles. *Methods Pharmacol.* **5,** 1–12.

126. Paucek, P., and Garlid, K. D. (1993) Reconstituted K^+ flux via the partially purified K^+/ATP channel from cardiac sarcolemmal. *Biophys. J.* **64,** A311.

127. Garlid, K. D., and Beavis, A. D. (1985) Swelling and contraction of the mitochondrial matrix. II. Quantitative application of the light scattering technique to solute transport across the inner membrane. *J. Biol. Chem.* **260,** 13434–13441.

128. Beavis, A. D., Lu, Y., and Garlid, K. D., (1993) On the regulation of K^+ uniport in intact mitochondria by adenine nucleotides and nucleotide analogs. *J. Biol. Chem.* **68,** 997–1004.

129. Matlib, M. A., and O'Brien, P. J. (1976) Properties of rat liver mitochondria with intermembrane cytochrome *c*. *Arch. Biochem. Biophys.* **173**, 27–33.

130. Guy, H. R., and Durell, S. R. (1994) Using sequence homology to analyze the structure and function of voltage-gated ion channel proteins. *Soc. Gen. Physiol. Ser.* **49,** 197–212.

131. Faivre, J. F., and Findlay, I. (1989) Effects of tolbutamide, glibenclamide and diazoxide upon action potentials recorded from rat ventricular muscle. *Biochim. Biophys. Acta* **984,** 1–5.

132. Paucek, P., Schindler, P. A., Yarov-Yarovoy, Y., and Garlid, K. D. (1996) Regulation of partially purified K_{ATP} channel from cardiac sarcolemma by nucleotides and K^+ channel openers. *Biophys. J.* **70,** A311.

133. Thuringer, D., and Escande, D. (1989) Apparent competition between ATP and the potassium channel opener RP 49356 on ATP-sensitive K^+ channels of cardiac myocytes. *Mol. Pharmacol.* **36,** 897–902.

134. Flatt, P. R., Shibier, O., Szecowka, J., and Berggren, P.-O. (1994) New perspectives on the actions of sulphonylureas and hyperglycaemic

sulphonamides on the pancreatic beta-cell. *Diabete Metab. (Paris)* **20,** 157–162.

135. Cole, W. C. (1993) ATP-sensitive K^+ channels in cardiac ischemia: an endogenous mechanism for protection of the heart. *Cardiovasc. Drugs Ther.* **7,** 527–537.

136. Murry, C. E., Jennings, R. B., and Reimer, K. A. (1986) Preconditioning with ischemia: a delay of lethal cell injury in ischemic myocardium. *Circulation* **74,** 1124–1136.

137. Escande, D., Thuringer, D., Leguern, S., and Cavero, I. (1988) The potassium channel opener cromakalim (BRL 34915) activates ATP-dependent K^+ channels in isolated cardiac myocytes. *Biochem. Biophys. Res. Commun.* **154,** 620–625.

138. Szewczyk, A., Mikolajek, B., Pikula, S. and Nalecz, M.J. (1993) Potassium channel openers induce mitochondrial matrix volume changes via activation of ATP-sensitive K+ channel. *Pol. J. Pharmacol.* **45**, 437–443.

139. Cuppoletti, J., Baker, A. M., and Malinowska, D. H. (1993) Cl^- channels of the gastric parietal cell that are active at low pH. *Am. J. Physiol.* **264**, C1609–C1618.

140. Ehrlich, B. E. (1992) Incorporation of ion channels in planar lipid bilayers: How to make bilayers work for you. In *The Heart and Cardiovascular System*, 2nd Ed. (Fozzard, H. A., Haber, E., Jennings, R. B., Katz, A. M., and Morgan, H. E., eds.), pp. 551–560, Raven Press, New York.

141. Kakar, S. S., Mahdi, F., Li, X., and Garlid, K. D. (1989) Reconstitution of the mitochondrial non-selective Na^+/H^+ (K^+/H^+) antiporter into proteoliposomes. *J. Biol. Chem.* **264**, 5848–5851.

142. Grover, G., and Garlid, K. D. (1998) ATP-sensitive potassium channels: a review of their pharmacology in myocardial ischemia. *J. Mol. Cell. Cardiol.*, in press.

143. Mironova, G. D., Fedotcheva, N. I., Makarov, P. R., Pronevich, L. A., and Mironov, G. P. (1981) A protein of the bovine heart mitochondria inducing channel potassium conductivity in bilayer lipid membranes. *Biophysics* **26,** 458–465.

144. Goding, J. W. (1986) Generation of conventional antibodies. In *Monoclonal Antibodies Principles and Practice,* pp. 281–293, Academic Press, San Diego, CA.

145. Smith, D. E., and Fischer, P. A. (1984) Identification, developmental regulation, and response to heat shock of two antigenically related forms of a major nuclear envelope protein in Drosophila embryos: application of an improved method for affinity purification of antibodies using polypeptides immobilized on nitrocellulose blots. *J. Cell Biol.* **99,** 20–28.

146. Wessel, D., and Flügge, U. I. (1984) A method for the quantitative recovery of protein in dilute solution in the presence of detergents and lipids. *Anal. Biochem.* **138,** 141–143.

147. Laemmli, U. K. (1970) Cleavage of structural proteins during the assembly of the head of bacteriophage T4. *Nature* **227,** 680–685.

148. Sammons, D. W., Adams, L. D., and Nishizawa, E. E. (1981) Ultrasensitive silver-based color staining of polypeptides in polyacrylamide gels. *Electrophoresis* **2,** 135–140.

149. Kramer, W., Oekonomopulos, R., Pünter, J., and Summ, H.-D. (1988) Direct photoaffinity labeling of the putative sulfonylurea receptor in rat beta-cell tumor membranes by [3H]glibenclamide. *FEBS Lett.* **229,** 355–359.

150. Schwanstecher, M., Loser, S., Chudziak, F., Bachmann, C., and Panten, U. (1994) Photoaffinity labeling of the cerebral sulfonylurea receptor using a novel radioiodinated azidoglibenclamide analogue. *J. Neurochem.* **63,** 698–708.

151. Schwanstecher, M., Loser, S., Chudziak, F., and Panten, U. (1994) Identification of a 38-kDa high affinity sulfonylurea-binding peptide in insulin-secreting cells and cerebral cortex. *J. Biol. Chem.* **269,** 17768–17771.

152. Bryan, J., and Aguilar-Bryan, L. (1997) The ABCs of ATP-sensitive potassium channels: more pieces of the puzzle. *Curr. Opin. Cell Biol.* **9,** 553–559.

153. Garlid, K. D., Beavis, A. D., and Ratkje, S. K. (1989) On the nature of ion leaks in energy-transducing membranes. *Biochim. Biophys. Acta* **976,** 109–120.

154. Martin, W. H., DiResta, D. J., and Garlid, K. D. (1986) Kinetics of inhibition and binding of dicyclohexylcarbodiimide to the 82,000-dalton mitochondrial K^+/H^+ antiporter. *J. Biol. Chem.* **261,** 12300–12305.

155. Tusnady, G. E., Bakos, E., Varadi, A., and Sarkadi, B. (1997) Membrane topology distinguishes a subfamily of the ATP-binding cassette (ABC) transporters. *FEBS Lett.* **402**, 1–3.

156. Higgins, C. F. (1992) ABC transporters: from microorganisms to man. *Annu. Rev. Cell Biol.* **8,** 67–113.

157. Brdiczka, D., and Wallimann, T. (1994) The importance of the outer mitochondrial compartment in regulation of energy metabolism. *Mol. Cell. Biochem.* **133–134,** 69–83.

BIBLIOGRAPHICAL SKETCH

Vladimir Yarov-Yarovoy was born in Moscow, Russia, on November 30, 1967. He attended Moscow State University in Moscow, Russia, and in 1993 earned a Master of Science in Biophysics. In 1993, Vladimir joined the laboratory of Dr. Keith D. Garlid in the Department of Biochemistry and Molecular Biology at the Oregon Graduate Institute of Science and Technology.

List of Publications

Garlid, K. D., Paucek, P., Yarov-Yarovoy, V., Sun, X., and Schindler, P. (1996) The mitochondrial K_{ATP} channel as a receptor for potassium channel openers. *J. Biol. Chem.* **271**, 8796–8799.

Paucek, P., Yarov-Yarovoy, V., Sun, X., and Garlid, K. D. (1996) Inhibition of the mitochondrial K_{ATP} channel by long chain acyl-CoA esters and activation by guanine nucleotides. *J. Biol. Chem.* **271**, 32084–32088.

Mironova, G. D., Skarga,Yu. Yu., Grigoriev, S. M., Yarov-Yarovoy, V. M., Alexandrov, A. V., and Kolomytkin, O. V. (1996) The ATP-dependent potassium channel from rat liver mitochondria. 1. Isolation, purification, and reconstitution in a bilayer lipid membrane. *Membr. Cell Biol.* **10**, 429–437.

Yarov-Yarovoy, V., Paucek, P., Jaburek, M., and Garlid, K. D. (1997) The nucleotide regulatory sites on the mitochondrial K_{ATP} channel face the cytosol. *Biochim. Biophys. Acta.* **1321**, 128–136.

Garlid, K. D., Paucek, P., Yarov-Yarovoy, V., Murray, H. N., Darbenzio, R. B., D'Alonzo, A. J., Lodge, N. J., Smith, M. A., and Grover, G. J. (1997) Cardioprotective effect of diazoxide and its interaction with mitochondrial ATP-sensitive potassium channels: possible mechanism of cardioprotection. *Circulation Res.* **81**, 1072–1082.

Jaburek, M., Yarov-Yarovoy, V., Paucek, P., and Garlid, K. D. (1998) State-dependent inhibition of the mitochondrial K_{ATP} channel by glyburide and 5-hydroxydecanoate. *J. Biol. Chem.* **273**, 13578–13582.

Paucek, P., Yarov-Yarovoy, V., and Garlid, K. D. (1998) Photoaffinity labeling and purification of mitoSUR, the sulfonylurea receptor of the mitochondrial K_{ATP} channel. *J. Biol. Chem.*, submitted.